UNIVERSIDADE FEDERAL DE SANTA CATARINA

CENTRO DE CIÊNCIAS DA SAÚDE

PROGRAMA DE PÓS-GRADUAÇÃO EM FARMÁCIA

Rafael Nicolay Pereira

Avaliação de Complexos de Sílica Mesoporosa (SBA-15) com Fármacos (Naproxeno e Estavudina)

Dissertação apresentada ao Programa de Pós-Graduação em Farmácia como requisito parcial à obtenção do grau de Mestre em Farmácia.

Orientador: Prof. Dr. Marcos Antonio Segatto Silva

Florianópolis – SC

2009

UNIVERSIDADE FEDERAL DE SANTA CATARINA

CENTRO DE CIÊNCIAS DA SAÚDE

PROGRAMA DE PÓS-GRADUAÇÃO EM FARMÁCIA

Avaliação de Complexos de Sílica Mesoporosa (SBA-15) com Fármacos (Naproxeno e Estavudina)

Dissertação apresentada por Rafael Nicolay Pereira ao Programa de Pós-Graduação em Farmácia como requisito parcial à obtenção do grau de Mestre em Farmácia.

Orientador: Prof. Dr. Marcos A. Segatto Silva

Florianópolis

2009

"Avaliação de Complexos de Sílica Mesoporosa (SBA-15) com Fármacos (Naproxeno e Estavudina)"

POR

Rafael Nicolay Pereira

Dissertação julgada e aprovada em sua forma final pelo Orientador e membros da Banca Examinadora, composta pelos Professores Doutores:

Banca Examinadora:

Hellen K. Stulzer

Profa. Dra. Hellen Karine Stulzer (UEPG– Membro Titular)

Profa. Dra. Angela Machado de Campos (UFSC - Membro Titular)

Simone Gonçalves Cardoso

Profa. Dra. Simone Gonçalves Cardoso (UFSC - Membro Titular)

Prof. Dr. Marcos Antônio Segatto Silva (UFSC – Orientador)

Profa. Dra. Elenara Lemos Senna
Coordenadora do Programa de Pós-Graduação em Farmácia da UFSC

Florianópolis, 30 de abril de 2009.

Dedico este trabalho aos meus pais, Alceu e Liria, pelo exemplo de vida e por todo o apoio e empenho que tem depositado em mim. Dedico ainda ao meu irmão, ao qual possuo grande admiração, e a Luisa pelo apoio indispensável na realização desse trabalho.

AGRADECIMENTOS

Ao meu orientador Prof. Dr. Marcos Antônio Segatto Silva, pela oportunidade dada, pela confiança depositada e além de tudo pela amizade criada durante todo este período que trabalhamos juntos e que, certamente irá perdurar ao longo dos anos. Agradeço ainda pela contribuição de minha formação profissional e pessoal. Muito obrigado ZICZIRA.

Aos meus pais, por todo o apoio, compreensão, confiança e carinho durante todos estes anos. Pessoas com as quais aprendi honestidade, disposição, vontade e muita garra. Obrigado pai e mãe por tudo o que vocês fizeram.

Ao meu irmão Maurício, pessoa pela qual tenho grande admiração pela garra, sabedoria e disposição. Agradeço pela amizade, carinho e grande apoio e incentivo. Obrigado meu irmão. À Claudia, irmã que não tive, mas que já faz parte de nossa família.

À Luisa, pessoa que tenho imensa admiração por sua sinceridade, companheirismo e garra invejáveis. Pessoa a qual devo muito desse trabalho pelas palavras de conforto, credibilidade e também, não poderia deixar de mencionar, na revisão do inglês. Muito obrigado linda.

À professora Simone, pela amizade, companheirismo e paciência com todos nós durante a realização de projetos em parceria.

À professora Hellen, pelo apoio e disposição na realização deste trabalho.

À Arlene, que teve papel fundamental no meu ingresso no curso de pós-graduação.

Ao Alexander, Alexandre, Raphaela, Thiago, Marcela e Antonio, pessoas que fizeram e fazem parte de meu convívio desde o início da universidade e que se tornaram grandes amigos.

Aos amigos do laboratório, Charise, Cassiana, Gislaine, Silvinha, Monika, Patrik, Gaby e Amarílis pelo convívio e amizade durante todo esse tempo.

Aos grandes amigos Fábio (Japa) e Bruno (Cane) pela amizade, companheirismo, apoio e pelas brincadeiras nas horas vagas. Saibam que sempre poderão contar comigo para todas as horas. Obrigado.

Aos amigos Paulo, Larissa e Aureana pela amizade e convívio durante horas de trabalho e até mesmo durantes os churrascos.

Aos amigos do Laboratório e colegas do pós-graduação Karen, Silvana, Geison, Jadel, Tiaguinho, Dani, Carine e Leticia pelo convívio.

As grandes amigas Tati e Andréa pelo apoio, convívio e risadas.

Aos técnicos de laboratório Solange, Sandra e Nilson, aos professores e funcionários do programa de pós-graduação em Farmácia e a todos aqueles que direta ou indiretamente me auxiliaram na realização deste trabalho.

"Ser desafiado na vida é inevitável. Ser derrotado é opcional". *(Roger Crawford)*

SUMÁRIO

LISTA DE TABELAS

LISTA DE FIGURAS

Introdução

Capítulo 1

Capítulo 2

APENDICE

LISTA DE ABREVIATURAS

Δm	Variação de massa
Δ*H* fusão	Variação da entalpia de fusão
DRXP/XRPD	Difração de raios-X de pó (*X – ray powder diffraction*)
DSC	*Diferencial scanning calorimetry* (Calorimetria exploratória diferencial)
DRIFT	*Diffuse reflectance infrared Fourier transform spectroscopy*
HPLC/CLAE	*High Performance Liquid Chromatography / Cromatografia L'iquida de Alta Eficiência*
FTIR	*Fourier Transform Infrared Spectroscopy*
MEV	*Microscopia eletrônica de varredura*
TG	*Thermogravimetry* (Termogravimetria)
T*onset*	*Temperatura onset*
SBA-15	*Santa Bárbara Amorphous 15*
SBA-15/NAP	*Complexo sílica/naproxeno*
SBA-15/STAV	*Complexo sílica/estavudina*
MCM-41	*Mobil Composition Matter*
AINEs	*Antinflamatório não-esteroidal*
IUPAC	*União Internacional de Química Pura e Aplicada*
HIV	*Vírus da Himunodeficiência*
COX	*Cicloxigenase*
FDA	*Food and Drugs Administration*
RT	*Transcriptase Reversa*

OMS	*Material Mesoporoso Ordenado*
d4T	*Estavudina*
SEM	*Scanning Eletronic Microscopy*
SBAn	*Santa Bárbara Amorphous n*
DNA	*Deoxirribonucleic Acid*
PG	*Prostaglandinas*
MCM	Móbil Company Matter
SAXS	Small Angle X-ray Spectroscopy

RESUMO

Materiais mesoporosos têm recebido muita atenção devido as suas características atrativas como estrutura de mesoporos estáveis, grande área superficial (acima de 1500 m^2/g), grande volume de poro, tamanho de poro regulável (2-10 mn) e superfície com caráter hidrofílico. Recentemente uma nova aplicação para a sílica mesoporosa como liberação de fármacos tem sido explorada devido a sua natureza não-tóxica e boa biocompatibilidade. SBA-15 é uma sílica mesoporosa ordenada com características adequadas e boa estabilidade térmica. Por esta razão, a SBA-15 é um potencial candidato a um sistema de liberação de fármacos. O naproxeno é um derivado do ácido propiônico e o naproxeno sódico é seu sal. É um fármaco antiinflamatório não-esteroidal (AINEs) que inibe a síntese de prostaglandinas. O naproxeno é um fármaco lipossolúvel, praticamente insolúvel em água a pH baixos e facilmente solúvel em pH mais elevados, é solúvel em etanol e metanol. Seu coeficiente de partição octanol/água a pH 7.4 é de cerca de 2.A estavudina é um antiretroviral representante da classe de inibidores de transcriptase reversa e é comumente utilizada na terapia contra o HIV. A estavudina, também chamada de d4T, é um fármaco hidrofílico, solúvel em água e parcialmente solúvel em etanol. Outra importante característica é seu coeficiente de partição (Log *P*(octanol/água)): −0.72 (ou 0.14)**.** Este valor lhe confere a característica hidrofílica o que explica sua solubilidade em água. O objetivo do trabalho foi avaliar a complexação de SBA-15 com dois fármacos modelos (naproxeno e estavudina). Algumas técnicas foram usadas: TG, DSC, FTIR, MEV e CLAE. A partir dos resultados obtidos foi possível observar a

complexação do naproxeno com a SBA-15, o que não ocorreu com a estavudina. Isso se deve ao fato de o naproxeno possuir característica de solubilidade semelhante a sílica mesoporosa SBA-15, facilitando a complexação. O controle do pH influenciou na ligação do naproxeno com os grupos funcionais da sílica. O percentual de fármaco presente na sílica foi quantificado por CLAE e resultou em cerca de 32 %.

Palavras-chave: SBA-15, naproxeno, estavudina, complexação.

ABSTRACT

Mesoporous silica materials have been received attention due to their attractive features such as stable mesoporous structure, high surface area (up to 1500 m^2/g), large pore volume (up to 1.2 cm^3/g), regular and adjustable nano-pore sizes (2–10 nm) and a hydrophilic surface character. Recently, a new application of mesoporous silica as a drug delivery system has been explored due to their non toxic nature and good biocompatibility. SBA-15 is an ordered mesoporous silica with a large surface area, uniform hexagonal channels and remarkable hydrothermal stability. For this reason, SBA-15 is a potential candidate for drug delivery systems since its pore size is easily controlled according to the synthesis conditions and the presence of swelling agents. Naproxen is a member of the arylacetic acid derivative of propionic acid and naproxen sodium is the sodium salt. It is a nonsteroidal anti-inflammatory drug (NSAIDs) that inhibit prostaglandin synthesis. The NSAIDs are used in a variety of painful conditions, including the treatment of postoperative pain. Naproxen is lipid-soluble, practically insoluble in water at low pH and freely soluble in water at high pH, soluble in ethanol (96 per cent) and in methanol. The octanol/water partition coefficient of naproxen at pH 7.4 is 1.6 to 1.8. Stavudine is an antiretroviral representative of nucleoside reverse transcriptase (RT) inhibitors class (NRTIs) and is commonly used in the HIV therapy**.** Stavudine, also named d4T, is a hydrophylic drug, soluble in water, sparingly soluble in ethanol (96 per cent) and slightly soluble in methylene chloride. Other important characteristic is its partition coefficient (Log *P*(octanol/water)): −0.72 (or 0.14)**.** This value confers

the hydrophilic characteristic which explains the high water solubility. The aim of the present work was available the complexes of SBA-15 silica and drugs. Some techniques were uses: TGA, DSC, FTIR, SEM and HPLC. From the results it was possible to observe the complexation of naproxen with SBA-15 which was not observed with stavudine. This result is due to the fact that naproxen has similar solubility characteristics of the SBA-15 mesoporous silica. The pH control influenced the binding of naproxen with the functional groups of silica. The percentage of drug loading in the silica was quantified by HPLC and resulted in about 32 %.

Keywords: SBA-15, naproxen, stavudine, complexation.

1.INTRODUÇÃO

1. INTRODUÇÃO

Em 1992 a companhia Móbil Oil descobriu uma nova família de materiais sintéticos à qual nomeou M41S. Estes materiais possuem características interessantes pois adsorvem moléculas volumosas, possuem tamanho de poros de 2 a 10 nm e um elevado volume de poro (1 cm^3/g), sendo capaz de adsorver uma quantidade grande de moléculas. Além disso, possuem uma área superficial bastante elevada (500 – 1000 m^2/g). A Figura 1 representa a classificação de tamanho de poro **[1]**.

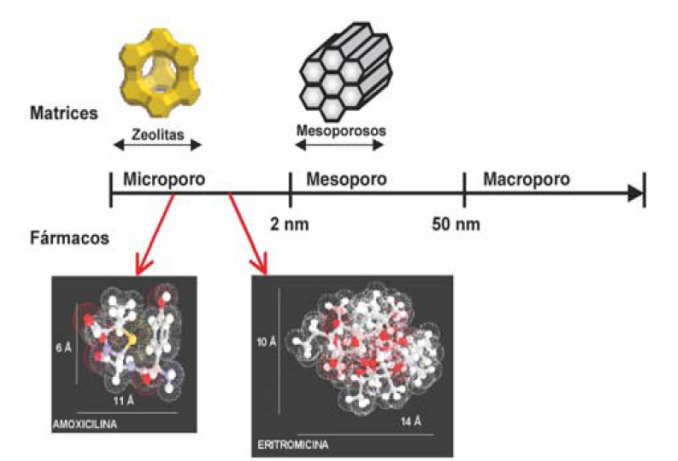

Figura 1 – Classificação IUPAC de materiais em função do tamanho de poro **[1]**.

Os materiais mesoporosos são ainda classificados de acordo com os tipos de poros. A MCM-41 e a SBA-15 possuem poros unidirecionais com empacotamento hexagonal e poros longitudinais como mostra a Figura 2. As diferenças estruturais de vários tipos de materiais mesoporosos é apresentada na Tabela 1 **[1]**.

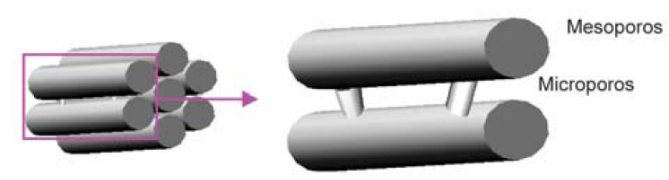

Figura 2 – Esquema ilustrativo do sistema de poros da SBA-15.

TABELA 1 - Características de Estruturas Mesoporosas. Adaptado da referência 1.

MATERIAL	ESTRUTURA	TIPO DE PORO
FSM-16	HEXAGONAL PLANA	CANAIS
MCM-41	HEXAGONAL PLANA	CANAIS
MCM-48	CUBICA BICONTÍNUA	CANAIS
MCM-50	LAMINAR	BICAPA
SBA-1	CUBICA	2 CAVIDADES
SBA-2	HEXAGONAL 3D	CAVIDADES/CANAIS
SBA-6	HEXAGONAL 3D	CAVIDADES
SBA-8	ROMBICA	?
SBA-15	**HEXAGONAL PLANA**	**CANAIS**
FDU-1	CUBICA 3D	CAVIDADES/CANAIS
MASU	HEXAGONAL DESORDENADA	CANAIS

Estudos de toxicidade demonstraram que estes materiais silicosos somente são problemáticos quando na forma de ácido silícico, porém esta forma reage com o cálcio do organismo diminuindo sua concentração. Além disso, a formação de sua forma ácida é muito baixa, sendo considerada insignificante. Dessa forma não há uma toxicidade destes materiais no organismo **[1]**.

Materiais silicosos possuem algumas características de interface de superfície interessantes, desempenhando um papel importante no processo de adsorção. As características de superfície do adsorvente determinam a natureza das ligações entre adsorvente e adsorbante. Diferentes técnicas são utilizadas para caracterizar a superfície do adsorbante e isto é de grande importância no entendimento do processo de complexação. Para investigar o comportamento dos poros da sílica revestida com polímeros de siloxano, podem ser realizadas técnicas de adsorção de nitrogênio, para a área de superficie e porosidade da sílica e da sílica revestida com polímero, além de técnicas termogravimétricas de alta resolução para a determinação do comportamento térmico da sílica. No tratamento térmico a superfície hidrofílica da sílica gradualmente muda para superfície hidrofóbica pela eliminação irreversível de um par de hidroxilas adjacentes. A temperatura de transição depende da origem e morfologia da amostra **[2]**.

Um considerável esforço tem sido direcionado à síntese de nanomateriais com estruturas de poros bem definidas, sendo estas de grande interesse na possibilidade de obtenção de silicatos mesoporosos com estruturas ordenadas **[3]**.

Estudos recentes levaram à descoberta de sílicas mesoporosas com estrutura hexagonal, as quais apresentam elevada área superficial (700 a 1000 m^2/g), tamanho de poros grande (5 a 9 nm) e espessura fina de parede do poro (3,5 a 5,3 nm), sendo a SBA15 um exemplo destas sílicas. Essas características fazem destes materiais matrizes adequadas para a incorporação e liberação, quando em condições apropriadas, de uma série de biomoléculas. As características da SBA15 preparada em diferentes temperaturas e o comportamento desse sistema com relação

ao micreoencapsulamento de um fármaco modelo pode ser investigado. Foi observado que materiais envelhecidos a elevadas temperaturas não apresentam microporosidades, e esse fato pode influenciar no controle da liberação do fármaco **[4]**.

A aplicabilidade de materiais mesoporosos como à silica SBA-15, como matriz para liberação de fármacos, está sendo estudada para estabelecer a influência da arquitetura e tamanho do poro neste processo de liberação. Este tipo de material, geralmente associado à biomoléculas, pode ser introduzido no organismo sem ser rejeitado como resultado de um processo inflamatório no local de implantação, tornando possível sua utilização como matriz de liberação de fármacos **[5]**.

Material mesoporoso é, atualmente, um campo de intensa pesquisa devido ao seu alto potencial de aplicações. Uma série de mesoestruturas inorgânicas, como MCM41, HMS, SBAn etc., têm sido sintetizadas com diferentes esquemas modelos **[5, 6]**.

Os dois fármacos escolhidos como modelo na complexação com a sílica mesoporosa SBA-15 foram o naproxeno e a estavudina.

O naproxeno é um derivado do ácido propiônico com atividade analgésica e antiinflamatória, o qual é amplamente utilizado no tratamento de doenças reumáticas. Este fármaco tem sido muito estudado em artrite reumatóide sendo tão efetivo quanto a aspirina, porém melhor tolerado, conduzindo a um maior número de adeptos ao tratamento contínuo. Por esta razão, médicos agora preferem indicar derivados do ácido propiônico, como o naproxeno, em detrimento à aspirina para pacientes com artrite reumatóide. Em estudos comparativos com outros fármacos antiinflamatórios não esteroidais,

assim como indometacina, ibuprofeno, fenoprofeno e outros, todos os fármacos demonstraram eficácia similar embora o naproxeno seja algumas vezes preferido devido a sua melhor tolerância **[7, 8]**.

O naproxeno também é efetivo em doenças degenerativas de articulações, embora estudos futuros bem delineados sejam necessários para definir mais claramente sua ação comparada com outros fármacos como diclofenaco ou diflunisal. Resultados de outros estudos demonstraram que o naproxeno é uma alternativa eficaz tanto quanto a fenilbutazona ou a indometacina em espondilite e a aspirina em artrite reumatóide juvenil **[7,8]**.

Naproxeno e naproxeno sódico são fármacos antiinflamatórios não-esteroidais (AINEs) que inibem a síntese de prostaglandinas **[10].**

De maneira geral, AINEs são inibidores da enzima cicloxigenase, a qual catalisa o metabolismo do ácido araquinóide para prostaglandinas, prostaciclinas e tromboxanos. A isoforma 1 da cicloxigenase é expressa em muitos tecidos, onde medeia as funções fisiológicas como citoproteção da mucosa gástrica e regulação de agregação plaquetária. Sua inibição pode contribuir para muitos efeitos colaterais comuns dos AINEs, incluindo ulceração e hemorragia gástrica **[11].**

Cicloxigenase (COX) é a enzima limitante que converte ácido araquidônico em prostaglandinas e possui importante papel em várias desordens do Sistema Nervoso Central (SNC). A COX existe em duas isoformas: COX-1 e COX-2. A COX-1 é constitutivamente expressa pelo corpo ao passo que a COX-2 é indetectável em muitos nos tecidos sob condições basais **[12,13].** Também há relatos que a COX-2 está

presente em alguns neurônios cerebrais **[14]** e sua expressão é aumentada em doenças neurológicas **[15]**.

O mecanismo de ação em efeitos de estresse ainda não é bem entendido, mas muitos estudos de processos inflamatórios vêm sendo desenvolvidos nos últimos anos **[16].**

Contudo, a isoforma COX-1 não tem recebido muita atenção como uma fonte importante de prostaglandinas, embora esteja associada com a homeostase dos tecidos e reações de catálise idênticas a alguns produtos pró-inflamatórios no local da inflamação **[17].**

Um esquema da ação dos AINEs na inibição da COX está representado na **Figura 3**, abaixo.

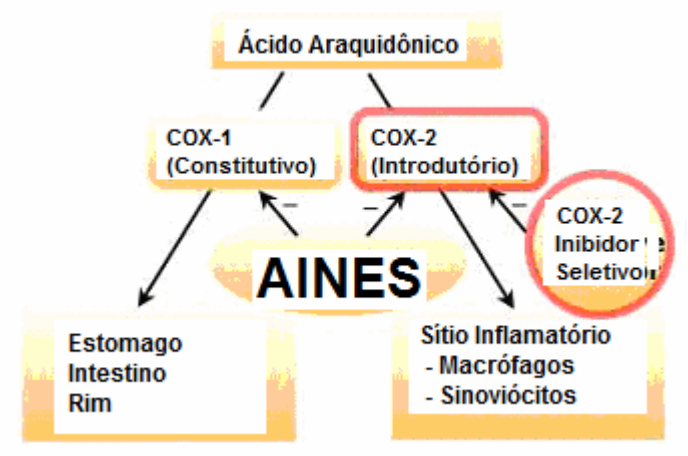

Figura 3 – Esquema da ação dos AINEs na inibição da COX **[18].**

Algumas das Ações de AINEs [12]:

- Inibição da síntese de prostaglandinas (PG):
- Inibição da COX-1 ou COX-2 ou ambas, impedindo a formação de PG.
- Antagonismo dos receptores das PG.
- Inibição da liberação de histamina dos mastócitos.
- Inibição da migração de leucócitos PMN (polimorfonucleares) e monócitos, reduzindo a quimiotaxia.
- Redução da permeabilidade capilar, diminuindo o edema e vermelhidão.
- Inibição da liberação da PGE1 na área pré-óptica do hipotálamo anterior, inibindo o mecanismo da febre.

O naproxeno é um derivado do ácido propiônico e naproxeno sódico é o sal sódico **[19].** Sua fórmula molecular é $C_{14}H_{14}O_3$ e possui Peso Molecular de 230,3. Os nomes químicos para o naproxeno e naproxeno sódico são ácido (S)-6-metoxi-α-metil-2- naftalenoacético e ácido (S)-6-metoxi-α-metil-2-naftalenoacetico sal sódico, respectivamente **[20,21].** O naproxeno e o naproxeno sódico possuem a estrutura representada na **figura 4**.

Em relação às características físico-químicas, o naproxeno é um pó branco, praticamente sem odor, cristalino, solúvel em álcool, álcool desidratado e álcool metílico e em clorofórmio sendo também facilmente solúvel em éter. Além disso, é solúvel em lipídeos,

praticamente insolúvel em água a baixo pH e facilmente solúvel em água a pH mais elevado. O coeficiente de partição octanol/água (Log P) a pH 7,4 é de 1,6 a 1,8. Esta característica lhe confere caráter lipofílico, o que pode ser observado em sua baixa solubilidade em água **[20,21]**. O naproxeno é extensivamente metabolizado a 6-0-desmetil naproxeno e tanto a base quanto seus metabólitos não induzem metabolização de enzimas **[21]**.

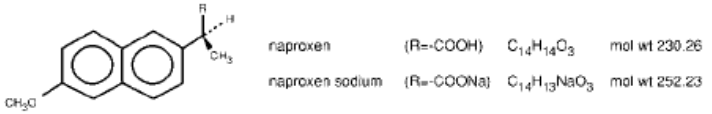

Figura 4: Representação da estrutura do naproxeno e naproxeno sal sódico **[21].**

Problemas no trato gastrointestinal superior como dispepsia são comuns e podem também ocorrer a qualquer tempo durante a terapia com NSAID. Portanto, médicos e pacientes devem permanecer alertas em relação à ulceração mesmo na ausência de sintomas prévios no trato gastrointestinal. Dessa forma NSAIDs devem ser prescritos com extrema precaução em pacientes com histórico de ulcerações ou lesões gastrointestinais **[22-27].**

Em relação ao fármaco estavidina, este é ampolamente utilizado no tratamento contra o HIV. Em nível mundial, diariamente mais de 6800 pessoas são infectadas com o HIV (vírus da imunodeficiência humana) e mais de 5700 pessoas morrem de SIDA (síndrome da imunodeficiência adquirida). Isto se deve ao fato de que grande parte da população têmdificuldades de acesso tanto à prevenção da doença quanto ao tratamento adequado. A pandemia do HIV continua o mais

grave desafio das doenças infecciosas para a saúde pública mundial **[28].**

Uma análise das tendências globais e regionais sugere que a pandemia já formou dois padrões distintos: epidemias generalizadas sustentadas na população de muitos países africanos, especialmente na parte sul do continente; e epidemias no resto do mundo, que são essencialmente concentradas entre as populações de maior risco, como homossexuais, usuários de drogas injetáveis, profissionais do sexo e seus parceiros sexuais **[28-34].**

Em 2007, avanços na metodologia de detecção de epidemias de HIV aplicadas em uma ampla faixa de dados de diferentes países têm resultado em substanciais mudanças na estimativa do números de casos de pessoas vivendo com o HIV em todo o mundo. Entretanto a interpretação qualitativa da severidade e implicações de pandemias mudou pouco. O número estimado de pessoas com HIV em todo o mundo, em 2007, foi de 33,2 milhões, uma redução de 16 % comparado

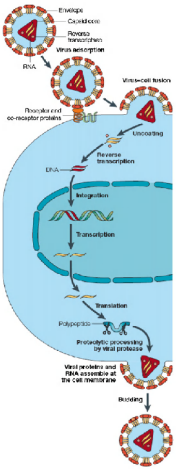

com o estimado em 2006 (39,5 milhões) **[32].** A maior razão para esta redução foi o exercício intensivo da Índia para avaliar a epidemia de HIV, que resultou em uma maior revisão das estimativas desse país. Uma importante reavaliação feita pela África do Sul também contribuiu para esta redução. Da diferença total nas estimativas publicadas em 2006 e 2007, 70 % foram devidas a mudanças em apenas seis países: Angola, Índia, Quênia, Moçambique, Nigéria e Zimbábue **[32].**

Em 2008, 25 anos após o surgimento do HIV (Human Immunodeficiency Virus), foi descoberto o agente etiológico da Síndrome da Imudodeficiência Adquirida (SIDA), ou AIDS (Acquired Immune Deficiency Syndrome) e exatamente 25 compostos anti-HIV foram formalmente aprovados para uso clínico no tratamento da AIDS. Estes compostos se dividem em seis categorias: a) ***Nucleosídeos Inibidores da Transcriptase Reversa (NRTIs)*** – (zidovudina, didanosídeo, estavudina, lamivudina, abacavir, zalcitabina e entricitabina); b) ***Nucleotídeo Inibidor da Transcriptase Reversa (NtRTIs)*** – (tenofovir); c) ***Não-nucleosídeo Inibidor de Transcriptase Reversa (NNRTIs)*** – (nevirapina, delavirdina, efavirenz e estravirina); d) ***Inibidor de Protease (Pis)*** – (saquinavir, ritonavir, indinavir, nelfinavir, amprenavir, lopinavir, atazanavir, fosanprenavir, tripanavir, darunavir); e) ***Inibidor de Entrada na Célula*** – Inibidor de fusão (FIs – enfuvirtide) e Inibidor de Co-recepção (Cris – maraviroc); e***) Inibidor de Integrase (INIs)*** – (raltegravir). Estes compostos devem ser usados em regimes de combinação para atingir um maior benefício, tolerância e diminuir riscos de desenvolvimento de resistência **[35].**

Na **figura 5** pode-se observar o ciclo de replicação do vírus da imunodeficiência humana (HIV), destacando os principais alvos de intervenção terapêutica.

Fig. 5. Ciclo de replicação do vírus da imunodeficiência humana (HIV), destacando os principais alvos de intervenção terapêutica: interação (co-)receptor; fusão célula-vírus; transcrição reversa (pela transcriptase reversa); integração e processo proteolítico (por protease). De acordo com De Clercq **[36].**

Inibidor Nucleosídeo de Transcriptase Reversa (NRTIs)

A Tanscriptase Reversa (RT – Reverse Transcriptase, em inglês) associada ao HIV é atualmente o alvo de três classes de inibidores: Inibidor RT nucleosídeo (NRTIs); Inibidor Nucleotídeo RT (NtRTIs); e Inibidor Não-nucleosídeo RT (NNRTIs). Os NRTIs e NtRTIs interagem com o sítio catalítico da enzima, ao passo que os NNRTIs interagem com um sítio alostérico a curta distancia do sítio catalítico (ca. 15 Å) **[35].**

Como os NRTIs e NtRTIs interagem com o sítio de ligação do substrato, eles necessitam ser fosforilados para as formas trifosfato e difosfato, respectivamente. Existem atualmente (em 2008) sete NRTIs que são formalmente aprovados para o tratamento de infecções por HIV: zidovudina (AZT); didanosina (ddI); zalcitabina (ddC); estavudina (d4T) (**figura 6, estavudina**); lamivudina (3TC); abacavir (ABC); e emtricitabina ((-)FTC).

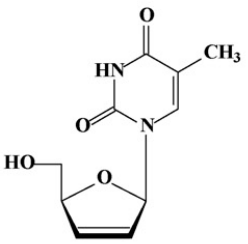

Stavudine
2',3'-Didehydro-2',3'-dideoxythymidine
(d4T)
Zerit®

Figura 6. Fórmula estrutural de nucleosídeo inibidor de transcriptase reversa (NRTIs) - estavudina.

Como um inibidor de substrato normal, o ddNTP irá inibir a incorporação deste substrato para o crescimento da cadeia de DNA; como um substrato alternativo, irá inibir a cadeia (como ddNMP), atuando como uma cadeia de terminação (desde que o ddNMP esteja sem o grupo 3'-hidroxil requerido para um posterior alongamento da cadeia). Este modo de ação é exemplificado para o AZT na **figura 7** baseado em dados originais de Mitsuya et al. **[32]** e Furman et al**. [37],** mas é válido para todos os análogos ddNTP uma vez feitas as mudanças necessárias.

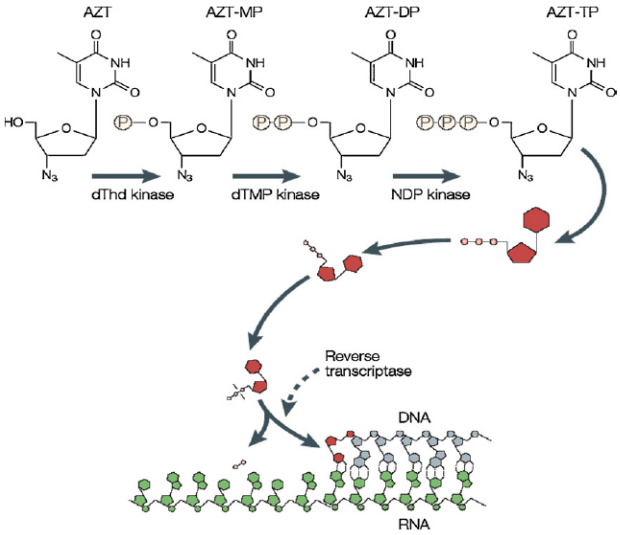

Figura 7. Mecanismo de ação da zidovudina (AZT). Segue a fosforilação para sua forma trifosfato (AZT-TP). AZT atua como um inibidor competitivo/substrato alternativo em relação ao dTTP na reação da transcriptase reversa. De acordo com De Clercq **[9].**

Combinação de fármacos Anti-HIV: Terapia com Alta Atividade Antirretroviral (HAART)

Desde 1996, o regime de combinação de fármacos anti-HIV se tornou amplamente aceito. O que já é prática comum para o tratamento de tuberculose (ex: combinação de três tuberculostáticos) foi introduzido para o tratamento da AIDS tendo recebido uma sigla própria, HAART, para Terapia com Alta Atividade Antiretroviral. A combinação de três (ou mais) compostos antiretrovirais é baseada nos mesmos objetivos gerais do tratamento da tuberculose: (i) obter sinergismo entre diferentes compostos atuando em alvo molecular diferente; (ii) diminuir a dose individual e reduzir seus efeitos colaterias tóxicos; e (iii) diminuir a probabilidade de desenvolvimento de resistência **[36].**

Dos 25 compostos formalmente licenciados para uso clínico, alguns ainda não são amplamente disponíveis e outros não foram completamente avaliados ou amplamente prescritos. No entanto, apesar do número dos medicamentos disponíveis não serem muitos, eles já são considerados suficientes para permitir um grande número de combinações. Ainda que o número de combinações possíveis de fármacos anti-HIV têm crescido rapidamente, o número de comprimidos que são administrados diariamente para todas as combinações vem sendo drasticamente reduzido, de mais de 20 comprimidos/dia em 1996 para apenas um comprimido/dia em 2006 **[28,30,32,33].**

A estavudina, aprovada pelo FDA (Food and Drug Administration), é um análogo nucleosídeo pirimidínico sintético sendo formalmente chamada de d4T. Seu nome químico é 1-(2,3-Dideoxi-β-D-*glicer*-pent-2-enofuranosil)timina e apresenta a seguinte fórmula molecular: $C_{10}H_{12}N_2O_4$ =224.2, com ponto de fusão de 174 °C.

Apresenta-se como pó cristalino branco ou quase branco e fotossensível. A estavudina é solúvel em água, dimetilacetamida e dimetilsulfóxido e parcialmente solúvel em álcool, acetonitrila e diclorometano. Este fármaco também exibe polimorfismo. Outra característica importante é seu Coeficiente de Partição - Log *P*(octanol/água): −0.72 (também cotado como 0.14) **[37-43].** Esse valor lhe confere uma característica hidrossolúvel, o que explica sua fácil solubilidade em água.

A estavudina é um potente inibidor da replicação do HIV em concentrações similares à zidovudina. Este fármaco entra rapidamente nas células por difusão não-facilitada. Em uma variedade de sistemas celulares, é seqüencialmente fosforilada a suas formas 5'-mono, di- e trifosfato **[37,38].** A forma 5'-trifosfato é o inibidor da transcriptase reversa sendo que a ativação para a forma 5'-monofosfato por timidina quinase celular é o passo metabólico limitante **[39].** A estavudina monofosfato não acumula intracelularmente e a taxa de mono- a di- e trifosfato é relativamente constante, variando de 1:1:1 para 1:1:3 **[40].** Isto contrasta com a zidovudina, na qual a forma monofosfato acumula em grandes níveis devido ao metabolismo limitado para a forma difosfato. A concentração intracelular de estavudina trifosfato aumenta na proporção da concentração extracelular do fármaco original. Em comparação, níveis de zidovudina intracelular mostram uma baixa relação concentração-resposta em relação à concentração extracelular de zidovudina **[40,41].** Uma vez formado o trifosfato, tanto para estavudina quanto para zidovudina, este possui meia-vida intracelular de aproximadamente 3,5 h **[39].**

A síntese da estavudina foi primeiramente relatada por Horwitz et al. (1966) **[42].** Como para outros compostos dideonucleosídeos,

estavudina-5'-trifosfato é inibidor da replicação retroviral por competir com desoxitimidina trifosfato endógena como substrato para a transcriptase reversa do HIV e por bloquear o alongamento da cadeia de DNA após a incorporação no DNA viral **[43].** Quer pela inibição competitiva, quer pela terminação da cadeia, o mecanismo intracelular de ação predominante é desconhecido **[44].**

A estavudina demonstrou ser um antiretroviral com potente atividade quando usado em monoterapia em pacientes assintomáticos ou com infecção severa, bem como eficácia clínica comparada a de pacientes tratados com zidovudina **[45-48].** Além disso, estavudina e lamivudina possuem maior atividade ou sinergia em relação à espécies de HIV-1 resistente e sensível à zidovudina em estudos *in vitro*. Nesse estudo foi demonstrado que o tratamento prolongado com estavudina geralmente não está associado com o desenvolvimento de resistência viral ao fármaco. Atualmente, a combinação de dois nucleosídeos análogos é o principal regime de tratamento antiretroviral para infecções com HIV-1. Um exemplo importante desta combinação é a associação entre estavudina e lamivudina, que demonstrou um efeito aditivo *in vitro,* bem como ausência de sobreposição de toxicidade e resistência cruzada **[49-51].**

Levando-se em conta todas essas considerações a respeito da SBA-15, percebe-se o potencial desta estrutura mesoporosa para hospedar a liberação de fármacos sob condições apropriadas, usando uma molécula modelo.

O naproxeno foi escolhido por ser um antiinflamatório amplamente utilizado na gerência da dor e no tratamento da enxaqueca e da dor de cabeça. Além disso, sua característica de solubilidade é

foco deste trabalho, uma vez que se propõe a avaliação de complexação de fármacos com características de lipossolubilidade.

A estavudina, outro fármaco utilizado, foi escolhida por possuir características físico-químicas opostas ao naproxeno, possuindo logP de 2 e pKa de 4,5. Além disso é um dos antiretrovirais mais utilizados, principalmente em terapias de associação, no tratamento do HIV.

Sendo assim, propõe-se a utilização da sílica SBA-15 para avaliar a complexação e quantificação do naproxeno e da estavudina na sílica mesoporosa.

2. OBJETIVOS

2.1. Objetivo Geral

Avaliar o potencial de uma estrutura mesoporosa (sílica SBA-15), em função das características físico-químicas, em servir de matriz para fármacos modelo (naproxeno e estavudina).

2.2. Objetivos Específicos

a) Caracterizar a sílica e os fármacos através de técnicas analíticas como DSC, TG, IV, DRX e MEV.

b) Realizar a complexação dos fármacos com a sílica SBA-15.

c) Avaliar a ocorrência da complexação através de técnicas analíticas como DSC, TG, IV, DRX e MEV.

d) Determinar a eficiência de complexação por CLAE.

3. REFERÊNCIAS

[1] Villarejo A.L.D., Regí M.V. Liberación de fármacos en matrices biocerámicas: Avances y perspectivas. Ed. Realigraf. Madrid, Espana, 2006.

[2] Parida S. K., Dash S., Patel S., Mishra B.K. Adsorption of organic molecules on silica surface. Advances in Colloid and Interface Science 121 (2006) 77–110.

[3] Matos J. R., Jaroniec M., Mercuri L.P. Comparative thermogravimetric and adsorption study of highly ordered mesoporous materials. Journal of Colloid and Interface Science: - APR 1 2006, Holanda, v. 296, n. 1, p. 377-380, 2006.

[4] Zhu-Zhu Li, Li-Xiong Wen, Lei Shao, Jian-Feng Chen. Fabrication of porous hollow silica nanoparticles and their applications in drug release control. Journal of Controlled Release 98 (2004) 245– 254.

[5] Kruk M., Celer E. B., Matos J. R., Pikus S. and Jaroniec M. Synthesis of FDU-1 Silica with Narrow Pore Size Distribution and Tailorable Pore Entrance Size in the Presence of Sodium Chloride. *J. Phys. Chem. B* 2005, *109,* 3838-3843.

[6] Fantini M.C.A., Matos J.R., Silva L.C. C., Mercuri L.P., Chiereci G.O., Celer E.B., Jaroniec M. Ordered mesoporous silica: microwave synthesis. Materials Science and Engineering B 112 (2004) 106–110.

[7] Brogden RN, Heel RC, Speight TM, Avery GS. Naproxen up to date: a review of its pharmacological properties and therapeutic efficacy and use in rheumatic diseases and pain states. Drugs. 1979 Oct; 18(4):241-77.

[8] Todd PA, Clissold SP. Naproxen: a reappraisal of its pharmacology, and therapeutic use in rheumatic diseases and pain states. Drugs 1990; 40: 91–137. PubMed

[9] Mason L, et al. Single dose oral naproxen and naproxen sodium for acute postoperative pain. Available in The Cochrane Database of Systematic Reviews; Issue 4. Chichester: John Wiley; 2004 (accessed 24/04/06). PubMed

[10] Fricke JR, Halladay SC and Francisco CA: Efficacy and safety of naproxen sodium and ibuprofen for pain relief after oral surgery. Current Therapeutic Research 1993, 54(6):619-27.

[11] Steinbach G., et.al. The Effect of Celecoxib, a Cyclooxygenase-2 Inhibitor, in Familial Adenomatous Polyposis. The New England Journal of Medicine, 2000; 342:1946-1952.

[12] Padi, S.S.V., Kulkarni, S.K., 2004. Differential effects of naproxen and rofecoxib on the development of hypersensitivity following nerve injury in rats. Pharmacol. Biochem. Behav. 79, 349–358.

[13] Willingale, H.L., Gardiner, N.J., McLymont, N., Gible, S., Grubb, B.D., 1997. Prostanoids synthesized by cyclooxygenase isoforms in the rat spinal cord and their contribution to the development of neuronal hyperexcitability. Br. J. Pharmacol. 122, 1593–1604.

[14] Breder, C.D., Dewitt, D., Kraig, R.P., 1995. Characterization of inducible cyclooxygenase in rat brain. J. Comp. Neurol. 355, 296–315.

[15] Asanuma, M., Miyazaki, I., Ogawa, N., 2004. Neuroprotective effects of nonsteroidal anti-inflammatory drugs on neurodegenerative diseases. Curr. Pharm. Des. 10, 695–700.

[16] Black, P.H., 2002. Stress and the inflammatory response, a review of neurogenic inflammation. Brain Behav. Immun. 16, 622–653.

[17] Dhir As, Padi S.S.V., Naidu P. S., Kulkarni S. K. Protective effect of naproxen (non-selective COX-inhibitor) or rofecoxib (selective COX-2 inhibitor) on immobilization stress-inducedbehavioral and biochemical alterations in mice. European Journal of Pharmacology 535 (2006) 192–198

[18] Silakova, J.M., Hewett, J.A., Hewett, S.J., 2004. Naproxen reduces excitotoxic neurodegeneration in vivo with an extended therapeutic window. J. Pharmacol. Exp. Ther. 309, 1060–1066.

[19] Analgesics Anti-inflammatory Drugs and Antipyretics. In: Martindale, The Complete Drug Reference 32th edition. Edited by: Parfitt K. London, Pharmaceutical Press; 1999:61-62.

[20] USP 30/ NF 25. United States Pharmacopeia & National Formulary (2007) 30 ed. Rockville, United States Pharmacopeial Convention.

[21] Farmacopéia Portuguesa VII, 2° vol., Lisboa, p. 509, 2002

[22] Court H and Volans GN, "Poisoning After Overdose With Nonsteroidal Anti-inflammatory Drugs," Adverse Drug React Acute Poisoning Rev , 1984, 3(1):1-21.

[23] "Drugs for Pain," Med Lett Drugs Ther , 2000, 42(1085):73-8.

[24] Graham DY, "Prevention of Gastroduodenal Injury Induced by Chronic Nonsteroidal Anti-inflammatory Drug Therapy," Gastroenterology , 1989, 96(2 Pt 2 Suppl):675-81.

[25] Jacobi J, Fraser GL, Coursin DB, et al, "Clinical Practice Guidelines for the Sustained Use of Sedatives and Analgesics in the Critically Ill Adult," Crit Care Med , 2002, 30(1):119-41.

[26] Smolinske SC, Hall AH, Vandenberg SA, et al, "Toxic Effects of Nonsteroid Anti-inflammatory Drugs in Overdose. An Overview of

Recent Evidence on Clinical Effects and Dose-Response Relationships," Drug Saf , 1990, 5(4):252-74.

[27] Vale JA and Meredith TJ, "Acute Poisoning Due to Nonsteroidal Anti-inflammatory Drugs," Med Toxicol , 1986, 1(1):12-31.

[28]UNAIDS. AIDS epidemic update : December 2007.

[29]UNAIDS (2007). Comparing adult antenatal-clinic based HIV prevalence with prevalence from national population based surveys in sub-Saharan Africa. UNAIDS presentation. Accessed 17 November 2007 at http://data.unaids.org/pub/Presentation/2007/survey_anc_2007_en.pdf.

[30] UNAIDS Reference Group on Estimates, Modelling, and Projections (2006). Improving parameter estimation, projection methods, uncertainty estimation, and epidemic classification. Report of a meeting of the UNAIDS Reference Group on Estimates, Modelling, and Projections, Prague, Czech Republic, 29 Nov—1 Dec. http://data.unaids.org/pub/Report/2007/2006prague_report_en.pdf.

[31] UNAIDS Reference Group on Estimates, Modelling and Projections (2002). Improved methods and assumptions for the estimation of the HIV/AIDS epidemic and its impact: recommendations of the UNAIDS Reference Group on Estimates, Modelling and Projections. AIDS, 16: W1–W16.

[32] UNAIDS/WHO (2006). AIDS epidemic update: December 2006. UNAIDS, Geneva 2006. UNAIDS/06.29E. ISBN 92 9 173542 6.

[33] WHO, UNAIDS, UNICEF (2007). Towards universal access: scaling up priority HIV/AIDS interventions in the health sector: progress report. April. Geneva. ISBN 978 92 4 159539 1.

[34] WHO (2003). World health report: 2003: shaping the future. Geneva. ISBN 92 4 156243 9.

[35] De Clercq E. Anti-HIV drugs: 25 compounds approved within 25 years after the discovery of HIV. Int. J. Antimicrob. Agents (2008), doi: 10.1016/j.ijantimicag.2008.10.010.

[36] De Clercq E. Strategies in the design of antiviral drugs. Nat Rev Drug Discov, 2002; 1:13–25.

[37] Furman PA, Fyfe JA, St Clair MH, Weinhold K, Rideout JL, Freeman GA, et al. Phosphorylation of 3'-azido-3'-deoxythymidine and selective interaction of the 5'-triphosphatewithhumanimmunodeficiency virus reverse transcriptase. Proc Natl Acad Sci U S A 1986;83:8333–7.

[38] August, E. M., M. E. Marangiu, T. S. Lin, and W. H. Prusoff. 1988. Initial studies on the cellular pharmacology of 39-deoxythymidin-29-ene (d4T): a potent and selective inhibitor of human immunodeficiency virus. Biochem. Pharmacol. **33:**4419–4422.

[39] Ho, H.-T. and Hitchcock, M.J.M. (1989) Cellular pharmacology of 2',3'-dideoxy-2',3'-didehydrothymidine, a nucleoside analog active against human immunodeficiency virus. Antimicrob. Agents Chemother. 33, 844-849.

[40] Balzarini, J., Herdewijn, P. and De Clercq, E. (1989a) Differential patterns of intracellular metabolism of 2',3'-didehydro-2',3'-dideoxythymidine and 3'-azido-2',3'-dideoxythymidine, two potent anti-human immunodeficiency virus compounds. J. Biol. Chem. 264, 6127-6133.

[41] Martin, J.C., Hitchcock, M.J.M., Fridland, A., Ghazzouli, I., Kaul, S., Dunkle, L.M., Sterzycki, R.Z. and Mansuri, M.M. (1990) Comparative studies of 2',3'-didehydro-2',3'-dideoxythymidine (D4T)

with other pyrimidine nucleoside analogues. Ann. N.Y. Acad. Sci. 616, 22-28.

[42] Horwitz, J.P., Chua, J., Da Rooge, M.A., Noel, M. and Klundt, I.L. (1966) The formation of 2',3'-unsaturated pyrimidine nucleosides via a novel /3-elimination reaction. J. Org. Chem. 31, 205-211.

[43] Yarchoan, R., Mitsuya, H., Myers, C.E. and Broder, S. (1989) Clinical Pharmacology of Y-azido-2',Y-dideoxythymidine (zidovudine) and related dideoxynucleosides. New Engl. J. Med. 321,726-738.

[44] Lea A. P.; Faulds D. Stavudine: A review of its pharmacodynamic and pharmacokinetic properties and clinical potential in HIV infection. Drugs. 1996, 51, pp. 846-864.

[45] Katlama C., Valantin M., Matheron S., Coutellier A., Calvez V., Descamps D., Longuet C., Bonmarchand M., Tubiana R., De Sa M., Lancar R., Agut H., Brun-Vezinet F. and Costagliola D. Efficacy and Tolerability of Stavudine plus Lamivudine in Treatment-Naive and Treatment-Experienced Patients with HIV-1 Infection. Annals of International Medicine. (1998).129, 525-531.

[46] Griffith BP, Brett-Smith H, Kim G, Mellors JW, Chacko TM, Garner RB, et al. Effect of stavudine on human immunodeficiency virus type 1 virus load as measured by quantitative mononuclear cell culture, plasma RNA, and immune complex-dissociated antigenemia. J Infect Dis. 1996; 173:1252-5.

[47] Murray HW, Squires KE, Weiss W, Sledz S, Sacks HS, Hassett J, et al. Stavudine in patients with AIDS and AIDS-related complex: AIDS Clinical Trials Group 089. J Infect Dis. 1995; 171 Suppl 2:S123-30.

[48] Petersen EA, Ramirez-Ronda CH, Hardy WD, Schwartz R, Sacks HS, Follansbee S, et al. Dose-related activity of stavudine in patients

infected with human immunodeficiency virus. J Infect Dis. 1995; 171 Suppl 2:S131-9.

[49] Merrill DP, Moonis M, Chou TC, Hirsch MS. Lamivudine or stavudine in two- and three-drug combinations against human immunodeficiency virus type 1 replication in vitro. J Infect Dis. 1996; 173:355-64.

[50] USP 30/ NF 25. United States Pharmacopeia & National Formulary (2007) 30 ed. Rockville, United States Pharmacopeial Convention.

[51] Britsh Pharmacopoeia. The Stationery Office on behalf of the Medicines and Healthcare products Regulatory Agency. CD-ROM version 11.0, London

CAPÍTULO 1

1. REVISÃO SÍLICA

Publicação científica - Pereira R. N., Murakami F.S., Valente B. R., Rodrigues P.O, Matos R. J., Mercuri L. P., Silva M. A. S.

A ser submetido - Microporous and Mesoporous Materials.

MESOPOROUS MATERIALS: A REVIEW OF THE CHARACTERISTICS AND APPLICABILITY IN PHARMACEUTICAL SCIENCES

Pereira R. N.[1], Murakami F.S.[1], Valente B. R.[1], Rodrigues P.O[1], Matos R. J.[2], Mercuri L. P.[3], Silva M. A. S .[1]

[1]*Universidade Federal de Santa Catarina, Laboratório de Controle de Qualidade, Campus Universitário Trindade, 88.040-900, Florianópolis, Brazil.*

[2]*Universidade de São Paulo - Instituto de Química da Universidade de São Paulo. Av. Lineu Prestes, 748 – Laboratório de Análise Térmica Prof. Dr. Ivo Giolito. Butantã. 05508-900 - São Paulo, SP – Brazil.*

[3]*Universidade Federal de São Paulo – Departamento de Ciências Exatas e da Terra -Campus Diadema, Av. Arthur Ridel, 275 - Bairro Eldorado, 09972-270, Diadema - SP-Brazil.*

[1] **e-mail:** *rafael_nicolay@yahoo.com.br*

ABSTRACT

Mesoporous silica materials have been received much attention due to their attractive features such as stable mesoporous structure, high surface area (up to 1500 m^2/g), large pore volume (up to 1.2 cm^3/g), regular and adjustable nano-pore sizes (2–10 nm) and a hydrophilic surface character. Recently, a new application of mesoporous silica as a drug delivery system has been explored due to their non toxic nature and good biocompatibility. SBA-15 is an ordered mesoporous silica with a large surface area, uniform hexagonal channels and remarkable hydrothermal stability. For this reason, SBA-15 is a potential candidate for drug delivery systems since its pore size is easily controlled

according to the synthesis conditions and the presence of swelling agents. The aim of this work is to review mesoporous materials (designated OMS), especially SBA-15, including characteristics and applicability in pharmaceutical sciences.

Keywords: OMS's, SBA-15, applicability, drug release.

1. INTRODUCTION

The first report about the synthesis of a new zeolite that didn't have a natural counterpart was described in 1948 and only after the 1950's the zeolite synthesis technology was introduced in large scale. Additionally, the first natural zeolite was discovered in 1956 and since than efforts has been made in order to synthesize new zeolites **(1)**.

In the early 1990's, a family of highly ordered mesoporous silicates M41S materials was firstly reported by scientists from Mobil Oil Research and Development. These mesoporous silicates with highly ordered structures (similar to those for the liquid crystals), narrow pore size distribution (from 1.5–40 nm) and ultrahigh surface area (800–2000 m^2/g) have been attracting much attention of the materials community due to their potential applications in the separation of large molecules, drug delivery, sensors and devices **(2-4)**.

The discovery of ordered mesoporous silicas by Mobil scientists opened a new realm of materials sciences **(5-10)**. After the discovery of MCM (Mobil Composition of Matter) 41, the first mesoporous solid synthesized that showed a regularly ordered pore arrangement and a very narrow pore-size distribution., the studies were focused on the following main subjects: (1) the characterization; (2) the mechanisms of

formation; (3) the synthesis of new materials based on the MCM-41 synthesis concept; (4) the morphology control; and (5) the technical applications of MCM-41 and related mesoporous materials **(11,12).** After that, the ordered mesoporous materials synthesis were used as a new approach in several research areas such as catalysis, biosensors, separation and drug delivery systems mainly because of their special characteristics, high surface area and narrow pore size distribution in wide mesoporous region (2–50 nm) **(4)**.

According to the IUPAC definition, porous materials are divided into three classes: microporous (< 2 nm), mesoporous (2-50 nm) and macroporous (> 50 nm). Well-known members of the microporous class are the zeolites which provide excellent aluminosilicate network. Larger pores are present in porous glasses and porous gels, which were known as mesoporous materials at the time of the discovery of MCM-41. However, they show disordered pore system with broad pore-size distributions **(4,13,14).**

This OMS's (2 nm < pore size < 50 nm), have attracted much attention because of their emerging applications in drug delivery. The majority of ordered mesoporous materials have a two dimensionally ordered array of cylindrical pores of uniform size disposed parallel to each other and separated by thin walls. MCM-41 (Mobil Composition of Matter number forty one) and SBA-15 (Santa Barbara Amorphous number fifteen) probably are the most investigated materials of this class **(15,16).**

In 1998, Zhao et al. synthesized a new type of mesoporous material called SBA-15 with uniform two-dimensional hexagonal structure. Compared with microporous zeolites, this material is

characterized by larger pore sizes up to approximately 30 nm and allows bulky molecules to enter into the pores. It has higher hydrothermal stability and thicker pore wall (3.1 – 6.4 nm) compared with mesoporous MCM-41 materials. For these reasons, SBA-15 is presented as a potential material to be used as a versatile catalyst and/or catalytic support for conversion of large molecules **(17,18).**

2. INTERFACE CHARACTERISTICS OF SILICA

The interface involving silica surface plays an important role in the adsorption process. The surface characteristics of the adsorbate determine the nature of the union between adsorbate and adsorbent. Different techniques are in use in order to characterize the surface of the adsorbents **(19).** For example, to investigate the behaviour of porous silica coated with siloxane polymers, nitrogen adsorption technique was used to evaluate surface area and porosity of the silica and the polymer coated silica; also, the high-resolution thermogravimetric technique was used to study the thermal behaviour of silica. It was found that the interactions between the silica and the polymer rendered a uniform layer of siloxane polymer on silica surface **(20).**

3. CHARACTERIZATION OF MESOPOROUS MATERIALS

3.1 IR Characteristics of Silica Surface

FTIR (Fourier Transform Infrared) is known to provide surface information of materials for the identification of chemical groups **(18).** IR spectra have been used to characterize divided silica in the region of 3200–3800 cm^{-1} corresponding to νOH stretching mode of silanols**.** A broad band appears around 3530 cm^{-1} due to the hydrogen-bonded

silanol. The advent of another band around 3715 cm^{-1} suggests the presence of terminal (isolated) silanols which behave as proton acceptors and have their own free protons for additional hydrogen bonds **(19, 21-31).** However it is difficult to differentiate between single (isolated) and geminal silanols because their properties are almost similar **(19, 23).** Exchange studies with heavy water show that some silanols, called internal silanol, are not accessible to water molecules. These groups absorb in the range of 3650–3670 cm^{-1} **(19).**

Rochester & Trebilco, 1979 (32) studied the IR spectral characteristics of silica surface by using a suitable designed optical compartment. To avoid the interaction of water with the silanol groups, the spectra were run in presence of non polar solvents just after heat treatment (423–1023 K) of the silica. The 3750 cm^{-1} band due to OH stretching vibration was found to shift to 3705 cm^{-1} when preheated (873 K) silica was immersed in heptane or 2,2,4- trimethyl pentane. The magnitude of shifting, however, was found to vary for different liquids and thus it can be a measure of the strength of the interaction between isolated silica surface OH groups and organic molecules present at the silica surface. When silica was heated at 423 K and cooled to room temperature it exhibited a broad spectrum with maximum absorption at 3535 cm^{-1}. The band was attributed to lateral hydrogen bonding interactions of adjacent silanols. When silica was immersed in 2,2,4-trimethyl pentane, the absorption band shifted to 3490 cm^{-1} indicating that the lateral hydrogen bonding was sustained. Also, **Jal et al., 2004 (33)** synthesized nanosilica and compared the IR spectral characteristics of the silica with the earlier reported data **(Table 1).** They observed

spectral characteristics indicanting the presence of molecular water adsorbed on the silica surface.

Additionally, the FTIR spectroscopy technique was used by **McCool & Lawrence, 2006 (34)** to estimate the surface area of porous and non-porous silica powders by comparing the integrated area of the band due to isolated silanol groups on different silica**.** Using fumed silica as a calibrant, an accuracy of around 7% in the surface area of several silica materials was obtained when compared to the surface area computed by BET (Braunaver/Emmet/Teller) nitrogen adsorption techniques. Considering structural parameters, charge distribution, force field and other features, the Si–OH and Si–OD stretching and bending vibrations were determined theoretically by **Carteret, 2006 (35).** The values were reported to be in the range of 790–1030 cm^{-1} for Si–OH and 790–1010 cm^{-1} for Si–OD.

Table 1 - IR spectral characteristics of the silica with the earlier reported data. Adapted from ref. **36 – 56.**

Frequency ***(cm^{-1})***	***Position assignment***	***Values reported ealier***
462	***Si-O* bond rockig**	**465-475**
800	***O-H* bending (silanol)**	**800-870**
970-980	***Si-OH* bond stretching**	**935-980**
1102	**Asymmetric *Si-O-Si* stretching in SiO_4 tetrahedron**	**1050-1150**
1630	***O-H* bending (molecular water)**	**1625**
3000-4000	***O-H* stretching and adsorbed water**	**3000-3800**
3755	***O-H* stretching**	**3740-3750**

3.2 Adsorption Isotherm

The surface area of a powder sample can be computed using the particle size distribution, which can be obtained through one of the methods outlined previously. Two methods are commonly available that permit direct calculation of the surface area. In the first method, the quantity of a gas or liquid solute that is adsorbed onto the sample of powder to form a monolayer is a direct function of the surface area of the sample. The second method depends on the rate at which a gas or liquid permeates a layer of powder and this is related, among other factors, to the surface area exposed to the permeant **(57).**

Particles with a large and specific area are considered good adsorbents for the adsorption of gases and solutes from a solution. After the determination of the adsorbent surface, the volume in cubic centimeters of the gas adsorbed per gram of adsorbent may be plotted against the pressure of the gas at constant temperature to give a type II isotherm **(57).** Considering the pressure effect, the adsorbed layer is monomolecular at low pressure and becomes multimolecular at higher pressures **(57).**

On the other hand, the adsorption phenomenon at the solid/liquid interface involves the change in concentration of the solution. Adsorption isotherm is constructed by measuring the concentration of the adsorbate in the medium before and after adsorption, at a fixed temperature. This is generally used to study the interaction between the adsorbate and the surface of the adsorbent and to know about the structure of the adsorbed layer **(57).**

3.3 Thermalanalytical Studies

Thermoanalysis has been used for the rapid evaluation of purity, kinetics decomposition and physical properties of drugs. Moreover, this technique provided an alert for compatibility problems and indicated the most favorable directions to follow in order to get a successful formulation.

The most widely used thermoanalytical techniques are differential scanning calorimetry (DSC) and thermogravimetry/derivate thermogravimetry (TG/DTG). In these techniques, a physical property of a substance and/or its reaction products is measured as a function of a controlled temperature program **(58-63).**

In the mesoporous materials field, the amount of drug present in its crystalline form in the pores of the mesoporous material can be distinguished and estimated from a melting point depression using DSC. If the compound in the pores is in a non crystalline state, the melting point depression cannot be detected. However, the amount of the crystalline drug on the surface of the microparticles can still be quantified **(64,65).**

The overall amount of loaded drug can also be quantified with TG. In the TG measurement, the drug is desorbed after decomposing, which is detected as a temperature-dependent weight decrease. If the drug substance reacts with the microparticles after decomposing, the TG measurements can give underestimated drug loading values. Nevertheless, together with the other three quantification methods described above, TG is an important and powerful tool to analyze the drug loadings reliably **(64,65).**

3.4 Zeta Potential

Zeta potential is a measure of the magnitude of the repulsion or attraction between particles. Its measurement brings detailed insights about the dispersion mechanism and it is the key to the electrostatic dispersion control. The measurement of zeta potential is an extremely important parameter across a wide range of industries including brewing, ceramics, pharmaceuticals, medicine, mineral processing and water treatment **(66).**

When a new suspension or emulsion is formulated, the measurement of the stability of the candidate formulations in a variety of conditions represents one of the biggest consumers of time. Zeta potential can be used to test candidate formulations to reject inappropriate ones at early stages reducing the costs of the stability study. This can also lead to an understanding of the mechanisms of stability, and thus helping with the research into product quality improvements **(66).** For this reason, zeta potential can be used to evaluate the interaction of mesoporous materials with drugs. When the zeta potential is largely positive or negative, the size of particles is sub-micron and the colloidal suspension is stable. On the contrary, in the composition region where the particle charge is close to neutrality, the colloidal suspension is settled due to the increase in size of aggregated particles **(67, 68).**

Xu et.al, 2003 (69), studied the surface charge properties and dispersion stability of aqueous silica suspensions. To do this, the zeta potential was measured versus barium acetate and zinc acetate concentration, at pH 6.0. Also, EDTA was used to chelate the bivalent metal ions, so that the charge of counterion was reduced. They observed

that the complexation of bivalent counterions favors the increase of the negative zeta potential and the dispersion stability of aqueous silica suspension **(69).**

In general, the zeta potential is an important factor controlling the dispersion stability of silica suspensions, which results in the existence of an energy barrier preventing the proximity of the particles. According to the DLVO theory, the energy barrier arises as a result of the electrical double layer force and the Van der Waals forces. The magnitude of zeta potential describes the height of the energy barrier. A minimum of surface charge is needed for the dispersion of powders in aqueous suspension. If an electrolyte is added to a colloidal suspension, this will cause marked compression of the electrical double layer around the silica particles and the reduction of surface charge **(69, 70).**

Surface charge properties of silica powder in aqueous suspensions were determined in terms of the zeta potential using electrophoresis technique. **Figure 1** shows a diagram of typical zeta potential versus pH value obtained for the silica powder in the absence of any additives. It is readily apparent that exist an intimate relation between zeta potential and pH. The isoelectric point (IEP) of the powder is at about pH 1.70 **(69)**. There are some differences with the results from other researchers **(71).** This may arise from the difference in production, store, and surface properties of the silica powder. The powder surface is negatively charged in a wide pH range. The farther the pH is from isoelectric point, the greater is the absolute value of the zeta potential. The surface charge of silica comes from the dissociation of the silanol groups, so in this case the pH controls the zeta potential of silica powder through the process described by Xu et al., 2003 **(69)**.

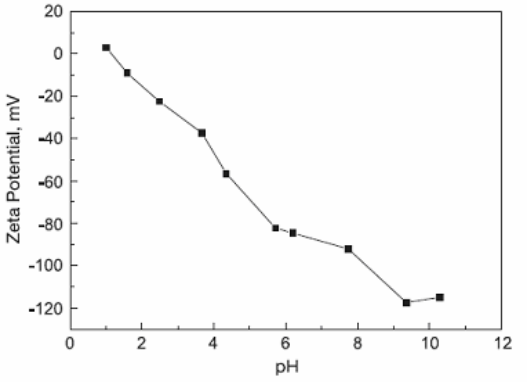

Figure 1 – Zeta potential of silica powder as a function of pH. Adapted from ref. **69.**

3.5 DRX (X-ray Diffraction)

The X-ray diffraction method has been used in order to characterize the formation of hexagonal mesostructured materials. Small-angle X-ray scattering/X-ray diffraction is the best technique for studying micellar structures and shapes having short- and long-range order. Short acquisition times and an adaptable experimental setup have made it the most-used technique in time-resolved and even temperature-resolved *in situ* experiments. Nevertheless, the acquisition times required when using low-flux X-ray sources are not compatible with the requirements for time-resolved measurements. Hence, SAXS/XRD experiments must be performed using a high-flux X-ray source such as synchrotron radiation, making this type of experiment quite expensive and difficult to access **(72).**

Beck et.al, 1992 (6), studied MCM-41 X-ray diffraction. The exact structural nature of the silicate/aluminosilicate framework in the

pore walls of these materials is uncertain. However, the presence of distinct reflections in the X-ray diffraction data suggests a framework with long range regularity. The ***hkO*** reflections can be indexed on a hexagonal lattice, but the observation of only ***hkO*** reflections in the experimental diffraction data **(Figure 2)** is unusual for material ordered in three dimensions **(6).**

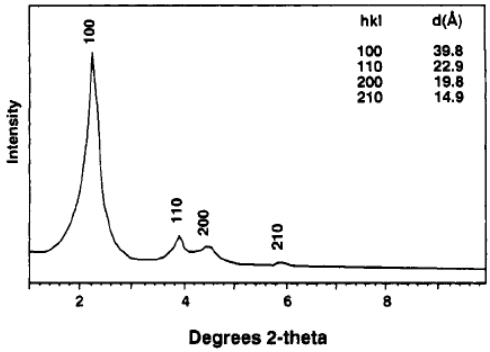

Figure 2. Powder X-ray diffraction pattern of calcined MCM-41. Adpated from **(6).**

In other work, **Aburto et.al, 2005 (73)**, studied SBA-16 mesoporous materials and used X-ray diffraction (XRD) to characterize this material. The X-ray diffraction (XRD) pattern of the parent material (SBA-16 40 A˚, **Figure 3**) shows three well-resolved peaks with lattice spacings of 112.6, 79.6, and 65 A˚, respectively. These values can be indexed as 110, 200, and 211 diffractions associated with cubic symmetry and a lattice constant (a) of 158.8 A˚ corresponding to SBA-16 **(73).**

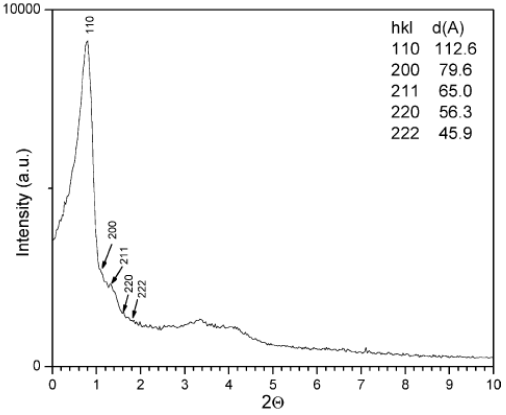

Figure 3 - X-ray diffraction pattern of a SBA-16 mesoporous material with a 40 A˚ pore size. Adpated from ref. **73**.

3.6 Scanning Electron Microscopy (SEM)

Scanning Electron Microscopy (SEM) can provide a high resolution image of a surface in three dimensions (topography), but the bulk of the specimen is not imaged. On the other hand, Transmission Electron Microscopy (TEM) does give high-resolution information of a sample, but the three-dimensional information is projected into a 2D image and the information in third dimension is lost. Nowadays, there are several electron microscopic techniques that can characterize intact materials in three-dimensions with nanometer scale resolution, however, some of them have become available to scientific materials only recently **(74, 75).**

Characterization of mesopores is mostly performed using nitrogen physiosorption and electron microscopy. In **Figure 4a,** a series of electron microscopy images of SIL-SIO_2 are given, which were obtained with SEM and TEM. The backscattered electron (BE) image in **figure**

4a shows many large zeolite particles sticking out of amorphous carbon agglomerate. In **figure 4b** a secondary electron (SE) image of one of these zeolite crystals is shown. From this image it is clear that there is partial contact between the carbon and the zeolite crystal. In **figure 4c** the SE image gives a closer look at the interface between the carbon and the zeolite crystal. **Figure 4d** a SE image is given which shows the zeolite crystals after the carbon has beeen burned away **(76).**

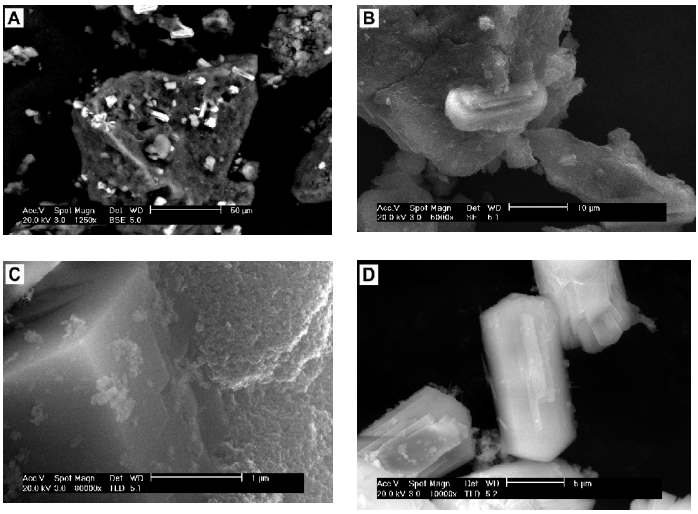

Figure 4 – Electron microscopy of SIL-SIO_2 with the carbon matrix present (a-c) and after burning off the carbon matrix (d); (a) Backscattered Electrons image (SEM), (b-d) Secondary Electrons image (SEM). Adapted from ref. **76**.

Yang & Zhao, 2005 (77) studied morphology control of mesoporous materials. By using SBA-15 nanorods with uniform lengths and highly ordered hexagonal mesostructures as templates, they have

synthesized OMCs with the same rod-like morphology **(Figure 5).** The SEM shown rods feature well-ordered mesostructured arrays, large pore sizes (up to 5.8 nm) and surface areas exceeding 1800 $m^2.g^{-1}$. Also showed the comparison of images obtained by SEM and TEM, these materials mesopores **(77).**

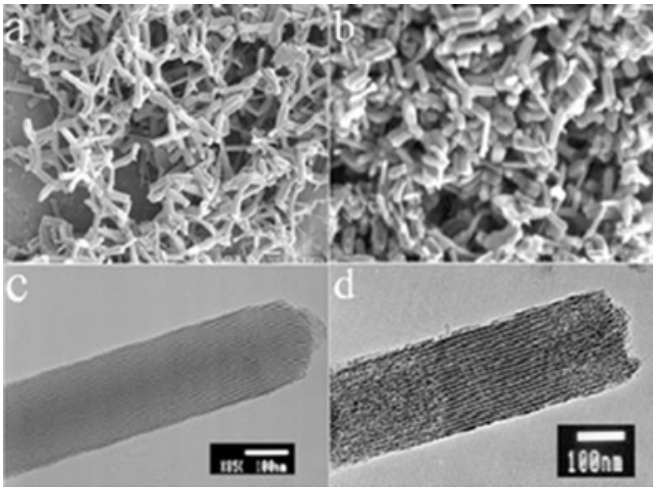

Figure 5 - a) SEM image and c) TEM image of calcined SBA-15 nanorods. b) SEM image and d) TEM image of mesoporous carbon nanorods replicated by using SBA-15 silica rods as templates. Adapted from ref. **77**.

4. APPLICABILITY IN PHARMACEUTICAL SCIENCES

The application of nanotechnology in biomedical research carries tremendous potential for drug administration. While most of the research has been focused on diagnostic systems the interest in microdevices for therapeutic applications has also increased significantly **(78, 22, 79, 80, 65).**

Initially, therapeutic applications of silicon based systems were directed towards implanted devices **(81, 82, 65, 83, 84, 24, 25)** with other administration routes, such as oral delivery **(85, 65, 26).** Recent reports on the advantages of mesoporous materials as drug delivery vehicles have encouraged research in novel applications, supporting also conventional dosage forms, and several potential materials for this purpose have been reported **(86, 87, 88, 89, 65).**

Main efforts in the studies of mesoporous materials as drug delivery vehicles have been focused on sustained/controlled drug release **(87, 88, 89, 65, 26).** The potential of mesoporous materials to improve the permeability of large, hydrophilic drug substances has also been explored in combination with classical permeation enhancers **(86, 65, 26).** Further, mesoporous materials offer a potential mean to increase the dissolution of poorly soluble drugs through effects on surface area or crystallinity.

At pore sizes only a few times larger than the drug molecule, the formation of crystalline material is restricted by the confined space of the pores, thus retaining the drug in its noncrystalline, amorphous form. The amorphous form is known to exhibit higher dissolution rates than the crystalline phase, especially when solubility is limited by high crystal energy **(90, 65, 91).** Drug delivery strategies providing the potential to tailor the physical state of a compound will be of increasing importance in drug development, since it is estimated that 40% of potential lead candidates suffer from poor solubility, a great part of which may be related to high crystal energy **(92, 65, 93).**

Porous silicon (PSi) has some advantages compared to synthesised mesoporous materials when drug delivery vehicles are

considered. The fabrication of PSi is a simple procedure, where the porosity and pore size can easily be tuned by anodization parameters **(65, 94, 95).** Depending on the morphology, PSi could be tailored as a biodegradable, bioactive or stable material **(96, 97, 65, 93, 95).** In addition, the chemistry surface of PSi can easily be modified to produce favourable surfaces for drug adsorption **(83, 32, 98, 99, 65).**

Salonen et al, 2005 (65), in their work, used five model drugs, antipyrine, ibuprofen, griseofulvin, ranitidine and furosemide, to study drug loading into the microparticles and subsequent drug release behaviour. The compounds were chosen to represent a wide range of solubilities with additional differences in acid/base character and lipophilicity, while also representing drugs of different biopharmaceutical classification (BCS) **(65, 100).** The dissolution was studied at the pH-values 5.5, 6.8 and 7.4 representative of different parts of the small intestine. The **Table 2** shows drug loading utilizing different methods.

Table 2 – Degrees of drug loading (%, w/w) determined from TCPSi microparticles utilizing different methodsm. Adapted from ref. 65.

Drug	TG	Pycno metry	N_2 sorption	Average load[a]	HPLC	DSC[b]
Antipiryne	54.1	52.7	-	53.4	44.5	14.5
Ibuprofen	30.8	33.0	27.4	30.4	28.2	0.2
Griseofulvin	12.5	20.5	-	16.5	12.4	0.25
Ranitidine HCl	10.3	11.8	17.5	13.2	8.8	[c]
Furosemide	43.0	39.6	41.2	41.3	39.1	0.0

[a] Average load a mean value of TG, pycnometry and N_2 sorption results.

[b] Crystallised substance found on the surface of the micropaticles.

[c] Decomposition during melting.

The surface properties form an essential aspect in the design of porous silicon particles to be used in drug delivery. The currently used types of surface treatments, thermal carbonization (TCPSi) and thermal oxidation (TOPSi) showed that in addition to the effects regarding the stability of the particles in the presence of aqueous or organic solvents, surface properties significantly affect compound affinity towards the particle. In addition to the surface properties, the chemical nature of the drug and the loading solution seem to be critical to the loading process. This is reflected in the obtained loading efficiencies, which varied between 9% and 45% with TCPSi particles. The most inadequate method was found to be the N_2 sorption method, which is a commonly used method in these kinds of studies. The release rate of a loaded drug was found to depend on the characteristic dissolution behaviour of the drug substance. When the dissolution rate of the unloaded drug was high, the microparticles caused a slightly delayed release. However, with poorly dissolving drugs, the loading into the mesoporous microparticles clearly improved the dissolution. In addition, pH dependency of the dissolution was reduced when the drug substance was loaded into the microparticles **(65).**

Physical Characterization of Microparticles and Determination of Drug Load

Drug delivery strategies providing the potential to tailor the physical state of a compound will be of increasing importance in drug development, since it is estimated that 40% of potential lead candidates

suffer from poor solubility, a great part of which may be related to high crystal energy **(65).**

The samples were characterised with thermogravimetry (TGA 7, N_2 gas purge), differential scanning calorimetry (DSC; N_2 gas purge), helium pycnometry and N_2 ad/desorption studies. The pore size distributions were calculated from the N_2 desorption values on the basis of density functional theory. The X-ray diffraction (XRD) measurements were performed on a Bragg– Brentano h/2h reflection geometry **(65).** Isothermal microcalorimetry (IMC) measurements were performed in closed glass ampoules. The details about the characterization methods have been reported recently **(65, 101).** Particle size distributions were determined with a laser diffractometer.

TG, DSC, helium pycnometry and N_2 adsorption were used in the quantification of all the drug loadings and XRD when needed. The wide variety of the methods is important, not only to obtain reliable results, but also to distinguish the drug in the pores from that on the surface of the particles and to verify the physical state of the drug loaded into the pores. Since the helium pycnometry and N_2 adsorption methods (BET and BJH) apply gas penetration in the measurement, severely erroneous results could be obtained if the drug substance remains on the surface of the microparticles and blocks the pores preventing the gas penetration into the pores. When in its crystalline form in the pores, the amount of drug can be distinguished and estimated from a melting point depression using DSC. If the compound in the pores is in a non crystalline state, the melting point depression cannot be detected **(65, 101).** However, the amount of the crystalline drug on the surface of the microparticles can still be quantified.

The overall amount of loaded drug can also be quantified with TG. In the TG measurement, the drug desorbs after decomposing, which is detected as a temperature-dependent weight decrease. Unfortunately, if the drug substance reacts with the microparticles after decomposing, the TG measurements could give underestimated drug loading values. In other work, **Vallet-Regi et al, 2001 (102)**, explored a new potential property of MCM-41, its capability of acting as a convenient reservoir for controlled drug delivery systems. Their group introduced ibuprofen into two MCM-41 materials with different pore sizes and subsequently the *in vitro* drug release process in a simulated body fluid was studied. This mesoporous material (MCM-41) was characterized by XRD and N_2 adsorption techniques. Two procedures were used to charge the material with ibuprofen:

In method 1 the drug was dissolved in hexane and the extracted MCM-41 sample was added, stirring for 24 h and preventing the evaporation of hexane. A UV spectrophotometer was used to control the amount of ibuprofen absorbed by the sample at 273 nm. That amount was determined by UV spectrometry and thermogravimetry, resulting, in both cases, in 30 wt % with respect to the powdered starting material. *In method 2* the initial powder without drug was pressed at the same conditions as described below. The disks were soaked in a solution of ibuprofen in hexane for 3 days. The absorption process is slower in this case, but it reached the same ratio in weight (30%) **(102).**

The release profile was obtained by soaking the samples in 90 mL of a simulated body fluid, SBF (1 mg of ibuprofen of the sample per mL of fluid), and measuring the drug concentration in the fluid by a UV-VIS spectrophotometer. Every sample (either powder or disk) was

characterized by XRD, Thermogravimetry, and N_2 adsorption. The thermogravimetric analyses (TGA) were carried out between 30 and 900 °C in air (flow rate 100 $mL.min^{-1}$ with a heating rate of 10 °C/min). The surface area and pore size of the material were determined by N_2 adsorption. Additionaly, the effective uptake of ibuprofen by the mesoporous materials when immersed into the hexane solution of the drug can be monitored by TG, which indicates a maximum of 30 wt % of ibuprofen. Indeed, the mesopore filling with ibuprofen molecules can be assessed by N_2 adsorption **(102).**

As proposed by the different behaviors of the material when the ibuprofen was introduced before or after the conformation could be explained by assuming that when the powdered material is charged with ibuprofen, the compression of the drug-matrix mixture leads to a decrease of pore size and, eventually, to a narrowing or closing of the pore cavity. This could induce a slow or even incomplete release of ibuprofen due to diffusion constraints. Nevertheless, if the starting MCM-41 material is compacted before ibuprofen loading, the uptake and release of the ibuprofen would take place following the same unrestricted diffusion pathway through the mesopore network **(102)**. This preliminary study demonstrated the feasibility of designing reliable drug delivery systems by appropriate choice of the matrix and the organic molecule.

Furthermore, **Horcajada et al, 2004 (103)** have studied the influence of the pore diameter of MCM-41 matrices covering a wide range of sizes in the *in vitro* releasing profile of the drug under stirring conditions. In order to do that, they have performed the synthesis of small pore size MCM-41 samples, from gels containing mixtures of

octyl and decyltrimethylammonium cations. Once achieved the synthesis of MCM-41, a comparative study of ibuprofen release in ordered mesoporous materials was executed between materials obtained from surfactants with 16, 12 and 8 atoms of carbon, where pore size ranges between 3.6 and 2.5 nm. Ibuprofen was adsorbed from a hexane solution as already reported for **Vallet-Regí et al. 2001 (102),** and the amount adsorbed and delivered was monitored by UV spectrometry, thermogravimetry (TG) and elemental analysis. The release profile was obtained by soaking the samples in a solution simulating body fluid composition (SBF), maintaining the ratio ml SBF/mg IBU adsorbed equal to 1. The SBF solution was kept at 37 ^{o}C and pH was regulated at 7.3–7.4. The *in vitro* assays were carried out by soaking the disks, mounted vertically in a special platinum scaffold, into the SBF solution in polyethylene containers maintained at 37 ^{o}C. The samples were characterized by XRD, TG, chemical analysis and N_2 adsorption. As observed by XRD patterns of MCM-41 synthesised materials **(Figure 6)** showed a characteristic intense low angle reflection, which should correspond to the (100) reflection. The (110) and (200) reflections were not distinguishable, as it is usually observed for MCM-41 samples prepared from surfactants having short hydrocarbon chain.

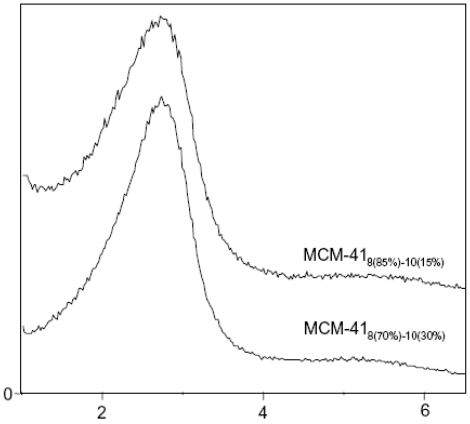

Figure 6 – XRD patterns of calcined MCM-41. Adapted from ref. **102**.

Also, **Figure 7** shows the nitrogen isotherms for MCM-41 and the pore size distribution, whereas BET surface areas and pore volumes are collected in Table 1.

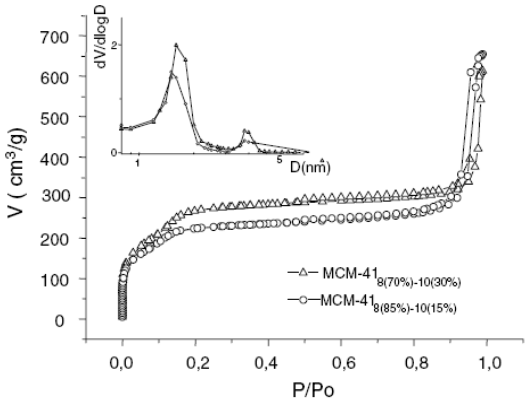

Figure 7 - Nitrogen isotherms and pore size distribution of calcined MCM-418. Adapted from ref. **102**

As it can be observed in **Table 3**, the pore volumes for both samples are higher than those previously reported for MCM-41 materials synthesised from C8 surfactant **(104, 103).**

Table 3 – Characterization of MCM-41 calcined samples. Adapted from ref. **103**.

	***d*(100) (nm)**	**α_o (nm)**	***Dp* - (nm)**	**S_{BET} (m^2/g)**	***Vp*** **(cm^3/g)**	***Vp*** **$_{(p/po=0.5)}$ (cm^3/g)**
MCM-41 16	3.9	4.42	3.6	1157	0.98	0.84
MCM-41 12	3.65	3.84	3.3	1087	0.85	0.67
MCM-41 8(70%)-10(30%)	3.4	3.9	2.7	936	0.95	0.44
MCM-41 8(85%)-10(15%)	3.4	3.9	2.5	768	1.012	0.37

The isotherms show the characteristic pore filling step of structural pores, which is essentially completed at p=p0 of ca. 0.2. The stepped increase of nitrogen adsorbed at p=p0 above ca. 0.90 can be attributed to the capillary condensation in interparticulate secondary pores [5]. As it can be observed in Table 1, the pore volumes for both samples are higher than those previously reported for MCM-41 materials synthesised from C8 surfactant **(103).**

However, this difference seems to be due basically to the abundant interparticulate porosity, as it can be observed when the volume for p=p0 ¼ 0:5 is calculated (Table 1). Besides, the unit cell is larger than that of other C8-derived materials [5,7], which suggests that a mixed micelle containing both C8 and C10 surfactants is playing the

structure directing role in the assembling process leading to these materials **(103).**

Table 4 shows the results of ibuprofen content and delivery from different pore sized MCM-41 materials**.**

Table 4 – Results of ibuprofen content and delivery from different pore size MCM-41 materials. Adapted from ref. **103**.

	Mg IBU/g	% wt IBU	*Vp*[a] *(m^3/g)*	mg IBU/g (24h)	*t* (h)[b]	*K* (mg/g $h^{1/2}$)
MCM-41_{16}	337	34	0.42	207	48	61.0
MCM-41_{12}	233	23	0.45	114	48	37.0
MCM-41 8(70%)-10(30%)	150	19	0.37	63	55[c]	13.7
MCM-41 8(85%)-10(15%)	106	11	0.41	43	55[c]	10.0

[a] Total pore volume after ibuprofen adsorption.

[b] Time required for complete liberation.

[c] Delivery not completed.

Comparing these results with those obtained for MCM-41 synthesised from surfactants containing hydrocarbon chains of 12 and 16 atoms of carbon, there is a clear tendency to adsorb less amount of drug as the carbon chain length decreases (Table 4) **(103).**

Moreover, after 24 h of assay, the quantities of ibuprofen delivered to the media by the samples with the biggest and the smallest pore size are different by a factor of five, Table 4. Therefore, a dosage of this drug as a function of the pore size of the MCM-41 host can be

afforded, and hence also the amount of drug delivered to the media at targeted times can be controlled **(103).**

Ibuprofen was introduced in both materials, in order to study the influence of pore size in drug adsorption. This approach was carried out as previously reported **(102, 103)** and the quantities of ibuprofen adsorbed were measured by TG and elemental analysis. The main conclusions about this study are that the amount of ibuprofen adsorbed from a hexane solution is directly related with the pore size, and a close packing of ibuprofen molecules inside the channels have been found only for MCM-41 materials with pore size larger than 2.7 nm.

Comparatively, in a study with SBA-15, **Doadrio et al, 2004 (88)** developed a mesoporous silica formulation for the controlled release of drug substances using gentamicin sulphate as a model drug. In addition, a new method based on the use of a HPLC methodology for gentamicin release measurements was proposed in the same work.

This new HPLC method is simpler and more effective than the HPLC standardized method **(88, 104)** which is based in a colorimetric method. Considering the new HPLC method, two objectives were achieved: to use a simple methodology with a low volume of sample and to reduce the time of analysis. In order to evaluate the delivery process, two different procedures were adopted: *In method 1*, the gentamicin sulphate was dissolved in water and the calcined SBA-15 powder was added over a period of 3 days at room temperature with stirring. The saturated solution of the drug was used. *In method 2*, the calcined powders were conformed in 0.1 g disk (13x3 mm) by uniaxial (2.75 MPa) and isostatic pressure (3 MPa) **(88).** For both methods, the powder and disk were soaked in a gentamicin sulphate solution in water at pH =

7 by addition of NaOH 4% (30 mg/ml, drug/solid = 6:1) for 3 days. The release profile was obtained by soaking the two drug-loaded SBA-15 samples, SBA-15- GP (in powder) and SBA-15-GD (in disk), in 40 ml of a simulated body fluid (SBF) at 37 ^{o}C under stirring **(88, 105)**.

The gentamicin concentration in the solution was measured through a HPLC system. All the samples were characterized by XRD and N_2 adsorption. Also, the surface area and pore size of the material were determinated by N_2 adsorption. The experiments have shown that the pH of the solution affects significantly the drug adsorption into the SBA-15 pores. The pH of the solution must be raised to 7 upon NaOH addition to favor a maximum amount of drug adsorbed (20% wt for SBA-15), while without change the original pH solution, the maximum drug adsorption is about 6 wt.%. In addition, the SBA-15-G presents similar N_2 adsorption isotherms to that from SBA-15 material. However, the overall N_2 adsorption amounts decrease for all relative pressures, indicating the presence of the drug adsorbed at the SBA-15 network **(88).**

The gentamicin was released out of the structure of SBA-15 during 48 h just upon immersion into solution. Chromatograms from gentamicin liberation showed one peak, at retention time of 1.1 min, indicated in **Figure 8**. Chromatogram from gentamicin standard solution showed the same peak at 1.1 min. Additionally, two peaks due to impurities appeared at 7.4–7.6 min. The peaks at 1.1 min were identified by UV spectra, with absorption maxima at 358 and 275 nm **(see Figure 8B)**, as much in the gentamicin standard as in the gentamicin release. The chromatographic peaks of gentamicin were also identified by

comparing the UV spectra from the HPLC Diode Array Detector with the gentamicin standard spectrum obtained from the UV–VIS conventional detector **(88).**

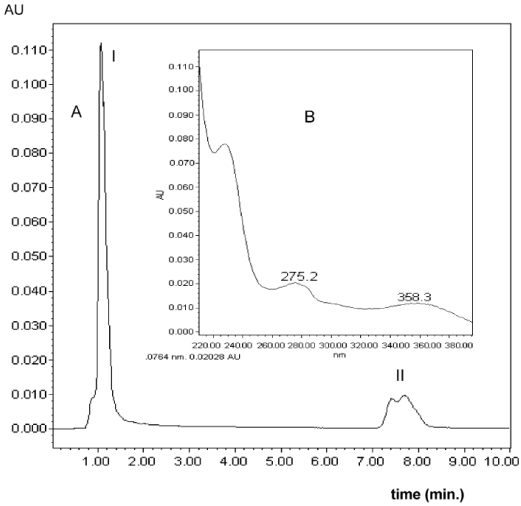

Figure 8 - (A) Chromatogram of gentamicin released in SBF at T=37 jC and 1 h of liberation. I: Gentamicin. tr = 1.1 min. II: Impurities. tr = 7.4–7.6 min. (B) UV spectrum. Adapted from ref. **88**.

The kinetics release of the drug was studied as a function of time and the results are shown in **Figure 10** for the SBA-15-GP and SBA-15-GD systems. As it can be observed, both systems presented a similar drug release profile. The release profiles exhibited a pronounced initial burst release effect of 60% (under 1 h), followed by a very slow release pattern. The initial burst is attributed to the immediate dissolution and release of the portion of the drug located on and near the surface of the disks. Indeed, the release rate from different systems achieves t80% values (release time of 80% of drug) of 2.5 and 7 h for the SBA-15-GP

and SBA-15-GD systems, respectively. Both of them presented a suitable controlled release profile. More than 70% of the drug was released after 3 h **(88).**

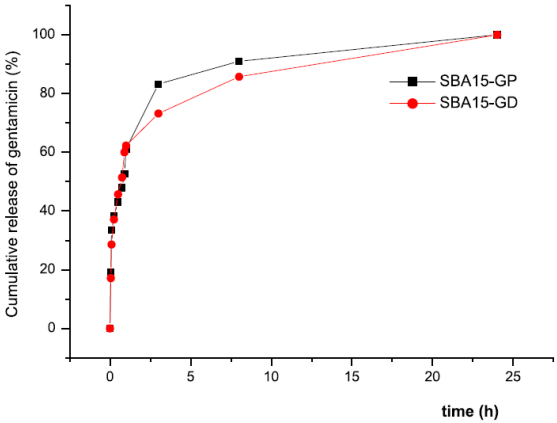

Figure 9 - Gentamicin (%) release from SBA-15 in powder (GP) and disk (GD). Adapted from ref. **88**.

This result can ensure maximum availability of the drug in the body. SBA-15-GP system has shown a slightly faster release profile compared with the SBA-15-GD system. This difference may be caused by a reduced diffusion for the disk system. Before liberation of the drug can occur, it must diffuse from inside the particle and it is more difficult for the disks, since the surface area to volume ratio of the powders is higher than the disks. So, the increase in the release rate of gentamicin can be caused by a reduced surface-to-bulk ratio since the powder is used.

5. FUTURE PROSPECTIVES

Silica surface can act as a template for the synthesis of high molecular weight polymers and biomolecules of medical importance. This template drug delivery technique can be seen as a promising experimental approach to the development of more specific and efficient drugs. Furthermore, taking into account the pharmaceutical sciences, this technique represents an important source of new mechanisms to improve the production, the effectiveness and the safety of the entire process, since the development till the final product, the new drug.

6. REFERENCES

[1] Davis M.E., Lobo R.F. Zeolite and Molecular Sieve Synthesis. *Chem. Mater. 1992, 4, 756 - 768.*

[2] Yang H., Zhao D. Synthesis of replica mesostructures by the nanocasting strategy. J. Mater. Chem. 2005, 15, 1217–1231.

[3] Cides da Silva L.C., Martins T.S., Santos Filho M., Teotônio E.E.S., Isolani P.C., Brito H.F., Tabacniks M.H., Fantini M.C.A., Matos J.R. Luminescent europium complexes encapsulated in cage-like cubic ordered mesoporous silica. Microporous and Mesoporous Materials 92 (**2006**) 94–100.

[4] Kisler J.M., Stevens G.W., O'Connor A.J. Adsorption of Proteins on Mesoporous Molecular Sieves. Mater.Phys.Mech. 4 (2001) 89-93

[5] Kipkemboi P., Fogden A., Alfredsson V., Flodstrom K. Triblock Copolymers as Templates in Mesoporous Silica Formation: Structural

Dependence on Polymer Chain Length and Synthesis Temperature. *Langmuir* 2001, *17,* 5398-5402.

[6] Beck J.S., VartUli J.C., Roth W.J., Leonowicz M.E., Kresge C.T., Schmitt K.D., Chu C.T-W., Olson D.H., Sheppard E.W., McCullen S.B., Higgins J.B., Schlenkert J.L. A New Family of Mesoporous Molecular Sieves Prepared with Liquid Crystal Templates. *J. Am. Chem. Sot.* 1992, *114,* 10834-10843.

[7] Inagaki S., Fukushima Y., Kuroda K. Synthesis of Highly Ordered Mesoporous Materials from a Layered Polysilicate. J . CHEM. SOC., CHEM. COMMUN., 1993.

[8] Kresge C.T., Leonowicz M.E., Roth W.J., Vartuli J.C., Beck J.S. Ordered mesoporous molecular sieves synthesized by a liquid-crystal template mechanism. *Nature* **1992**, *359*, 710-712.

[9] Shi L.Y., Wang Y.M., Ji A., Gao L., Wang Y. In situ direct bifunctionalization of mesoporous silica SBA-15. J. Mater. Chem., 2005, 15, 1392–1396.

[10] Shi K., Peng L.-M., Chen Q., Wang R., Zhou W. Porous crystalline iron oxide thin films templated by mesoporous silica. Microporous and Mesoporous Materials 83 (2005) 219–224.

[11] Ciesla U., Schuth F. Ordered mesoporous materials. Microporous and Mesoporous Materials 27 (1999) 131–149.

[12] Liang Y., Anwander R. Synthesis of pore-enlarged mesoporous organosilicas under basic conditions. Microporous and Mesoporous Materials 72(2 004) 153–165.

[13] Sing K.S.W., Everett D.H., Haul R.A.W. Moscou L., Pierotti R.A., Rouquerol J., Siemieniewska T. International Union of Pure and

Applied Chemistry. Pure & Appl. Chem., Vol. 57, No. 4, pp. 603—619, 1985.

[14] Gédéon A., Lassoued A., Bonardet J.L, Fraissard J. Surface acidity diagnosis and catalytic acidity of AlSBA materials obtained by direct synthesis. Micropporous and Mesoporous Materials 44 – 45 (2001) – 801-806.

[15] MeLllaerts R., Mols R., Jammaer J.A.G., Aerts C.A., Annaert P., Humbeeck J.V., Mooter G.V., Augustijns P., Martens J.A. Increasing the oral bioavailability of the poorly water soluble drug itraconazole with ordered mesoporous silica. European Journal of Pharmaceutics and Biopharmaceutics (2008).

[16] Feng X., Fryxell G.E., Wang L.Q., Kim A.Y., Liu J., Kemner K.M. Functionalized Monolayers on Ordered Mesoporous Supports. *Science* 276, 923 (1997)

[17] Hu W., Luo Q., Su Y., Chen L., Yue Y., Ye C., Deng F. Acid sites in mesoporous Al-SBA-15 material as revealed by solid-state NMR spectroscopy. Microporous and Mesoporous Materials 92 (2006) 22–30.

[18] Song S.W., Hidajat K., Kawi S. Functionalized SBA-15 Materials as Carriers for Controlled Drug Delivery: Influence of Surface Properties on Matrix-Drug Interactions. *Langmuir* 2005, *21,* 9568-9575.

[19] Parida S. K., Dash S., Patel S., Mishra B.K. Adsorption of organic molecules on silica surface. Advances in Colloid and Interface Science 121 (2006) 77–110.

[20] Bose A, Gilpin R.K, Jaroniec M. J Colloid Interface Sci 2001;240:224.

[21] Davydov V.Y, Zhuravlev L.T, Kiselev A.V. Russ J Phys Chem 1964;38:1108.

[22] Hockey J.A. Chem Ind (Lond) 1965;2:57.

[23] Peri J.B. J Phys Chem 1966;70:70.

[24] Hair M.L, Hertl W. J Phys Chem 1969;73:4269.

[25] Van Cauwelaert F.H, Jacobs P.A, Uylterhoeven B. J Phys Chem 1972; 76: 1434.

[26] Morrow B.A, Cody L.A, Lee L.S.M. J Phys Chem 1978; 82:2761.

[27] Van Roosmalen A.J, Moe J.C. J Phys Chem 1978;82:2748.

[28] Van Roosmalen A.J, Moe J.C. J Phys Chem 1979;83:2485.

[29] Ghiotti G, Garrone E, Moterra C, Boccuzzi F. J Phys Chem 1979;83: 2863.

[30] Hoffmann P, Knozinger F. Surf Sci 1987;188:181.

[31] Zhdano V.S.P, Kosheleva L.S, Titova T.I. Langmuir 1987;3:960.

[32] Rochester C.H, Trebilco D.A. J Chem Soc Faraday Trans I 1979;75:2211.

[33] Jal P.K, Sudarshan M, Saha A, Patel S, Mishra B.K. Colloids Surf A Physicochem Eng Asp 2004;240:173.

[34] McCool B., Murphy L., Tripp C.P. J Colloid Interface Sci. 2006;295:294.

[35] Carteret C. Spectrochim Acta Part A 2006;64:670.

[36] Bell R.J, Bird N.F, Dean P. J Phys Chem 1968;72:299.

[37] Morrow BA, McFarlan AJ. J Phys Chem 1992;96:1395.

[38] Hino M, Sato T. Bull Chem Soc Jpn 1971;44:33.

[39] Boccuzzi F, Coluccia S, Ghiotti G, Morterra C, Zecchina A. J Phys Chem 1978;82:1298.

[40] Lang S.J, Marrow B.A. J Phys Chem 1994;98:13314.

[41] Benesi H.A, Jones A.C. J Phys Chem 1959;63:179.

[42] Low M.J.D, Severda A.G, Arnold T.H. Spectrosc Lett 1983;16:207.

[43] Fukui K, Miyauchi H, Iwasawa Y. Chem Phys Lett 1997;274:133.

[44] Ferraro J, Manghari M. J Appl Phys 1972;43:4595.

[45] Civalleri B, Garrone E, Ugliengo P. Chem Phys Lett 1998;294:103.

[46] Zarzycki J, Naudin F. J Chim Phys Phys Chim Biol 1961;58:830.

[47] Ugliengo P, Garrone E. J Mol Catal 1989;54:439.

[48] Smirnov K.S, Smirnov E.P, Tsyganenko A.A. J Electron Spectrosc Relat Phenom 1990;54–55:815.

[49] Senchenya I.N, Garrone E, Ugliengo P. J Mol Struct Theochem 1996;368: 93.

[50] Ermoshin V.A, Smirnov K.S, Bougeard D. Surf Sci 1996;368:147.

[51] Orcel G, Phalippou J, Hench L.L. J Non-Cryst Solids 1986;88:114.

[52] Delia Valle R.G, Venuti E. J Chem Phys 1994;179:411.

[53] Wilson M, Madden P.A, Hemmati M, Angell C.A. Phys Rev Lett 1996;77:4023.

[54] Sarnthein J, Pasquarello A, Car R. Science 1997;275:1925.

[55] Taraskin SN, Elliot SR. Phys Rev B 1997;56:8605.

[56] Brinker J, Sherer W. Sol–Gel Science, The Physics and Chemistry of Sol–Gel Processing. New York: Academic Press; 1990. Chapter 9.

[57] Martin A., Swarbrick J., Cammarata A. Physical Pharmacy: Physical Chemical Principles in the Pharmaceutical Sciences, 3 edition, Lea & Febiger, Philadelphia, PA, 1983, 507-508.

[58] Bruni G., Amici L., Berbenni V., Marini A., Orlandi A. (2002) Drug excipient compatibility studies. *J. Therm. Anal. Calorim.* **68**: 561-73.

[59] Rodante F., Vecchio S., Catalani G., Toassetti M. (2002) Compatibility between active components of a commercial drug. *Il Farmaco*. **57**: 833-43.

[60] Vueba M.L., Veiga F., Sousa J.J., Pina M.E. (2005) Compatibility studies between ibuprofen or ketoprofen with cellulose ether polymer mixtures using thermal analysis. *Drug Dev. Ind. Pharm.* **31**: 943-949.

[61] Araújo, A.A.S., Storpirtis S., Mercuri L.P., Carvalho F.M.S., Santos Filho M., Matos J.R. (2003). Analysis of the antiretroviral zidovudine (AZT) and evaluation of the compatibility with excipients used in solid dosage forms. *Int. J. Pharm.* **260**: 303-14.

[62] Kiss D., Zeló R., Novak Cs., Éhen Zs. (2006) *J. Therm. Anal. Calorim.* **84**: 447-51.

[63] Pereira R.N., Valente B.R., Cruz A.P., Foppa T., Murakami F.S. & Silva M.A.S. Thermoanalytical Study of Atenolol and Commercial Tablets. *Lat. Am. J. Pharm.* 26 (3): 382-6 (2007).

[64] Lehto V.P., Vähä-Heikkilä K., Paski J., Salonen J. Use of Thermoanalytical Methods in Quantification of Drug Load in Mesoporous Silicon Microparticles. Journal of Thermal Analysis and Calorimetry, Vol. 80 (2005) 393–397.

[65] Salonen J., Laitinen L., Kaukonen A.M., Tuura J., Bjorkqvist M., Heikkila T., Vaha-Heikkila K., Hirvonen J., Lehto V.P.. Mesoporous silicon microparticles for oral drug delivery: Loading and release of five model drugs. Journal of Controlled Release 108 (2005) 362– 374.

[66] Malvern Instruments. In: http://www.malvern.co.uk/LabEng/products/IWTM/iwtm.htm Accessed: August 2008.

[67] Schaffazick R.S., Guterres S.S, Freitas L.L., Pohlmann R.A. Caracterização e estabilidade físico-química de sistemas poliméricos nanoparticulados para administração de fármacos. *Química Nova,* v. 26, n. 5, p. 726 - 737, 2003.

[68] Sonvico F., Cagnani A., Rossi A., Motta S., Di Bari M.T., Cavatorta F., Alonso M.J., Deriu A., Colombo P. Formation of self-organized nanoparticles by lecithin/chitosan ionic interaction.*International Journal of Pharmaceutics,* v. 324, p. 67–73, 2006.

[69] Xu G., Zhang J., Song G. Effect of complexation on the zeta potential of silica powder. Powder Technology 134 (2003) 218– 222.

[70] Verwey E.J., Overbeek J.T.G. Theory of the Stability of Lyophobic Colloid, Elsevier, Amsterdam, 1948, pp. 205–223.

[71] Gun'ko V.M., Zarko V.I., Leboda R., Voronin E.F., Chibowski E., Colloids Surf. A Physicochem. Eng. Asp. 132 (1998) 241.

[72] Baccile N., Teixeira C.V., Amenitsch H., Villain F., Lindén M. and Babonneau F. Time-Resolved in Situ Raman and Small-Angle X-ray Diffraction Experiments: From Silica-Precursor Hydrolysis to Development of Mesoscopic Order in SBA-3 Surfactant-Templated Silica. *Chem. Mater.* **2008,** *20,* 1161–1172.

[73] Aburto J., Ayala M., Jaimes I. B.-, Montiel C., Terre´s E., Domınguez J. M., Torres E. Stability and catalytic properties of chloroperoxidase immobilized on SBA-16 mesoporous materials. Microporous and Mesoporous Materials 83 (2005) 193–200.

[74] Bovin J.-O, Alfredsson V., Karlsson G., Carlsson A., Blum Z., Terasaki O., Ultramicroscopy 62 (1996), 277.

[75] Jong KP de, Koster AJ, Chem. Phys. Chem. 3 (2002), 776.

[76] Janssen A.H. Three-dimensional Transmission Electron Microscopy os Porous Catalysts. Chemical Sciences, 1976.

[77] Yang H. & Zhao D., Synthesis of replica mesostructures by the nanocasting strategy. Journal of Materials Chemistry, 2005.

[78] Davydov V.Y, Zhuravlev L.T, Kiselev A.V. J Phys Chem 1964;38:1108.

[79] Shawgo R.S., Greyson A.C. R., Li Y., Cima M.J. BioMEMS for drug delivery, Curr. Opin. Solid State Mater. Sci. 6 (2002) 329– 334.

[80] Niemeyer C.M., Mirkin C.A. Nanobiotechnology. Concepts, Applications and Perspectives, Wiley-VCH, Darmstadt, 2004.

[81] Santini J.T., Cima M.J., Langer R. A controlled release microchip, Nature 397 (1999) 335– 338.

[82] Leoni L., Desai T.A. Nanoporous biocapsules for the encapsulation of insulinoma cells: biotransport and biocompatibility considerations, IEEE Trans. Biomed. Eng. 48 (2001) 1335–1341.

[83] Peri J.B. J Phys Chem 1966;70:70.

[84] Peri J.B, Hansley A.L. J Phys Chem 1968;72:2926.

[85] Ahmed A., Bonner C., Desai T.A., Bioadhesive microdevices with multiple reservoirs: a new platform for oral drug delivery, J. Control. Release 81 (2002) 291–306.

[86] Foraker A., Walczak R., Cohen M., Boiarski T., Grove C., Swaan P. Microfabricated porous silicon particles enhance paracellular delivery of insulin across intestinal Coco-2 cell monolayer, Pharm. Res. 20 (2003) 110– 116.

[87] Cavallaro G., Pierro P., Palumbo F.S., Testa F., Pasqua L., Aiello R. Drug delivery devices based on mesoporous silicate, Drug Deliv. 11 (2004) 41– 46.

[88] Doadrio A.L., Sousa E.M.B., Doadrio J.C., Pe´rez-Pariente J., Izquierdo-Barba I., Vallet-Regi M. Mesoporous SBA-15 HPLC evaluation for controlled gentamicin drug delivery, J. Control. Release 97 (2004) 125–132.

[89] Muñoz B., Rámila A., Pérez-Pariente J., Diaz I., Vallet- Regi M. MCM-41 organic modification as drug delivery rate regulator, Chem. Mater. 15 (2003) 500–503.

[90] Hancock B.C., Parks M. What is the true solubility advantage for amorphous pharmaceuticals? Pharm. Res. 17 (2000) 397– 404.

[91] Ghiotti G, Garrone E, Moterra C, Boccuzzi F. J Phys Chem 1979;83: 2863.\

[92] Wilding I.R. In search of a single solution for complex molecules, Scrip Mag. (2001 May) 9– 11; K.R Horspool, C.A. Lipinski, Advancing new drug delivery concepts to gain the lead, Drug Deliv. Technol. 3 (2003) 34– 46.

[93] Hoffmann P, Knozinger F. Surf Sci 1987;188:181.

[94] Salonen J., Bjorkqvist M., Laine E., Niinisto L. Effects of fabrication parameters on porous p+-type silicon morphology, Phys. Status Solidi, A Appl. Res. 182 (2000) 249– 254.

[95] Zhdano V.S.P, Kosheleva L.S, Titova T.I. Langmuir 1987; 3:960.

[96] Canham L.T. Bioactive silicon structure fabrication through nanoetching techniques, Adv. Mater. 7 (1995) 1033– 1037.

[97] Canham L.T., Reeves C.L., Newey J.P., Houlton M.R., Cox T.I., Buriak J.M., Stewart M.P. Derivatized mesoporous silicon with dramatically improved stability in simulated human blood plasma, Adv. Mater. 11 (1999) 1505– 1507.

[98] Chazalviel, J.N.; Ozaram, F. Surface modification of porous silicon, in: L.T. Canham (Ed.), Properties of porous silicon, INSPEC, London, UK, 1997.

[99] Song, J.H.; Sailor, M.J. Chemical modification of crystalline porous silicon surfaces, Comments Inorg. Chem. 21 (1999) 69– 84.

[100] FDA Guidance for Industry, Waiver of In Vivo Bioavailability and Bioequivalence Studies for Immediate-Release Solid Oral Dosage Forms Based on a Biopharmaceutics Classification System, Food and drug administration, Baltimore, MD, 2000, www.fda.gov/cder/guidance/index.htm.

[101] Lehto, V.P.; Vaha-Heikkila, K.; Paski, J.; Salonen, J. Use of thermoanalytical methods in quantification of drug load in mesoporous silicon microparticles, J. Therm. Anal. Calorim. 80 (2005) 393– 397.

[102] Vallet-Regí, M.; Ramila, A.; Real, R.P. del; Perez-Pariente, J. Chem. Mater. 13 (2001) 308.

[103] Horcajada, P.; Ramila, A.; Perez-Pariente, J.; Vallet-Regí, M.. Influence of pore size of MCM-41 matrices on drug delivery rate. Microporous and Mesoporous Materials 68 (2004) 105–109.

[104] Waters. Gentamicin antibiotic drugs, Application Notebook, Waters Applications Note Library, http://www.waters.com, 2003.

[105] Bohner, M.; Lemaitre, J.; Landuty, P. V.; Zambelli, P.Y.; Markle, H.P.; Gander, B. Gentamicin-loaded hydraulic calcium phosphate bone cement as antibiotic delivery system, J. Pharm. Sci. 86 (5) (1997) 565–572.

CAPÍTULO 2

Publicação científica - Pereira R. N., Murakami F.S., Valente B. R., Rodrigues P.O, Matos R. J., Mercuri L. P., Silva M. A. S.

A ser submetido - Microporous and Mesoporous Materials.

PHYSICO CHEMICAL EVALUATION OF SBA-15 COMPLEXES – NAPROXENE AND STAVUDINE

Pereira R. N.[1], Murakami F.S.[1], Valente B. R.[1], Rodrigues P.O[1], Matos R. J.[2], Mercuri L. P.[3], Silva M. A. S .[1]

[1]*Universidade Federal de Santa Catarina, Laboratório de Controle de Qualidade, Campus Universitário Trindade, 88.040-900, Florianópolis, Brazil.*

[2]*Universidade de São Paulo - Instituto de Química da Universidade de São Paulo. Av. Lineu Prestes, 748 – Laboratório de Análise Térmica Prof. Dr. Ivo Giolito. Butantã. 05508-900 - São Paulo, SP – Brazil.*

[3]*Universidade Federal de São Paulo – Departamento de Ciências Exatas e da Terra -Campus Diadema, Av. Arthur Ridel, 275 - Bairro Eldorado, 09972-270, Diadema - SP-Brazil.*

[1] e-mail: *rafael_nicolay@yahoo.com.br*

ABSTRACT

Mesoporous silica materials have been received much attention due to their attractive features such as stable mesoporous structure, high surface area (up to 1500 m^2/g), large pore volume (up to 1.2 cm^3/g), regular and adjustable nano-pore sizes (2–10 nm) and a hydrophilic surface character. Recently, a new application of mesoporous silica as a drug delivery system has been explored due to their non toxic nature and good biocompatibility. SBA-15 is an ordered mesoporous silica with a large surface area, uniform hexagonal channels and remarkable hydrothermal stability. For this reason, SBA-15 is a potential candidate for drug delivery systems since its pore size is easily controlled

according to the synthesis conditions and the presence of swelling agents. The aim of the present work was available the complexes of SBA-15 silica and drugs. Also evaluate the amount of drug (stavudine and naproxen) present in SBA-15 silica by HPLC. To characterize the SBA-15, stavudine, naproxen and SBA-15 complexes, TGA, DSC, FTIR and SEM was employed.
Keywords: SBA-15, naproxen, stavudine, complexes.

1. INTRODUCTION

Since 1992, new ordered mesoporous solids have been synthesized **[1]**, greatly expanding their potential applicability in a number of fields. In terms of drug delivery systems, these mesoporous materials presents special characteristics such as highly ordered structures (similar to those for the liquid crystals), narrow pore size distribution (from 1.5–40 nm) and ultrahigh surface area (800–2000 m^2/g) which offer new possibilities for incorporating biological agents within silica samples and for controlling the kinetics of their release from the matrix **[2, 3, 4, 5]**. Among them, highly ordered hexagonal mesoporous silica structure SBA-15 has been synthesized by using commercially available block-copolymer surfactants in strong acid media **[6]**. This material is characterized by larger pore sizes up to approximately 30 nm and allows bulky molecules to enter into the pores. It has higher hydrothermal stability and thicker pore wall (3.1 – 6.4 nm) compared with other mesoporous materials **[7, 8].** Under appropriate conditions, its particular pore architecture makes SBA-15 suitable hosting and delivery candidate for a variety of molecules of

pharmaceutical interest, for example, stavudine and naproxen, drugs widely used in the HIV and pain therapy, respectively.

Stavudine is an antiretroviral representative of nucleoside reverse transcriptase (RT) inhibitors class (NRTIs) and is commonly used in the HIV therapy **[9].** The stavudine interacts with the catalytic site (that is the substrate-binding site) of the enzyme (RT) blocking HIV reproduction inside the cells **[9].** Stavudine, also named d4T, is a hydrophylic drug, soluble in water, sparingly soluble in ethanol (96 per cent) and slightly soluble in methylene chloride. Other important characteristic is its partition coefficient (Log *P*(octanol/water)): −0.72 (or 0.14) **[10, 11].** This value confers the hydrophilic characteristic which explains the high water solubility.

Naproxen is a member of the arylacetic acid derivative of propionic acid and naproxen sodium is the sodium salt. It is a nonsteroidal anti-inflammatory drug (NSAIDs) that inhibit prostaglandin synthesis **[12].** The NSAIDs are used in a variety of painful conditions, including the treatment of postoperative pain **[13].** Naproxen is lipid-soluble, practically insoluble in water at low pH and freely soluble in water at high pH, soluble in ethanol (96 per cent) and in methanol. The octanol/water partition coefficient of naproxen at pH 7.4 is 1.6 to 1.8 **[12].**

The application of nanotechnology in biomedical research carries tremendous potential for drug administration. While most of the research has been focused on diagnostic systems the interest in microdevices for therapeutic applications has also increased significantly **[13-17].**

Recently, a new application of mesoporous silica as a drug delivery system has been explored due to their non toxic nature and good biocompatibility. SBA-15 is an ordered mesoporous silica with a large surface area, uniform hexagonal channels and remarkable hydrothermal stability. For this reason, SBA-15 is a potential candidate for drug delivery systems since its pore size is easily controlled according to the synthesis conditions and the presence of swelling agents **[14, 15, 16].**

The aim of the present work was available the complexes of SBA-15 silica and drugs. Also evaluate the amount of drug (Stavudine and Naproxen) present in SBA-15 silica by HPLC. To characterize the SBA-15, stavudine, naproxen and SBA-15 complexes, TGA, DSC, FTIR and SEM was employed.

2. EXPERIMENTAL

2.1 Chemical and Reagents

SBA-15 was provided by Laboratório de Análise Térmica Prof. Dr. Ivo Giolito (USP – Brazil). Stavudine (L. KMT 247650) was a gift from UNIVILLE (Universidade de Joinville, Joinville, Brazil). Naproxen (L. ALL 18174, All Chemistry do Brasil Ltda.) was a gift from UP (Universidade Positivo, Curitiba, Brazil). Ultrapure water was provided by a Milli-Q® purification system (Millipore, USA). Other solvents and reagents used were of analytical grade.

2.2 Loading SBA-15 with Model Drugs

The assays to load SBA-15 with NAP (Naproxen) and SBA-15 with STAV (Stavudine) were conducted as described by **SOONG et.al 2005 [18],** with modifications. To load SBA-15 with NAP (Naproxen) and SBA-15 with STAV (Stavudine), 50 mg of the powder drug samples was added to 50 ml of solvents. Methanol was used for NAP and for STAV two solvents were tested, water and methanol. For both systems, the pH was controlled (NAP – pH 4.1 with HCl; STAV – pH 9.4 with NaOH). The systems with solvent plus drug were soaked for 2 h and after 50 mg of SBA-15 were added to each system. The solutions were soaked for 3 days under stirring. After 3 days, both samples were decanted and the supernatants were removed. The decanted samples were dried and subsequently used to the analytical processes **[18]**.

2.3 Thermoanalytical studies

The thermoanalytical analysis of the SBA-15 alone and of the complexes of NAP and STAV with SBA-15 were performed through the differential scanning calorimetry (DSC) and the thermogravimetry/derivate thermogravimetry (TG/DTG) techniques. The complex systems were prepared as described above. The TG/DTG measurement was performed on thermobalance TGA-50 (Shimadzu), under dynamic nitrogen atmosphere with the flow rate of 50 mL/min. Approximately 5 mg of sample was placed in platinum pan and heated from 30 °C to 400 °C in heating rate of 10 °C/min. The DSC measurement was performed in DSC-60 cell (Shimadzu), under

dynamic nitrogen atmosphere with the flow rate of 50 mL/min. Approximately 2 mg of sample was weight out and placed in a sealed aluminum pan. The analysis was scanned from 30 °C up to 400 °C with heating rate of 10 °C/min. **[19]**.

2.4 Diffuse Reflectance Infrared Fourier Transform Spectroscopy Analysis

The DRIFT spectra were recorded using a Shimadzu spectrometer; model FTIR Prestige, over the wavenumber range of 4000 - 400 cm^{-1}, using a nominal resolution of 4 cm^{-1} and averaging of 32 scans. The samples, SBA-15 and SBA-15 complexes, were diluted with approximately 2 % spectroscopic grade potassium bromide (KBr) (w/w). A background spectrum was obtained for each experimental condition. The software used for the differential analysis was GRAMS/32 V4.04 (Galactic Industries Corporation, Salem, NH, USA) **[20]**.

2.5 X- ray powder diffraction (XRPD)

The XRPD patterns were recorded on an X-ray diffractometer (Siemens model D5000). The samples were irradiated with monochromatized Cukα radiation (1.54056 A°) and analyzed between 10-120° (2 Θ). The voltage, current and pass time used were 40 kw, 40 mA and 1 s, respectively **[20]**.

2.6 Morphology Characterization

The morphology of the complexes was determined by scanning electron microscopy (SEM). SEM was carried out with a Hitachi S-3500N scanning electron microscope **[21].**

2.7 Drug Loading Studies

The SBA-15 silica was charged with stavudine and naproxen and the HPLC method was employed for calculate stavudine and naproxen amount in the complexes.

The HPLC analysis was performed on a Shimadzu LC-10A system (Kyoto, Japan) equipped with a LC-10AD pump, SPD-10AV UV detector (set at 271 nm for NAP and 270 nm for STAV), SCL-10Avp controller unit, and the sample injection performed via a Rheodyne 7125 valve with a 20 μL loop. A RP C18A Merck column (250 mm x 4.6 mm i.d., 5 μm particle size) was used. The mobile phase employed to naproxen was constituted of 750 ml acetonitrile, 735 ml water, and 15 ml glacial acetic acid at room temperature at a flow rate of 1.2 $mL.min^{-1}$. The injection volume was 20 μL for all standards and samples. Data acquisition was performed using CLASS-VP software by the measurement of detected peak areas **[20, 22].**

The mobile phase employed to stavudine was constituted of mobile phase constituted by 20% solution (v/v) of methanol in water in an isocratic system**,** at room temperature at a flow rate of 1.0 $mL.min^{-1}$. The injection volume was 20 μL for all standards and samples. Data

acquisition was performed using CLASS-VP software by the measurement of detected peak areas **[23].**

The assay was carried out with a sample and it was compared with five different concentration of the standard. For naproxen 100, 150, 200, 250 and 300 $\mu g.mL^{-1}$ was employed. For stavudine 2, 4, 5, 8 and 10 $\mu g.mL^{-1}$ was employed.

The SBA-15/NAP, SBA-15/STAV complexes and naproxen and stavudine drugs samples were diluted in mobile phase. The samples were sonicated for 1 hour and filtered in polyamid filter with 0.45 μm pore diameter.

3. RESULTS AND DISCUTIONS

3.1 Thermoanalytical studies (TGA/DSC)

Through the combination of the results measured with TG and DSC, reliable estimations for the degrees of drug loads can be obtained **[24].** The loading degrees obtained with the thermoanalytical methods can be comparable with the results obtained with HPLC.

Taking into account the mass loss of these systems evaluated with the thermoanalytical methods, the mass loss is proportional to the total drug content in the sample. On the other hand, when the drug is confined to small pores its melting temperature is depressed when compared with the melting temperature of bulk drug. Additionally, with the thermal analysis is possible to distinguish the drug located on the surface of the microparticles from that one confined into the pores since

the drug located on the external surfaces of the microparticles is considered as bulk material **[24].**

In order to evaluate the effectiveness of uptake of naproxen and stavudine by the mesoporous material, TG and DSC were used. The decomposition was monitored by TG and the TG curve displayed the weight loss of the complexes as described by **Zhu 2002 [25].**

DSC curve of NAP and SBA-15/NAP are presented in Figure 1. Naproxen showed one endothermic event of fusion (Figure 1C) at 154.0 ^{o}C and showed ΔH = -158.96 J/g. The complex SBA-15/NAP showed two endothermic events of fusion (Figure 1 A and B). The first endothermic event appeared at 147.7 ^{o}C with ΔH = - 44.3 J/g and second one appeared at 197.2 ^{o}C with ΔH = - 28.3 J/g (table 1). These events (Figure 1 - SBA-15/NAP) are probably related to the drug adsorbed on the surface of the silica and inside the pores. Additionally, it was observed that the fusion events of SBA-15/NAP occurred at temperatures about 10 °C less (for the first event) and 40 ^{o}C higher than the pure naproxen. These results demonstrate the occurrence of the complexation of naproxen and SBA-15.

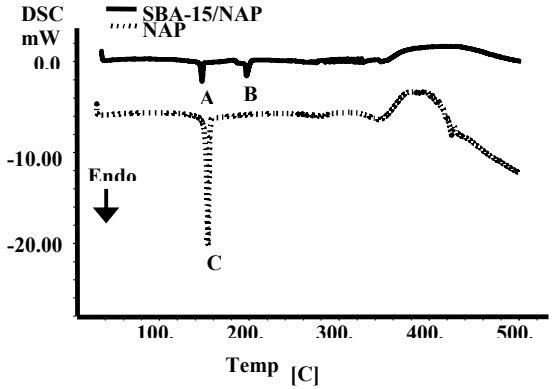

Figure 1 – DSC curve of SBA-15/NAP complex and NAP.

DSC curve of STAV and SBA-15/STAV are presented in Figure 2. Stavudine presented one endothermic event of fusion in 171.3 ^{o}C and showed ΔH = -271.64 J/g. The SBA-15/STAV complex showed one endothermic event which appeared at 125 ^{o}C with ΔH = - 254.65 J/g (Table 1). This endothermic event may be due to a small amount of drug adsorbed on silica.

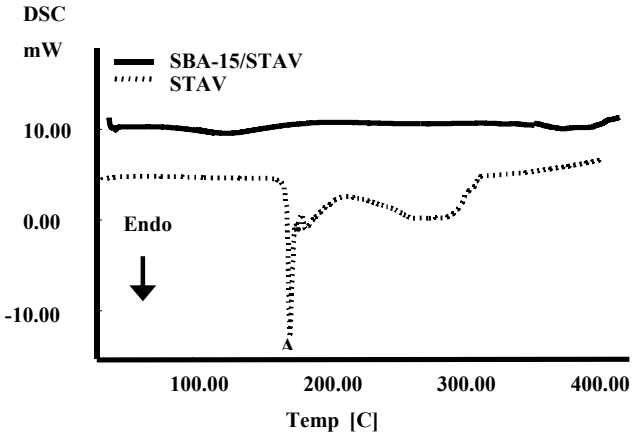

Figure 2 – DSC curve of SBA-15/STAV complex and STAV.

In general, to distinguish the drug adsorbed on the surface of the microparticles from that absorbed into the pores, the principle of thermoporometry on the DSC measurements can be employed. According to this principle, the drug held in the capillaries of porous material has a depressed melting temperature because of the higher pressure of the drug in cavities with a curved interface. On the other hand, the drug located on the external surface of the microparticles exhibits the normal melting temperature of the bulk drug **[24].**

Taking into account the principe of thermoporometry and the DSC results of SBA-15 complexes and the respective drugs, we can suggest that the complexation occurs just with naproxen, as demonstrated with the second peak on figure 1 while with the stavudine, there were no characteristic alterations in the curves (figure 2) that could infer the complexation with this drug and the silica **[26].**

In order to evaluate the mass loss of the systems, TGA studies were performed. TGA curve of NAP and SBA-15/NAP are presented in figure 3. Naproxen showed a weight loss event (97.95 %) which can be represented as the degradation of the drug. In the same way, SBA-15/NAP TGA also showed a weight loss event (57.50 %) for drug degradation (table 2). Considering that it was used a 1:1 ratio of naproxen and silica these results suggest that the drug was fully complexed with the silica.

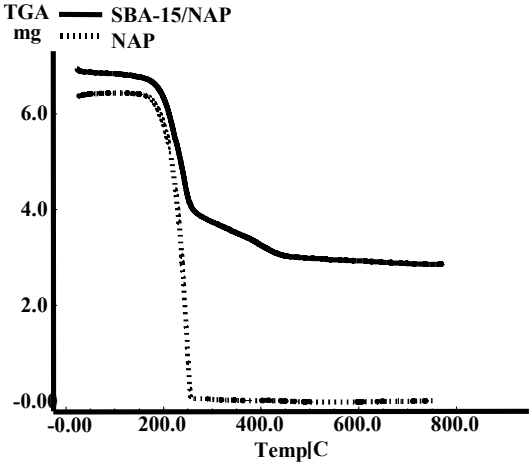

Figure 3 – TGA curve of SBA-15/NAP complex and NAP.

On the other hand, TGA curve of STAV and SBA-15/STAV (Figure 4) showed no significant event of mass loss however, a weight loss appeared in 75 ^{o}C. This event was due to the loss of adsorbed water (3 %) (table 2) suggesting that the complexation of SBA-15 and STAV didn't occur.

The combination of the information obtained from TG and DSC measurements gave a reliable estimation for the complexation of the drug to the mesoporous material. These results are in agreement with previous studies that described the complexation of mesoporous materials with different substances **[24].**

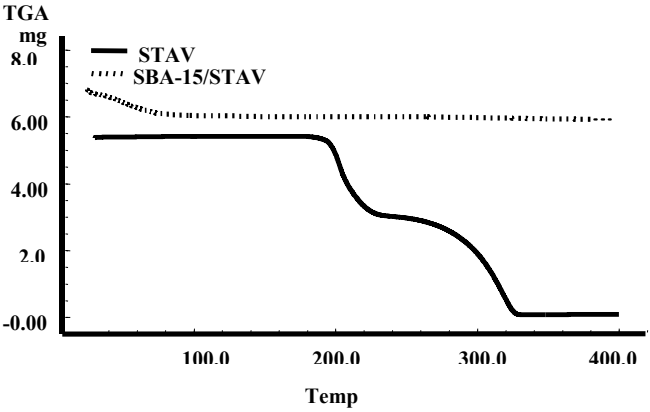

Figure 4 – TGA curve of SBA-15/STAv complex and STAV.

Table 1 – DSC analysis of drugs and complexes.

DSC	T_{peak} (^oC)	T_{onset} (^oC)	T_{endset} (^oC)	Weight (mg)	ΔH (J/g)
NAP	154.0	152.3	156.1	4.2	- 158.96
SBA/NAP	147.7 197.2	145.4 195.2	149.5 201.4	2.8	- 44.30 - 28.30
STAV	171.3	169.4	175.0	3.0	- 271.64
SBA/STAV	125.0	78.8	171.7	1.8	- 241.17

Table 2 – TGA analysis of drugs and complexes.

TGA	NAP	SBA/NAP	STAV	SBA/STAV
Weight (%)	97.95	57.50	99.21	3.00
$T_{(peak)}$ ^oC	248.53	243.42	203.24 and 319.6	47.74

3.2 Diffuse Reflectance Infrared Fourier Transform Spectroscopy Analysis (FTIR)

FTIR spectroscopy can provide surface information of materials for identification of chemical groups.

Figure 5 presents the transmission FTIR spectrum of SBA-15, in which the bands in 3500 - 3300 cm^{-1} were attributed to O-H groups. It was previously reported that in this region the spectrum has two strong peaks at about 3437 and 3326 cm^{-1}. The peak at 3436 cm^{-1} is due to silanol groups while the other peak is due to hydrogen-bonded water molecule **[27, 28].** Also, **t**he band around 1084 cm^{-1} is a typical asymmetric Si–

O–Si stretching attributed to the condensed silica network present in the samples. The Si–OH vibration band is present at 962 cm^{-1} as described by **Li 2007 [29].** In 802 cm^{-1} and 603 cm^{-1}, two bands are present. The first one is due to O-H bending band corresponding to silanol group; the second band is due to presence of Si-O bond rocking. These seven bands are characteristic of SBA-15, mainly three bands: 3436 cm^{-1}, 1084 cm^{-1} and 962 cm^{-1} and are in accordance with the literature concerning SBA-15 FTIR spectrum **[30].**

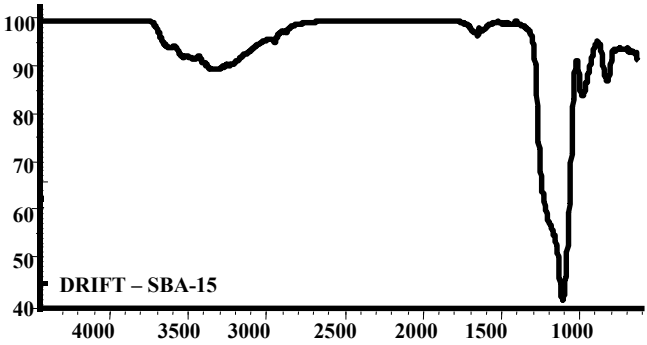

Figure 5 – DRIFT of SBA-15.

NAPROXEN FTIR

Figure 6 shows the infrared spectrum of the naproxen. In agreement with the literature, a broad strong adsorption band at 3186 cm^{-1} is observed which can be attributed to the OH combination stretching vibrations of hydroxyl groups and physically adsorbed water **[31]**. In addition, adsorption bands at 2975 and 2939 cm^{-1} are due to the asymmetric and symmetric stretching vibrations of $–CH_3$ groups, respectively. Bands at 1681, 1597 and 1506 cm^{-1} are assigned to

adsorption of skeletal stretching vibrations of aromatic rings as also described in **[32]**. 1728, 1394 and 1260 cm^{-1} were attributed to υ_cC=O stretching vibration, –COOH bend/stretch and stretch/bend vibrations, respectively. The bands at 1027 and 856 cm^{-1} were assigned to absorption of C–O–C in naproxen, while 1173 cm^{-1} was due to the absorption of C–O. The bands presented in the characteristic region of the spectrum are related to the functional groups of naproxen **[33]** and are shown in table 4.

The interaction of the drug with the mesoporous matrix of the silica promotes a relative band displacement which may suggest links between the hydrogen of silanol groups and the functional groups of naproxen **[34].**

Table 3 – FTIR analysis of naproxen.

Frequency (cm^{-1})	*Position assignment*
856	**C-O-C adsorption**
1027	**C-O-C adsorption**
1173	**C-O adsorption**
1260	**-COOH *stretching/bend* vibration**
1394	**-COOH *bend/stretching* vibration**
1506, 1597, 1681	**Skeletal *stretching* vibration aromatic rings**
1728	***υ_c* C=O *stretching***
2939	**CH3 *symmetric stretching***
2975	**CH3 *asymmetric stretching***
3186	**OH *stretching/adsorbed H2O***

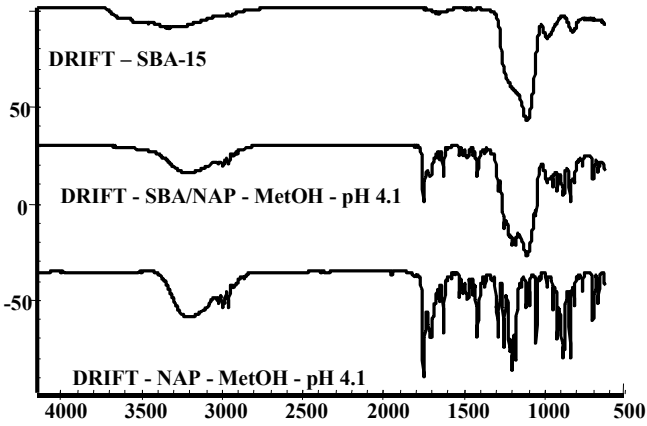

Figure 6 – DRIFT of SBA-15, SBA-15/NAP complex and NAP.

STAVUDINE

The characteristic bands of stavudine **(Figure 7)** are O-H stretching at 3500 cm^{-1}, N-H stretching of secondary amide at 3300 – 3200 cm^{-1}, C=O stretching at 1700 cm^{-1}. The N-H bending band at 1615 cm^{-1} and N-H wagging out-of-plane appears at 800–666 cm^{-1} and 3100 – 3060 $cm^{-}1$. As can be shown in **Table 4** and **figure 9**, the infrared bands are in accordance with those described for stavudine in the literature **[35]**.

Table 4 – FTIR analysis of stavudine.

Frequency (cm^{-1})	*Position assignment*
800-660	**N-H *wagging out-of-plane***
1615	**N-H *bending***
1700	**C=O *stretching***
3100	**N-H *wagging* out-of-plane**
3300-3200	**N-H *stretching***
3500	**O-H *stretching***

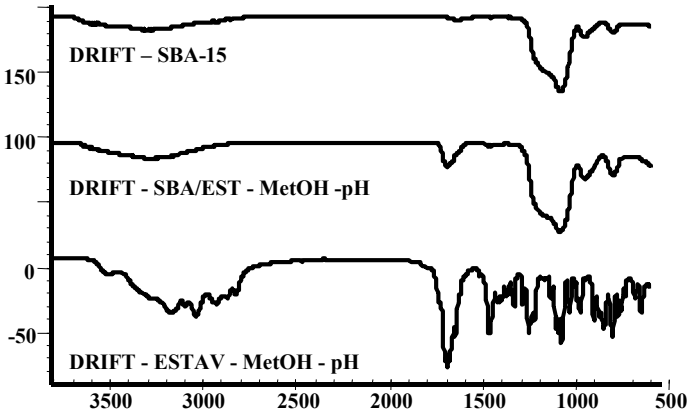

Figure 7 – DRIFT of SBA-15, SBA-15/STAV complex and STAV.

Comparatively, the FTIR spectrum of SBA-15/NAP, **Fig. 6,** exhibits absorption bands similar to those observed in the pattern of NAP. This behavior can be indicative of interactions between species with opposite charges arising from hydrogen bonding, which suggests a probable complexation of SBA-15 groups and Naproxen. On the other hand, the FTIR spectrum of SBA-15/STAV **(Figure 7)** did not show

similar absorption bands observed in the patterns of STAV. This behavior can be indicative that no one interaction was occurred with SBA-15 groups and Stavudine. These results are in accordance with TGA and DSC analyses and confirm that naproxen is complexed in SBA-15 and stavudine is not adequate to complexation with SBA-15.

3.3 X- ray powder diffraction (XRPD)

X-ray diffraction is widely applied in the characterization of powder sample, specially in this case, mesoporous materials and drug powders.

The **Figure 8** shows the high angle XRD patterns of samples of pure silica SBA-15. The SBA-15 sample exhibited typical XRD patterns of SBA-15 mesoporous materials **[36].** The powder XRD analysis of SBA-15 showed diffraction peaks in lower 2Θ angles due to its hexagonal structure. The **Figure 8** displays the reflection of SBA-15 and agrees with that reported by **FAGUNDES 2006 [2].** The broad peaks at around 2Θ 3° and 2Θ 21° are typical peaks of the amorphous silica composition of the SBA-15 sample **[37]**. In this figure, the broad band centered at 2Θ 21° can be assigned to the characteristic reflection from amorphous SiO_2 **[30].** This result confirms that the SBA-15 is an amorphous material and the diffraction peaks are in accordance with literature **[2, 30, 36, and 37].**

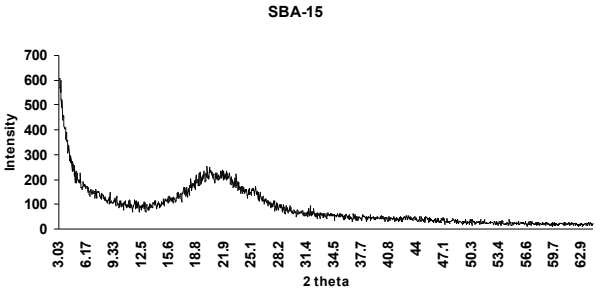

Figure 8 –XRD of SBA-15.

X-ray diffraction is a proven tool to study crystal lattice arrangements and yields very useful information on degree of sample crystallinity drug. Naproxen is a crystalline powder and its characterization was performed by powder XRD. **Figure 9** shows the XRD patterns of naproxen samples. As it can be seen on **Figure 9**, the values of naproxen sample are in the 2Θ 6, 13 and 2Θ 20-23 Â. These values confirm that naproxen is a crystalline powder **[38 – 40]**.

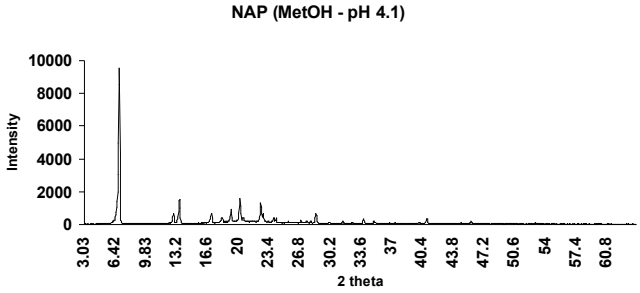

Figure 9 –XRD of NAP.

In addition, the X-ray powder diffraction pattern of pure drug reveals that the intensity of the peaks for the pure stavudine was sharped

[41]. For this reason the X-ray powder diffractometry was carried out to investigate the crystallinility of stavudine. As it can be observed in **Figure 10** the values of stavudine sample are in the 2Θ 9, 10, 19 and 23 . These values confirm that stavudine is a crystalline powder **[35].**

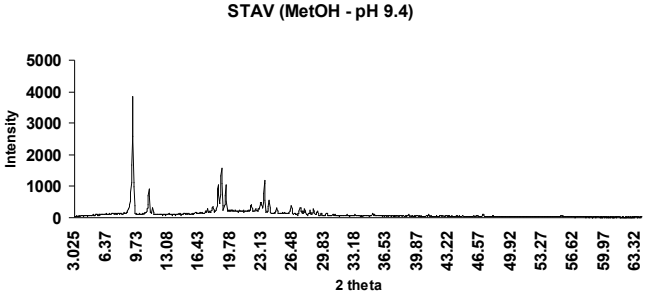

Figure 10 –XRD of STAV.

SBA-15/NAP COMPLEX

The XRD of SBA-15/NAP complex was performed to identify the peaks related to crystalline form of naproxen in the complex **[35]**. **Figure 11** shows the XRD patterns of SBA-15/NAP complex sample. When naproxen was incorporated into the mesoporous material (SBA-15), the complex peaks showed crystalline sharpness due to the complexation of the drug **[41]**. It can be seen from **Figure 11** that the values of SBA-15/NAP sample are in the 2Θ 6, 13 and 20-23. The shapes of these peaks are similar to that found in the naproxen alone **(Figure 6).** These results reinforce the profiles observed in the present work with the thermo analytical studies and demonstrate that the complex, drug and silica (SBA-15/NAP), was held successfully.

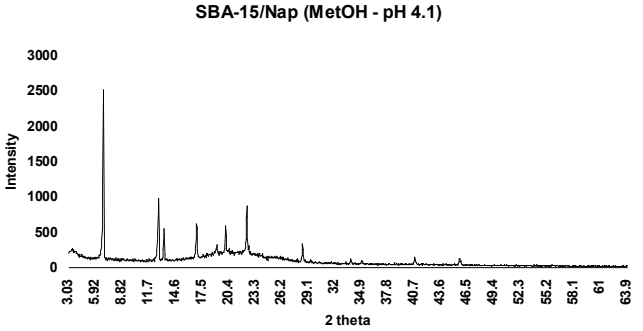

Figure 11 –XRD of SBA-15/NAP complex.

The XRD of SBA-15/STAV was performed to identify the peaks related to the crystalline form of stavudine. **Figure 12** shows the XRD patterns of SBA-15/STAV complex sample. When stavudine was incorporated into the mesoporous material, in this case SBA-15, the complex peaks showed amorphous sharpness which may be due to no complexation of the drug with the silica, as described by **GANGHI 2000 [41]**. The shapes of these peaks are similar to that found in the SBA-15 alone. This result is in accordance to that found in TGA/DSC analysis in this work.

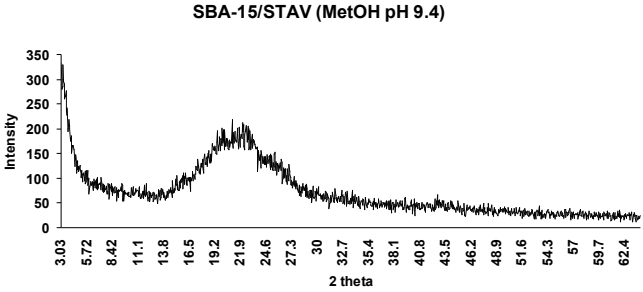

Figure 12 –XRD of SBA-15/STAV complex.

3.4 Morphology Characterization

Scanning Electron Microscopy (SEM) can provide a high resolution image of a surface in three dimensions (topography), but the bulk of the specimen is not imaged. Nowadays, there are several electron microscopic techniques that can characterize intact materials in three-dimensions with nanometer scale resolution, however, some of them have become available to scientific materials only recently **[42, 43]. Yang & Zhao, 2005 [44]** studied morphology control of mesoporous materials. By using SBA-15 nanorods with uniform lengths and highly ordered hexagonal mesostructures as templates, they have synthesized OMCs with the same rod-like morphology**.** The SEM showed rods feature well-ordered mesostructured arrays, large pore sizes (up to 5.8 nm) and surface areas exceeding 1800 $m^2.g^{-1}$. The SEM images showed in the present study are quite similar to those reported by **Yang an Zhao, 2005 [44]**. Comparatively, the two systems show similar arrangements proving strong evidence that the silica used in this work presents appropriated pores and surface characteristics as described in the literature **[44].**

Figure 13 shows SEM images of SBA-15 sample (E), naproxen (B), stavudine (D), SBA-15/NAP complex (A) and SBA-15/STAV complex (C). Figure 16 (F) shows the complex SBA-15/NAP in higher resolution, which allows a better visualization of the silica and the naproxen adsorbed on the SBA-15 surface. These results suggest that the complexation of SBA-15/NAP occurred successfully, confirming the results observed with TGA, DSC and FTIR analysis. Although in the SEM image the result was not so visible it was demonstrated that the complex of SBA-15/STAV was not formed agreeing with the previously

reported in this study. This could be explained by the fact that the images supplied may need additional simulations because of the difficulties of focusing as reported by **SOUZA 2006 [34]** and also by CHEN et al., 1995 concerning the morphological analysis of MCM-41.

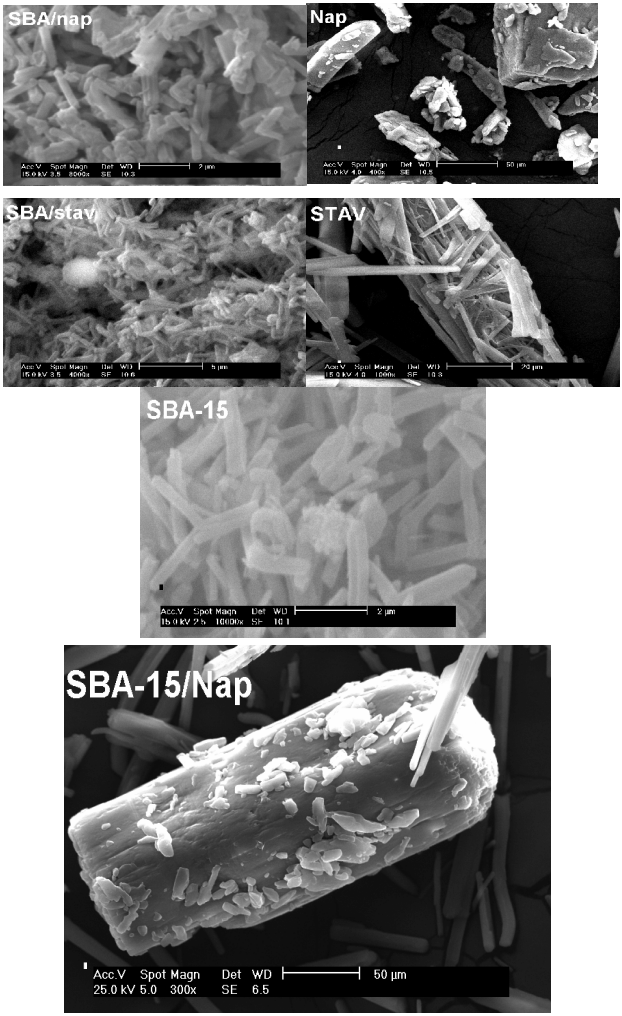

Figure 13 – Scanning Eletronic Microscopy (SEM) of SBA-15, SBA-15/NAP and SBA-15/STAV.

3.5 Drug Loading Studies (HPLC)

Drug concentrations in the samples were determined using an HPLC system. The loading of SBA-15/NAP was performed in a mobile phase (200 μg/ml). The load of SBA-15/NAP was 32.19 % **(Figure 14)** and was calculated from values obtained with the naproxen HPLC method **(Figure 15).** This may suggest interactions between naproxen and the SBA-15, since it was possible to quantify the burden of drug present in the sample. This result was in accordance that TGA, DSC, FTIR and XRD analysis and confirm that this techniques was successfully carried out.

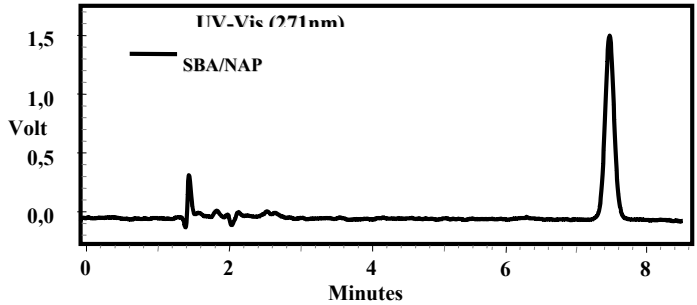

Figure 14 – HPLC chromatogram of SBA-15/NAP complex.

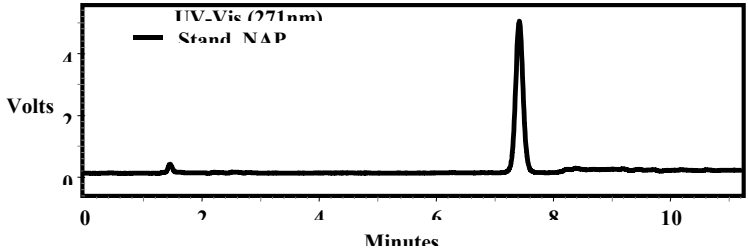

Figure 15 - HPLC chromatogram of Standard naproxen.

The loading of SBA-15/STAV was performed in a mobile phase (5 μg/ml). The load of SBA-15/STAV was not quantified due to the complexation was not occurred. The load of STAV was calculated from values obtained with the stavudine HPLC method **(Figure 16).** This result was in accordance that TGA, DSC, FTIR and XRD analysis and confirms that this technique was successfully carried out.

The calibrated plot naproxen, in the HPLC conditions **(see Figure 17),** at concentrations of 100, 150, 200, 250 and 300 $\mu g.ml^{-1}$, shows a good correlation coefficient of 0.999. The r^2, obtained from 3 consecutive injections of each concentration, is < 1.

Table 6 show the results of load naproxen load at SBA-15 using HPLC method. The average concentration drug loading at silica was 32.19 %, and presented SD 0.55 and coefficient of variance of 1.70 %.

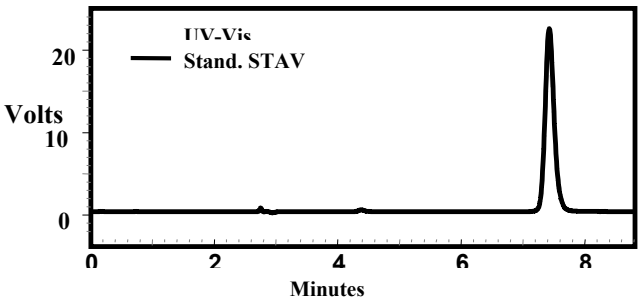

Figure 16 - HPLC chromatogram of stavudine standard.

Table 5 – Results of naproxen load at SBA-15 silica by HPLC method.

ACCURACY				STANDARD	
SAMPLE	Conc. µg/mL	Result		Rep	Area
		Area	%	1	44205
1	200	14070	31.49	2	45310
2	200	14293	31.99	3	44534
3	200	14436	32.31	**Average**	44683
4	200	14613	32.70	**SD**	567.3685
5	200	14196	31.77	**RSD %**	1.26
6	200	14702	32.90		
Average – 32.19 %		**SD - 0.55**		**RSD - 1.70%**	

These experiments have shown that the pH of the solution affects significantly the drug adsorption into the SBA-15 pores. The pH of the naproxen solution must be raised to 4 upon HCl addition to favor a maximum amount of drug adsorbed, while without change the original pH solution, the drug adsorption is not occur (result not shown) **[45].** The pH of the stavudine solution must be raised to 9.4 upon NaOH addition not favored a maximum amount of drug adsorbed due to hydrophilic characteristic of drug.

4. CONCLUSIONS

The TGA, DSC, FTIR, XRD, SEM and HPLC techniques were employed to evaluate complexation of SBA-15 and two model drugs (naproxen and stavudine). These techniques demonstrated that SBA-15 can be used as a matrix of drugs with hydrophobic characteristics, for

example naproxen. On the other hand, complexes of SBA-15 and stavudine not occurred, probably due to hydrophilic characteristic of stavudine. These experiments have shown that the pH of the solution affects significantly the drug adsorption into the SBA-15 pores. The pH control provides better results when compared to the complexation without pH control. The HPLC showed a percentage of complexation of naproxen around 32 %, which is in agreement with those found in the literature for other drugs model.

5. REFERENCES

[1] Davis M.E., Lobo R.F. Zeolite and Molecular Sieve Synthesis. *Chem. Mater. 1992, 4, 756 - 768.*

[2] L.B. Fagundes, T.G.F. Sousa, A. Sousa, V.V. Silva, E.M.B. Sousa. SBA-15-collagen hybrid material for drug delivery applications. Journal of Non-Crystalline Solids 352 (2006) 3496–3501.

[3] MATOS, J. R.; JARONIEC M.; MERCURI, L.P.; ZJ, L. Comparative thermogravimetric and adsorption study of highly ordered mesoporous materials. Journal of Colloid and Interface Science: - APR 1 2006, Holanda, v. 296, n. 1, p. 377-380, 2006.

[4] FANTINI, M.C.A.; MATOS, J.R.; SILVA, L.C. C.; MERCURI, L.P.; CHIERECI G.O.; CELER, E.B.; JARONIEC, M. Ordered mesoporous silica: microwave synthesis. Materials Science and Engineering B 112 (2004) 106–110.

[5] ZHU-ZHU Li, Li-XIONG WEN, LEI SHAO, JIAN-FENG CHEN. Fabrication of porous hollow silica nanoparticles and their applications

in drug release control. Journal of Controlled Release 98 (2004) 245–254.

[6] Zhao X. S., Lu G. Q., Whittaker A. K., Millar G. J., Zhu, H. Y. *J. Phys. Chem. B* **1997,** *101*, 6525-6531.

[7] Hu W., Luo Q., Su Y., Chen L., Yue Y., Ye C., Deng F. Acid sites in mesoporous Al-SBA-15 material as revealed by solid-state NMR spectroscopy. Microporous and Mesoporous Materials 92 (2006) 22–30.

[8] Song S.W., Hidajat K., Kawi S. Functionalized SBA-15 Materials as Carriers for Controlled Drug Delivery: Influence of Surface Properties on Matrix-Drug Interactions. *Langmuir* 2005, *21,* 9568-9575.

[9] Erik De Clercq. Anti-HIV drugs: 25 compounds approved within 25 years after the discovery of HIV. International Journal of Antimicrobial Agents (2008).

[10] USP 28 (2005) *"The United States Pharmacopoeia"* 28th ed, United Stated Pharmacopoeial Convenction, INC, Rockville, MD.

[11] BRITSH PHARMACOPOEIA. The Stationery Office on behalf of the Medicines and Healthcare products Regulatory Agency. CD-ROM version 11.0, London, 2007.

[12] FDA: available at **http://www.fda.gov/cber/infosheets/mphvzig020806.htm**. Accessed in 2007.

[13] Hockey J.A. Chem Ind (Lond) 1965;2:57.

[14] Salonen J., Laitinen L., Kaukonen A.M., Tuura J., Bjorkqvist M., Heikkila T., Vaha-Heikkila K., Hirvonen J., Lehto V.P.. Mesoporous silicon microparticles for oral drug delivery: Loading and release of five model drugs. Journal of Controlled Release 108 (2005) 362– 374.

[15] Davydov V.Y, Zhuravlev L.T, Kiselev A.V. J Phys Chem 1964;38:1108.

[16] Shawgo R.S., Greyson A.C. R., Li Y., Cima M.J. BioMEMS for drug delivery, Curr. Opin. Solid State Mater. Sci. 6 (2002) 329– 334.

[17] Niemeyer C.M., Mirkin C.A. Nanobiotechnology. Concepts, Applications and Perspectives, Wiley-VCH, Darmstadt, 2004.

[18] Todd PA, Clissold SP. Naproxen: a reappraisal of its pharmacology, and therapeutic use in rheumatic diseases and pain states. Drugs 1990; 40: 91–137. PubMed

[19] Rafael N. PEREIRA*, Bruno R. VALENTE, Ariane P. CRUZ, Talize FOPPA, Fabio S. MURAKAMI & Marcos A. S. SILVA.Thermoanalytical Study of Atenolol and Commercial Tablets. *Lat. Am. J. Pharm.* 26 (3): 382-6 (2007).

[20] Murakami, F. S.; Oliveira, P. R.; Bernardi, L. S.; Mendes, C.; Janissek, P. & Silva, M. A. S. Journal of Pharmaceutical and Biomedical Analysis. Submitted - JPBA-D-09-00019.

[21] Qingyi Lu, Feng Gao, Dongsheng Li and Sridhar Komarneni. Biomolecule and/or Microwave-Assisted Solvothermal Syntheses of Nanomaterials AJOMO – Journal of Materials, 2005.

[22] Fabio S. Murakami, Ariane P. Cruz, Rafael N. Pereira, Bruno R. Valente, and Marcos A. S. Silva. Development and Validation of a RP-HPLC Method to Quantify Omeprazole in Delayed Release Tablets. Journal of Liquid Chromatography & Related Technologies, 30: 113–121, 2007.

[23] Gisele Rodrigues da Silva, Felipe Antonacci Condessa, Gérson Antônio Pianetti, Elzíria de Aguiar Nunan e Ligia Maria Moreira de Campos. Desenvolvimento e validação de método por cromatografia

líquida de alta eficiência para determinação simultânea das impurezas timina e timidina na matéria-prima estavudina. *Quim. Nova,* Vol. 31, No. 7, 1686-1690, 2008.

[24] Lehto V.P., Vähä-Heikkilä K., Paski J., Salonen J. Use of Thermoanalytical Methods in Quantification of Drug Load in Mesoporous Silicon Microparticles. Journal of Thermal Analysis and Calorimetry, Vol. 80 (2005) 393–397.

[25] Kake Zhu, Bin Yue, Wuzong Zhou and Heyong He. Preparation of three-dimensional chromium oxide porous single crystals templated by SBA-15. Chemical Communications, 2002.

[26] Mellaerts Randy, Caroline A. Aerts, Jan Van Humbeeck, Patrick Augustijns, Guy Van den Mooter and Johan A. Martens. Enhanced release of itraconazole from ordered mesoporous SBA-15 silica materials. Chem. Commun., 2007, 1375–1377.

[27] S. Maria Chong and X. S. Zhao. Functionalization of SBA-15 with APTES and Characterization of Functionalized Materials. *J. Phys. Chem. B* 2003, *107,* 12650-12657.

[28] S.-W. Song, K. Hidajat, and S. Kawi. Functionalized SBA-15 Materials as Carriers for Controlled Drug Delivery: Influence of Surface Properties on Matrix-Drug Interactions. *Langmuir* 2005, *21,* 9568-9575.

[29] Junning Li, Tao Qi, Lina Wang, Changhou Liu, Yi Zhang. Synthesis and characterization of imidazole-functionalized SBA-15 as an adsorbent of hexavalent chromium. Materials Letters 61 (2007) 3197–3200.

[30] Yang H., Zhao D. Synthesis of replica mesostructures by the nanocasting strategy. J. Mater. Chem. 2005, 15, 1217–1231.

[31] Min Wei, Shuxian Shi, Ji Wang, Yong Li, and Xue Duan. Studies on the intercalation of naproxen into layered double hydroxide and its thermal decomposition by in situ FT-IR and in situ HT-XRD. Journal of Solid State Chemistry 177 (2004) 2534–2541.

[32] W.J. Hehre, L. Radom, P.V.R. Schleyer, AbInitio Molecular Orbital Theory [M], Wiley, New York, 1986, p. 227.

[33] SILVERSTEIN, R.M., BASSLER, G.C, MORRIL, T.C. Identificação Espectrométrica de Compostos Orgânicos. 5ª ed. Rio de Janeiro: 1994, 85p.

[34] SOUSA, E.M.B. Funcionalization of mesoporous materials with long alkil chains as a strategy for controlling drug delivery pattern. Journal of Materials Chemstry, v.16, p. 1-6, 2006.

[35] Sunit Kumar Sahoo, Abdul Arif Mallick, BB Barik and Prakash Ch Senapati. Formulation and *in vitro* Evaluation of Eudragit® Microspheres of Stavudine. *Tropical Journal of Pharmaceutical Research, Vol. 4, No. 1, June 2005, pp. 369-375.*

[36] Shoucang SHEN, Pui Shan CHOW, Fengxi CHEN, and Reginald Beng Hee TAN. Submicron Particles of SBA-15 Modified with MgO as Carriers for Controlled Drug Delivery. *Chem. Pharm. Bull.* 55(7) 985—991 (2007).

[37] Ye Wang, Xiaoxing Wang, Zheng Su, Qian Guo, Qinghu Tang, Qinghong Zhang, Huilin Wan. SBA-15-supported iron phosphate catalyst for partial oxidation of methane to formaldehyde. Catalysis Today 93–95 (2004) 155–161.

[38] True L. Rogers,et.al. Development and Characterization of a Scalable Controlled Precipitation Process to Enhance the Dissolution of

Poorly Water-Soluble Drugs. *Pharmaceutical Research, Vol. 21, No. 11, 2004.*

[39] Teófilo Donaires Flores. Functionalization of Inhalable Particles by Fluidized Bed Processing, Dissertação, 2008.

[40] Wan-Guo Hou & Zhi-Lin Jin. Synthesis and characterization of Naproxen intercalated Zn–Al layered double hydroxides. Colloid Polym Sci (2007) 285:1449–1454.

[41] R. B. Gandhi, J. B. Bogardus, D. E. Bugay, R. K. Perrone and M. A. Kaplan. Pharmaceutical relationships of three solid state forms of stavudine. International Journal of Pharmaceutics, Volume 201, Issue 2, 25 May 2000, Pages 221-237.

[42] Bovin J.-O, Alfredsson V., Karlsson G., Carlsson A., Blum Z., Terasaki O., Ultramicroscopy 62 (1996), 277.

[43] Jong KP de, Koster AJ, Chem. Phys. Chem. 3 (2002), 776.

[44] Yang H. & Zhao D., Synthesis of replica mesostructures by the nanocasting strategy. Journal of Materials Chemistry, 2005.

[45] Doadrio A.L., Sousa E.M.B., Doadrio J.C., Pe´rez-Pariente J., Izquierdo-Barba I., Vallet-Regi M. Mesoporous SBA-15 HPLC evaluation for controlled gentamicin drug delivery, J. Control. Release 97 (2004) 125–132.

CONSIDERAÇÕES GERAIS

CONSIDERAÇÕES GERAIS

A sílica SBA-15 foi complexada com dois fármacos modelo. Um dos fármacos de escolha foi o naproxeno, que apresenta características lipossolúveis, uma vez que possui Log P acima de 2. Além disso, possui pKa de 4,5, uma característica importante na obtenção dos complexos, pois estes foram desenvolvidos com o controle de pH em faixas próximas a seu pKa, a fim de facilitar a complexação pelo fato de o fármaco estar na sua forma ionizada. Outro fármaco escolhido na realização do trabalho foi a estavudina. Esta, por sua vez, apresenta característica hidrossolúvel, pois seu Log P é menor que 1. Seu pKa é 9,4 e, também tendo sido realizado o controle de pH da solução para ampliar a capacidade de complexação da sílica SBA-15.

Através dos resultados observou-se que o pH influenciou na complexação da SBA-15 com os fármacos, uma vez que tanto em relação ao naproxeno quanto a estavudina, não foi obtido resultado positivo sem seu controle.

Algumas técnicas de caracterização do material foram testadas tanto para a SBA-15 quanto para os respectivos complexos com os fármacos. As técnicas termoanalíticas realizadas foram Termogravimetria (TG) e Calorimetria Exploratória Diferencial (DSC). A termogravimetria forneceu resultados de perda de massa dos materiais (complexos, naproxeno e estavudina), referentes à degradação dos fármacos. Em relação a curva TG do complexo SBA-15/estavudina, ocorreu uma perda de massa de aproximadamente 50 %, sugerindo a total interação do fármaco com a sílica. A partir das curvas DSC foram evidenciados eventos endotérmicos referentes ao processo de fusão dos fármacos. Somente para o complexo SBA-15/naproxeno houve evento característico de fusão do fármaco. Para este complexo foram

observados dois eventos de fusão, um referente ao fármaco adsorvido na superfície da sílica e outro evento referente ao fármaco presente nos poros deste material. Ambos os valores de temperatura de fusão foram diferentes do encontrado para o fármaco sozinho, sugerindo uma interação do fármaco, tanto na superfície quanto nos poros da sílica.

Os resultados obtidos para análise de Infravermelho (IV) e Difração de raios-X (DRX) corroboraram com os encontrados nas técnicas termoanalíticas, confirmando os resultados. O FTIR do complexo SBA-15/naproxeno mostrou bandas referentes ao fármaco, porém com alguns deslocamentos, sugerindo mais uma vez o sucesso do processo de complexação com o napoxeno. O mesmo não foi observado para o complexo SBA-15/estavudina, uma vez que não houve aparecimentos de bandas referentes ao fármaco.

A Microscopia Eletrônica de Varredura (MEV) foi utilizada para caracterização morfológica dos materiais (SBA-15, naproxeno, estavudina e respectivos complexos). Através desta técnica foi possível a visualização dos resultados, principalmente no que se refere ao complexo da SBAS-15 com o naproxeno, onde se observou a presença do fármaco adsorvido na superfície da sílica mesoporosa. Em relação ao complexo SBA-15/estavudina, não foi possível observar a presença do fármaco, uma vez que este não complexou com a sílica. Além disso, um resultado mais visível não foi possível, uma vez que existe uma grande dificuldade de foco para a real visualização dos poros da sílica através desta técnica.

A fim de quantificar o percentual de fármaco presente nos poros e na superfície da sílica, foi realizada análise por Cromatografia de Alta Eficiência (CLAE), tanto para o complexo SBA-15/naproxeno quanto

SBA-15/estavudina. Estes resultados foram comparados tendo as matérias-primas dos fármacos como referência. Foi obtido resultado de 32 % de naproxeno presente no complexo SBA-15/naproxeno e não foi possível observar nenhum pico relativo a estavudina para seu respectivo complexo.

Tendo em vista os resultados obtidos, foi possível observar que a SBA-15 possui característica ideal na complexação com fármacos lipossolúveis, como o naproxeno, uma vez que possui características de poro semelhante. Além disso, percebe-se a real importância, durante a complexação, do controle de pH da solução a fim de se obter resultados mais adequados.

CONCLUSÕES E PERSPECTIVAS

CONCLUSÕES E PERSPECTIVAS

1. CONCLUSÕES

1 – A técnica de complexação, da sílica mesoporosa SBA-15, empregada demonstrou ser adequada para os fármacos modelos deste estudo.

2 – Através das combinações dos resultados de DSC e TG foi possível inferir que houve complexação somente com o fármaco naproxeno, uma vez observado o aparecimento de dois eventos endotérmicos característicos de adsorção superficial e adsorção nos poros da SBA-15. Em relação ao fármaco estavudina o mesmo não pode ser observado.

3 – A técnica de Infravermelho por Transformada de Fourier (FTIR) corroborou com os resultados apresentados nos estudos termoanalíticos, uma vez que para o fármaco naproxeno houve o aparecimento das bandas características deste fármaco com pequenos deslocamentos das bandas, indicando interação entre a SBA-15 e o fármaco. Em relação à estavudina, a técnica comprovou a não complexação dos materiais, ocorrendo apenas bandas características da sílica.

4 – No que se refere às análises de DRX da SBA-15, dos fármacos e dos complexos, foi possível observar que a sílica apresentou característica amorfa enquanto os dois fármacos modelo apresentaram regiões cristalinas. Em relação ao complexo SBA-15/naproxeno, houve o aparecimento de regiões cristalinas referentes ao fármaco, comprovando mais uma vez os resultados apresentados para o naproxeno analisado de maneira individual. Já o complexo SBA-15/estavudina não apresentou reflexões características do fármaco, comportando-se como material amorfo. Estes resultados complementam os resultados obtidos

anteriormente, em que somente o complexo SBA-15/naproxeno apresentaram resultados satisfatórios.

5 – As análises por microscopia eletrônica de varredura apresentam imagens referentes a SBA-15, sendo esta semelhante ao já relatado na literatura. Também foram realizados imagens dos fármacos em separado e imagens dos complexos com o naproxeno e estavudina. A imagem do complexo SBA-15/naproxeno permite uma boa visualização da sílica como naproxeno adsorvido em sua superfície. O mesmo não foi possível para o complexo SBA-15/estavudina.

6 – As análises por CLAE (cromatografia líquida de alta eficiência) foram ponto chave na confirmação da interação dos fármacos com a sílica. Além disso, foi possível quantificar o percentual de fármaco complexado na SBA-15. Em relação ao complexo SBA-15/naproxeno, o percentual de fármaco presente na sílica foi de cerca de 30 %, estado este resultado de acordo com o mencionado na literatura para materiais mesoporosos. Em relação ao complexo SBA-15/estavudina, como já esperado, não houve nenhum pico relativo ao fármaco, quando comprado com a referência.

7 – Todos estes resultados permitem concluir que somente o fármaco naproxeno complexou com a SBA-15 de maneira satisfatória. Isso se deve ao fato de a sílica apresentar característica hidrofóbica nos seu interior, semelhante ao que ocorre com o naproxeno. Além disso, o controle de pH foi extremamente importante na ligação do naproxeno com os grupos funcionais da sílica, permitindo uma complexação adequada. No que concerne a estavudina, mesmo com um controle de pH não houve complexação. Isto pode ser explicado pelo fato de este

fármaco apresentar característica hidrofílica, oposto ao apresentado pela SBA-15.

2. PERSPECTIVAS

1 – A técnica de funcionalização da sílica SBA-15 com grupamentos amino, por exemplo, poderia ser uma boa ferramenta para complexação com fármacos hidrofílicos como a estavudina.

2 – Testar diferentes proporções de sílica e fármaco a fim de determinar a estequiometria de complexação.

3 – Determinar o perfil de dissolução dos complexos para melhor compreender de que modo este material pode ser utilizado como futuro carreador de fármacos.

4 – Determinar a cinética de degradação do material através de analises termoanalíticas e determinar a estabilidade do fármaco quando em complexo.

5 – Desenvolver uma formulação com o complexo e realizar testes *in vivo* a fim de saber o real comportamento do material em condições fisiológicas.

REFERÊNCIAS

REFERÊNCIAS

Aburto J., Ayala M., Jaimes I. B.-, Montiel C., Terre´s E., Domınguez J. M., Torres E. Stability and catalytic properties of chloroperoxidase immobilized on SBA-16 mesoporous materials. Microporous and Mesoporous Materials 83 (2005) 193–200.

Ahmed A., Bonner C., Desai T.A., Bioadhesive microdevices with multiple reservoirs: a new platform for oral drug delivery, J. Control. Release 81 (2002) 291–306.

Analgesics Anti-inflammatory Drugs and Antipyretics. In: Martindale, The Complete Drug Reference 32th edition. Edited by: Parfitt K. London, Pharmaceutical Press; 1999:61-62.

Araújo, A.A.S., Storpirtis S., Mercuri L.P., Carvalho F.M.S., Santos Filho M., Matos J.R. (2003). Analysis of the antiretroviral zidovudine (AZT) and evaluation of the compatibility with excipients used in solid dosage forms. *Int. J. Pharm.* **260**: 303-14.

Asanuma, M., Miyazaki, I., Ogawa, N., 2004. Neuroprotective effects of nonsteroidal anti-inflammatory drugs on neurodegenerative diseases. Curr. Pharm. Des. 10, 695–700.

August, E. M., M. E. Marangiu, T. S. Lin, and W. H. Prusoff. 1988. Initial studies on the cellular pharmacology of 39-deoxythymidin-29-ene (d4T): a potent and selective inhibitor of human immunodeficiency virus. Biochem. Pharmacol. **33:**4419–4422.

Baccile N., Teixeira C.V., Amenitsch H., Villain F., Lindén M. and Babonneau F. Time-Resolved in Situ Raman and Small-Angle X-ray Diffraction Experiments: From Silica-Precursor Hydrolysis to

Development of Mesoscopic Order in SBA-3 Surfactant-Templated Silica. *Chem. Mater.* **2008,** *20,* 1161–1172.

Balzarini, J., Herdewijn, P. and De Clercq, E. (1989a) Differential patterns of intracellular metabolism of 2',3'-didehydro-2',3'-dideoxythymidine and 3'-azido-2',3'-dideoxythymidine, two potent anti-human immunodeficiency virus compounds. J. Biol. Chem. 264, 6127-6133.

Beck J.S., VartUli J.C., Roth W.J., Leonowicz M.E., Kresge C.T., Schmitt K.D., Chu C.T-W., Olson D.H., Sheppard E.W., McCullen S.B., Higgins J.B., Schlenkert J.L. A New Family of Mesoporous Molecular Sieves Prepared with Liquid Crystal Templates. *J. Am. Chem. Sot.* 1992, *114,* 10834-10843.

Bell R.J, Bird N.F, Dean P. J Phys Chem 1968;72:299.

Benesi H.A, Jones A.C. J Phys Chem 1959;63:179.

Bertin P., Lapicque F., Payan E., Rigaud M., Bailleul F., Jaeger S., Treves R., Netter P. Sodium naproxen: concentration and effect on inflammatory response mediators in human rheumatoid synovial fluid. European Journal of Clinical Pharmacology 92 (2006) 1–9.

Black, P.H., 2002. Stress and the inflammatory response, a review of neurogenic inflammation. Brain Behav. Immun. 16, 622–653.

Boccuzzi F, Coluccia S, Ghiotti G, Morterra C, Zecchina A. J Phys Chem 1978;82:1298.

Bohner, M.; Lemaitre, J.; Landuty, P. V.; Zambelli, P.Y.; Markle, H.P.; Gander, B. Gentamicin-loaded hydraulic calcium phosphate bone cement as antibiotic delivery system, J. Pharm. Sci. 86 (5) (1997) 565–572.

Bose A, Gilpin R.K, Jaroniec M. J Colloid Interface Sci 2001;240:224.

Bovin J.-O, Alfredsson V., Karlsson G., Carlsson A., Blum Z., Terasaki O., Ultramicroscopy 62 (1996), 277.

Breder, C.D., Dewitt, D., Kraig, R.P., 1995. Characterization of inducible cyclooxygenase in rat brain. J. Comp. Neurol. 355, 296–315.

Brinker J, Sherer W. Sol–Gel Science, The Physics and Chemistry of Sol–Gel Processing. New York: Academic Press; 1990. Chapter 9.

Britsh Pharmacopoeia. The Stationery Office on behalf of the Medicines and Healthcare products Regulatory Agency. CD-ROM version 11.0, London, 2007.

Brogden RN, Heel RC, Speight TM, Avery GS. Naproxen up to date: a review of its pharmacological properties and therapeutic efficacy and use in rheumatic diseases and pain states. Drugs. 1979 Oct; 18(4):241-77.

Bruni G., Amici L., Berbenni V., Marini A., Orlandi A. (2002) Drug excipient compatibility studies. *J. Therm. Anal. Calorim.* **68**: 561-73.

Canham L.T. Bioactive silicon structure fabrication through nanoetching techniques, Adv. Mater. 7 (1995) 1033– 1037.

Canham L.T., Reeves C.L., Newey J.P., Houlton M.R., Cox T.I., Buriak J.M., Stewart M.P. Derivatized mesoporous silicon with dramatically improved stability in simulated human blood plasma, Adv. Mater. 11 (1999) 1505– 1507.

Carteret C. Spectrochim Acta Part A 2006;64:670.

Cavallaro G., Pierro P., Palumbo F.S., Testa F., Pasqua L., Aiello R. Drug delivery devices based on mesoporous silicate, Drug Deliv. 11 (2004) 41– 46.

Chazalviel, J.N.; Ozaram, F. Surface modification of porous silicon, in: L.T. Canham (Ed.), Properties of porous silicon, INSPEC, London, UK, 1997.

Chong S. Maria and X. S. Zhao. Functionalization of SBA-15 with APTES and Characterization of Functionalized Materials. *J. Phys. Chem. B* 2003, *107,* 12650-12657.

Cides da Silva L.C., Martins T.S., Santos Filho M., Teotônio E.E.S., Isolani P.C., Brito H.F., Tabacniks M.H., Fantini M.C.A., Matos J.R. Luminescent europium complexes encapsulated in cage-like cubic ordered mesoporous silica. Microporous and Mesoporous Materials 92 (**2006**) 94–100.

Ciesla U., Schuth F. Ordered mesoporous materials. Microporous and Mesoporous Materials 27 (1999) 131–149.

Civalleri B, Garrone E, Ugliengo P. Chem Phys Lett 1998;294:103.

Court H and Volans GN, "Poisoning After Overdose With Nonsteroidal Anti-inflammatory Drugs," Adverse Drug React Acute Poisoning Rev , 1984, 3(1):1-21.

Davis M.E., Lobo R.F. Zeolite and Molecular Sieve Synthesis. *Chem. Mater. 1992, 4, 756 - 768.*

Davydov V.Y, Zhuravlev L.T, Kiselev A.V. J Phys Chem 1964;38:1108.

De Clercq E. Anti-HIV drugs: 25 compounds approved within 25 years after the discovery of HIV. Int. J. Antimicrob. Agents (2008), doi: 10.1016/j.ijantimicag.2008.10.010.

De Clercq E. Strategies in the design of antiviral drugs. Nat Rev Drug Discov, 2002; 1:13–25.

De Clercq Erik. Anti-HIV drugs: 25 compounds approved within 25 years after the discovery of HIV. International Journal of Antimicrobial Agents (2008).

Delia Valle R.G, Venuti E. J Chem Phys 1994;179:411.

Dhir As, Padi S.S.V., Naidu P. S., Kulkarni S. K. Protective effect of naproxen (non-selective COX-inhibitor) or rofecoxib (selective COX-2 inhibitor) on immobilization stress-inducedbehavioral and biochemical alterations in mice. European Journal of Pharmacology 535 (2006) 192–198

Doadrio A.L., Sousa E.M.B., Doadrio J.C., Pe´rez-Pariente J., Izquierdo-Barba I., Vallet-Regi M. Mesoporous SBA-15 HPLC evaluation for controlled gentamicin drug delivery, J. Control. Release 97 (2004) 125–132.

Drugs for Pain," Med Lett Drugs Ther , 2000, 42(1085):73-8.

Ermoshin V.A, Smirnov K.S, Bougeard D. Surf Sci 1996;368:147.

Fagundes L.B., T.G.F. Sousa, A. Sousa, V.V. Silva, E.M.B. Sousa. SBA-15-collagen hybrid material for drug delivery applications. Journal of Non-Crystalline Solids 352 (2006) 3496–3501.

Fantini M.C.A., Matos J.R., Silva L.C. C., Mercuri L.P., Chiereci G.O., Celer E.B., Jaroniec M. Ordered mesoporous silica: microwave synthesis. Materials Science and Engineering B 112 (2004) 106–110.

Farmacopéia Portuguesa VII, 2° vol., Lisboa, p. 509, 2002.

FDA Guidance for Industry, Waiver of In Vivo Bioavailability and Bioequivalence Studies for Immediate-Release Solid Oral Dosage Forms Based on a Biopharmaceutics Classification System, Food and drug administration, Baltimore, MD, 2000, www.fda.gov/cder/guidance/index.htm.

FDA: available at **http://www.fda.gov/cber/infosheets/mphvzig020806.htm**. Accessed in 2007.

Feng X., Fryxell G.E., Wang L.Q., Kim A.Y., Liu J., Kemner K.M. Functionalized Monolayers on Ordered Mesoporous Supports. *Science* 276, 923 (1997)

Ferraro J, Manghari M. J Appl Phys 1972;43:4595.

Flores T. D. Functionalization of Inhalable Particles by Fluidized Bed Processing, Dissertação, 2008.

Foraker A., Walczak R., Cohen M., Boiarski T., Grove C., Swaan P. Microfabricated porous silicon particles enhance paracellular delivery of insulin across intestinal Coco-2 cell monolayer, Pharm. Res. 20 (2003) 110– 116.

Fricke JR, Halladay SC and Francisco CA: Efficacy and safety of naproxen sodium and ibuprofen for pain relief after oral surgery. Current Therapeutic Research 1993, 54(6):619-27.

Fukui K, Miyauchi H, Iwasawa Y. Chem Phys Lett 1997;274:133.

Furman PA, Fyfe JA, St Clair MH, Weinhold K, Rideout JL, Freeman GA, et al. Phosphorylation of 3'-azido-3'-deoxythymidine and selective interaction of the 5'-triphosphatewithhumanimmunodeficiency virus reverse transcriptase. Proc Natl Acad Sci U S A 1986;83:8333–7.

Gandhi R. B., J. B. Bogardus, D. E. Bugay, R. K. Perrone and M. A. Kaplan. Pharmaceutical relationships of three solid state forms of stavudine. International Journal of Pharmaceutics, Volume 201, Issue 2, 25 May 2000, Pages 221-237.

Gédéon A., Lassoued A., Bonardet J.L, Fraissard J. Surface acidity diagnosis and catalytic acidity of AlSBA materials obtained by direct

synthesis. Micropporous and Mesoporous Materials 44 – 45 (2001) – 801-806.

Ghiotti G, Garrone E, Moterra C, Boccuzzi F. J Phys Chem 1979;83: 2863.

Graham DY, "Prevention of Gastroduodenal Injury Induced by Chronic Nonsteroidal Anti-inflammatory Drug Therapy," Gastroenterology , 1989, 96(2 Pt 2 Suppl):675-81.

Griffith BP, Brett-Smith H, Kim G, Mellors JW, Chacko TM, Garner RB, et al. Effect of stavudine on human immunodeficiency virus type 1 virus load as measured by quantitative mononuclear cell culture, plasma RNA, and immune complex-dissociated antigenemia. J Infect Dis. 1996; 173:1252-5.

Gun'ko V.M., Zarko V.I., Leboda R., Voronin E.F., Chibowski E., Colloids Surf. A Physicochem. Eng. Asp. 132 (1998) 241.

Hair M.L, Hertl W. J Phys Chem 1969;73:4269.

Hancock B.C., Parks M. What is the true solubility advantage for amorphous pharmaceuticals? Pharm. Res. 17 (2000) 397– 404.

Hehre W.J., L. Radom, P.V.R. Schleyer, AbInitio Molecular Orbital Theory [M], Wiley, New York, 1986, p. 227.

Hino M, Sato T. Bull Chem Soc Jpn 1971;44:33.

Ho, H.-T. and Hitchcock, M.J.M. (1989) Cellular pharmacology of 2',3'-dideoxy-2',3'-didehydrothymidine, a nucleoside analog active against human immunodeficiency virus. Antimicrob. Agents Chemother. 33, 844-849.

Hockey J.A. Chem Ind (Lond) 1965;2:57.

Hoffmann P, Knozinger F. Surf Sci 1987;188:181.

Horcajada, P.; Ramila, A.; Perez-Pariente, J.; Vallet-Regí, M.. Influence of pore size of MCM-41 matrices on drug delivery rate. Microporous and Mesoporous Materials 68 (2004) 105–109.

Horwitz, J.P., Chua, J., Da Rooge, M.A., Noel, M. and Klundt, I.L. (1966) The formation of 2',3'-unsaturated pyrimidine nucleosides via a novel /3-elimination reaction. J. Org. Chem. 31, 205-211.

Hou W. G & Zhi-Lin Jin. Synthesis and characterization of Naproxen intercalated Zn–Al layered double hydroxides. Colloid Polym Sci (2007) 285:1449–1454.

Hu W., Luo Q., Su Y., Chen L., Yue Y., Ye C., Deng F. Acid sites in mesoporous Al-SBA-15 material as revealed by solid-state NMR spectroscopy. Microporous and Mesoporous Materials 92 (2006) 22–30.

Inagaki S., Fukushima Y., Kuroda K. Synthesis of Highly Ordered Mesoporous Materials from a Layered Polysilicate. J . CHEM. SOC., CHEM. COMMUN., 1993.

Jacobi J, Fraser GL, Coursin DB, et al, "Clinical Practice Guidelines for the Sustained Use of Sedatives and Analgesics in the Critically Ill Adult," Crit Care Med , 2002, 30(1):119-41.

Jal P.K, Sudarshan M, Saha A, Patel S, Mishra B.K. Colloids Surf A Physicochem Eng Asp 2004;240:173.

Janssen A.H. Three-dimensional Transmission Electron Microscopy os Porous Catalysts. Chemical Sciences, 1976.

Jong KP de, Koster AJ, Chem. Phys. Chem. 3 (2002), 776.

Junning Li, Tao Qi, Lina Wang, Changhou Liu, Yi Zhang. Synthesis and characterization of imidazole-functionalized SBA-15 as an adsorbent of hexavalent chromium. Materials Letters 61 (2007) 3197–3200.

Katlama C., Valantin M., Matheron S., Coutellier A., Calvez V., Descamps D., Longuet C., Bonmarchand M., Tubiana R., De Sa M., Lancar R., Agut H., Brun-Vezinet F. and Costagliola D. Efficacy and Tolerability of Stavudine plus Lamivudine in Treatment-Naive and Treatment-Experienced Patients with HIV-1 Infection. Annals of International Medicine. (1998).129, 525-531.

Kipkemboi P., Fogden A., Alfredsson V., Flodstrom K. Triblock Copolymers as Templates in Mesoporous Silica Formation: Structural Dependence on Polymer Chain Length and Synthesis Temperature. *Langmuir* 2001, *17,* 5398-5402.

Kisler J.M., Stevens G.W., O'Connor A.J. Adsorption of Proteins on Mesoporous Molecular Sieves. Mater.Phys.Mech. 4 (2001) 89-93

Kiss D., Zeló R., Novak Cs., Éhen Zs. (2006) *J. Therm. Anal. Calorim.* **84**: 447-51.

Kresge C.T., Leonowicz M.E., Roth W.J., Vartuli J.C., Beck J.S. Ordered mesoporous molecular sieves synthesized by a liquid-crystal template mechanism. *Nature* **1992**, *359*, 710-712.

Kruk M., Celer E. B., Matos J. R., Pikus S. and Jaroniec M. Synthesis of FDU-1 Silica with Narrow Pore Size Distribution and Tailorable Pore Entrance Size in the Presence of Sodium Chloride. *J. Phys. Chem. B* 2005, *109,* 3838-3843.

Lang S.J, Marrow B.A. J Phys Chem 1994;98:13314.

Lea A. P.; Faulds D. Stavudine: A review of its pharmacodynamic and pharmacokinetic properties and clinical potential in HIV infection. Drugs. 1996, 51, pp. 846-864.

Lehto V.P., Vähä-Heikkilä K., Paski J., Salonen J. Use of Thermoanalytical Methods in Quantification of Drug Load in

Mesoporous Silicon Microparticles. Journal of Thermal Analysis and Calorimetry, Vol. 80 (2005) 393–397.

Leoni L., Desai T.A. Nanoporous biocapsules for the encapsulation of insulinoma cells: biotransport and biocompatibility considerations, IEEE Trans. Biomed. Eng. 48 (2001) 1335–1341.

Liang Y., Anwander R. Synthesis of pore-enlarged mesoporous organosilicas under basic conditions. Microporous and Mesoporous Materials 72(2 004) 153–165.

Low M.J.D, Severda A.G, Arnold T.H. Spectrosc Lett 1983;16:207.

Lu Qingyi, Feng Gao, Dongsheng Li and Sridhar Komarneni. Biomolecule and/or Microwave-Assisted Solvothermal Syntheses of Nanomaterials AJOMO – Journal of Materials, 2005.

Malvern Instruments. In: http://www.malvern.co.uk/LabEng/products/IWTM/iwtm.htm Accessed: August 2008.

Martin A., Swarbrick J., Cammarata A. Physical Pharmacy: Physical Chemical Principles in the Pharmaceutical Sciences, 3 edition, Lea & Febiger, Philadelphia, PA, 1983, 507-508.

Martin, J.C., Hitchcock, M.J.M., Fridland, A., Ghazzouli, I., Kaul, S., Dunkle, L.M., Sterzycki, R.Z. and Mansuri, M.M. (1990) Comparative studies of 2',3'-didehydro-2',3'-dideoxythymidine (D4T) with other pyrimidine nucleoside analogues. Ann. N.Y. Acad. Sci. 616, 22-28.

Mason L, et al. Single dose oral naproxen and naproxen sodium for acute postoperative pain. Available in The Cochrane Database of Systematic Reviews; Issue 4. Chichester: John Wiley; 2004 (accessed 24/04/06).

Matos J. R., Jaroniec M., Mercuri L.P. Comparative thermogravimetric and adsorption study of highly ordered mesoporous materials. Journal of Colloid and Interface Science: - APR 1 2006, Holanda, v. 296, n. 1, p. 377-380, 2006.

McCool B., Murphy L., Tripp C.P. J Colloid Interface Sci. 2006;295:294.

MeLllaerts R., Mols R., Jammaer J.A.G., Aerts C.A., Annaert P., Humbeeck J.V., Mooter G.V., Augustijns P., Martens J.A. Increasing the oral bioavailability of the poorly water soluble drug itraconazole with ordered mesoporous silica. European Journal of Pharmaceutics and Biopharmaceutics (2008).

Merrill DP, Moonis M, Chou TC, Hirsch MS. Lamivudine or stavudine in two- and three-drug combinations against human immunodeficiency virus type 1 replication in vitro. J Infect Dis. 1996; 173:355-64.

Morrow B.A, Cody L.A, Lee L.S.M. J Phys Chem 1978; 82:2761.

Morrow BA, McFarlan AJ. J Phys Chem 1992; 96:1395.

Muñoz B., Rámila A., Pérez-Pariente J., Diaz I., Vallet- Regi M. MCM-41 organic modification as drug delivery rate regulator, Chem. Mater. 15 (2003) 500–503.

Murakami Fabio S., Ariane P. Cruz, Rafael N. Pereira, Bruno R. Valente, and Marcos A. S. Silva. Development and Validation of a RP-HPLC Method to Quantify Omeprazole in Delayed Release Tablets. Journal of Liquid Chromatography & Related Technologies, 30: 113–121, 2007.

Murakami, F. S.; Oliveira, P. R.; Bernardi, L. S.; Mendes, C.; Janissek, P. & Silva, M. A. S. Journal of Pharmaceutical and Biomedical Analysis. Submitted - JPBA-D-09-00019.

Murray HW, Squires KE, Weiss W, Sledz S, Sacks HS, Hassett J, et al. Stavudine in patients with AIDS and AIDS-related complex: AIDS Clinical Trials Group 089. J Infect Dis. 1995; 171 Suppl 2:S123-30.

Niemeyer C.M., Mirkin C.A. Nanobiotechnology. Concepts, Applications and Perspectives, Wiley-VCH, Darmstadt, 2004.

Orcel G, Phalippou J, Hench L.L. J Non-Cryst Solids 1986;88:114.

Padi, S.S.V., Kulkarni, S.K., 2004. Differential effects of naproxen and rofecoxib on the development of hypersensitivity following nerve injury in rats. Pharmacol. Biochem. Behav. 79, 349–358.

Parida S. K., Dash S., Patel S., Mishra B.K. Adsorption of organic molecules on silica surface. Advances in Colloid and Interface Science 121 (2006) 77–110.

Pereira R.N., Valente B.R., Cruz A.P., Foppa T., Murakami F.S. & Silva M.A.S. Thermoanalytical Study of Atenolol and Commercial Tablets. *Lat. Am. J. Pharm.* 26 (3): 382-6 (2007).

Peri J.B, Hansley A.L. J Phys Chem 1968;72:2926.

Peri J.B. J Phys Chem 1966;70:70.

Petersen EA, Ramirez-Ronda CH, Hardy WD, Schwartz R, Sacks HS, Follansbee S, et al. Dose-related activity of stavudine in patients infected with human immunodeficiency virus. J Infect Dis. 1995; 171 Suppl 2:S131-9.

Randy Mellaerts, Caroline A. Aerts, Jan Van Humbeeck, Patrick Augustijns, Guy Van den Mooter and Johan A. Martens. Enhanced release of itraconazole from ordered mesoporous SBA-15 silica materials. Chem. Commun., 2007, 1375–1377.

Rochester C.H, Trebilco D.A. J Chem Soc Faraday Trans I 1979;75:2211.

Rodante F., Vecchio S., Catalani G., Toassetti M. (2002) Compatibility between active components of a commercial drug. *Il Farmaco.* **57**: 833-43.

Sahoo Sunit Kumar, Abdul Arif Mallick, BB Barik and Prakash Ch Senapati. Formulation and *in vitro* Evaluation of Eudragit® Microspheres of Stavudine. *Tropical Journal of Pharmaceutical Research, Vol. 4, No. 1, June 2005, pp. 369-375.*

Salonen J., Bjorkqvist M., Laine E., Niinisto L. Effects of fabrication parameters on porous p+-type silicon morphology, Phys. Status Solidi, A Appl. Res. 182 (2000) 249– 254.

Salonen J., Laitinen L., Kaukonen A.M., Tuura J., Bjorkqvist M., Heikkila T., Vaha-Heikkila K., Hirvonen J., Lehto V.P.. Mesoporous silicon microparticles for oral drug delivery: Loading and release of five model drugs. Journal of Controlled Release 108 (2005) 362– 374.

Santini J.T., Cima M.J., Langer R. A controlled release microchip, Nature 397 (1999) 335– 338.

Sarnthein J, Pasquarello A, Car R. Science 1997;275:1925.

Schaffazick R.S., Guterres S.S, Freitas L.L., Pohlmann R.A. Caracterização e estabilidade físico-química de sistemas poliméricos nanoparticulados para administração de fármacos. *Química Nova,* v. 26, n. 5, p. 726 - 737, 2003.

Senchenya I.N, Garrone E, Ugliengo P. J Mol Struct Theochem 1996;368: 93.

Shawgo R.S., Greyson A.C. R., Li Y., Cima M.J. BioMEMS for drug delivery, Curr. Opin. Solid State Mater. Sci. 6 (2002) 329– 334.

Shen Shoucang, Pui Shan CHOW, Fengxi CHEN, and Reginald Beng Hee TAN. Submicron Particles of SBA-15 Modified with MgO as

Carriers for Controlled Drug Delivery. *Chem. Pharm. Bull.* 55(7) 985—991 (2007).

Shi K., Peng L.-M., Chen Q., Wang R., Zhou W. Porous crystalline iron oxide thin films templated by mesoporous silica. Microporous and Mesoporous Materials 83 (2005) 219–224.

Shi L.Y., Wang Y.M., Ji A., Gao L., Wang Y. In situ direct bifunctionalization of mesoporous silica SBA-15. J. Mater. Chem., 2005, 15, 1392–1396.

Silakova, J.M., Hewett, J.A., Hewett, S.J., 2004. Naproxen reduces excitotoxic neurodegeneration in vivo with an extended therapeutic window. J. Pharmacol. Exp. Ther. 309, 1060–1066.

Silva Gisele Rodrigues da, Felipe Antonacci Condessa, Gérson Antônio Pianetti, Elzíria de Aguiar Nunan e Ligia Maria Moreira de Campos. Desenvolvimento e validação de método por cromatografia líquida de alta eficiência para determinação simultânea das impurezas timina e timidina na matéria-prima estavudina. *Quim. Nova,* Vol. 31, No. 7, 1686-1690, 2008.

Silverstein, R.M., Bassler, G.C, Morril, T.C. Identificação Espectrométrica de Compostos Orgânicos. 5ª ed. Rio de Janeiro: 1994, 85p.

Sing K.S.W., Everett D.H., Haul R.A.W. Moscou L., Pierotti R.A., Rouquerol J., Siemieniewska T. International Union of Pure and Applied Chemistry. Pure & Appl. Chem., Vol. 57, No. 4, pp. 603—619, 1985.

Smirnov K.S, Smirnov E.P, Tsyganenko A.A. J Electron Spectrosc Relat Phenom 1990;54–55:815.

Smolinske SC, Hall AH, Vandenberg SA, et al, "Toxic Effects of Nonsteroid Anti-inflammatory Drugs in Overdose. An Overview of Recent Evidence on Clinical Effects and Dose-Response Relationships," Drug Saf , 1990, 5(4):252-74.

Song S.W., Hidajat K., Kawi S. Functionalized SBA-15 Materials as Carriers for Controlled Drug Delivery: Influence of Surface Properties on Matrix-Drug Interactions. *Langmuir* 2005, *21,* 9568-9575.

Song, J.H.; Sailor, M.J. Chemical modification of crystalline porous silicon surfaces, Comments Inorg. Chem. 21 (1999) 69– 84.

Sonvico F., Cagnani A., Rossi A., Motta S., Di Bari M.T., Cavatorta F., Alonso M.J., Deriu A., Colombo P. Formation of self-organized nanoparticles by lecithin/chitosan ionic interaction.*International Journal of Pharmaceutics,* v. 324, p. 67–73, 2006.

Sousa, E.M.B. Funcionalization of mesoporous materials with long alkil chains as a strategy for controlling drug delivery pattern. Journal of Materials Chemstry, v.16, p. 1-6, 2006.

Steinbach G., et.al. The Effect of Celecoxib, a Cyclooxygenase-2 Inhibitor, in Familial Adenomatous Polyposis. The New England Journal of Medicine, 2000; 342:1946-1952.

Taraskin SN, Elliot SR. Phys Rev B 1997;56:8605.

The Japanese Pharmacopoeia, 4th Ed., p. 636-637, 2004.

Todd PA, Clissold SP. Naproxen: a reappraisal of its pharmacology, and therapeutic use in rheumatic diseases and pain states. Drugs 1990; 40: 91–137.

True L. Rogers,et.al. Development and Characterization of a Scalable Controlled Precipitation Process to Enhance the Dissolution of Poorly Water-Soluble Drugs. *Pharmaceutical Research, Vol. 21, No. 11, 2004.*

Ugliengo P, Garrone E. J Mol Catal 1989;54:439.

UNAIDS (2007). Comparing adult antenatal-clinic based HIV prevalence with prevalence from national population based surveys in sub-Saharan Africa. UNAIDS presentation. Accessed 17 November 2007 at http://data.unaids.org/pub/Presentation/2007/survey_anc_2007_en.pdf.

UNAIDS Reference Group on Estimates, Modelling and Projections (2002). Improved methods and assumptions for the estimation of the HIV/AIDS epidemic and its impact: recommendations of the UNAIDS Reference Group on Estimates, Modelling and Projections. AIDS, 16: W1–W16.

UNAIDS Reference Group on Estimates, Modelling, and Projections (2006). Improving parameter estimation, projection methods, uncertainty estimation, and epidemic classification. Report of a meeting of the UNAIDS Reference Group on Estimates, Modelling, and Projections, Prague, Czech Republic, 29 Nov—1 Dec. http://data.unaids.org/pub/Report/2007/2006prague_report_en.pdf.

UNAIDS. AIDS epidemic update : December 2007.

UNAIDS/WHO (2006). AIDS epidemic update: December 2006. UNAIDS, Geneva 2006. UNAIDS/06.29E. ISBN 92 9 173542 6.

USP 30/ NF 25. United States Pharmacopeia & National Formulary (2007) 30 ed. Rockville, United States Pharmacopeial Convention.

Vale JA and Meredith TJ, "Acute Poisoning Due to Nonsteroidal Anti-inflammatory Drugs," Med Toxicol , 1986, 1(1):12-31.

Vallet-Regí, M.; Ramila, A.; Real, R.P. del; Perez-Pariente, J. Chem. Mater. 13 (2001) 308.

Van Cauwelaert F.H, Jacobs P.A, Uylterhoeven B. J Phys Chem 1972; 76: 1434.

Van Roosmalen A.J, Moe J.C. J Phys Chem 1978;82:2748.

Van Roosmalen A.J, Moe J.C. J Phys Chem 1979;83:2485.

Verwey E.J., Overbeek J.T.G. Theory of the Stability of Lyophobic Colloid, Elsevier, Amsterdam, 1948, pp. 205–223.

Villarejo A.L.D., Regí M.V. Liberación de fármacos en matrices biocerámicas: Avances y perspectivas. Ed. Realigraf. Madrid, Espana, 2006.

Vueba M.L., Veiga F., Sousa J.J., Pina M.E. (2005) Compatibility studies between ibuprofen or ketoprofen with cellulose ether polymer mixtures using thermal analysis. *Drug Dev. Ind. Pharm.* **31**: 943-949.

Wang Ye, Xiaoxing Wang, Zheng Su, Qian Guo, Qinghu Tang, Qinghong Zhang, Huilin Wan. SBA-15-supported iron phosphate catalyst for partial oxidation of methane to formaldehyde. Catalysis Today 93–95 (2004) 155–161.

Waters. Gentamicin antibiotic drugs, Application Notebook, Waters Applications Note Library, http://www.waters.com, 2003.

Wei Min, Shuxian Shi, Ji Wang, Yong Li, and Xue Duan. Studies on the intercalation of naproxen into layered double hydroxide and its thermal decomposition by in situ FT-IR and in situ HT-XRD. Journal of Solid State Chemistry 177 (2004) 2534–2541.

WHO (2003). World health report: 2003: shaping the future. Geneva. ISBN 92 4 156243 9.

WHO, UNAIDS, UNICEF (2007). Towards universal access: scaling up priority HIV/AIDS interventions in the health sector: progress report. April. Geneva. ISBN 978 92 4 159539 1.

Wilding I.R. In search of a single solution for complex molecules, Scrip Mag. (2001 May) 9– 11; K.R Horspool, C.A. Lipinski, Advancing new drug delivery concepts to gain the lead, Drug Deliv. Technol. 3 (2003) 34– 46.

Willingale, H.L., Gardiner, N.J., McLymont, N., Gible, S., Grubb, B.D., 1997. Prostanoids synthesized by cyclooxygenase isoforms in the rat spinal cord and their contribution to the development of neuronal hyperexcitability. Br. J. Pharmacol. 122, 1593–1604.

Wilson M, Madden P.A, Hemmati M, Angell C.A. Phys Rev Lett 1996;77:4023.

Xu G., Zhang J., Song G. Effect of complexation on the zeta potential of silica powder. Powder Technology 134 (2003) 218– 222.

Yang H., Zhao D. Synthesis of replica mesostructures by the nanocasting strategy. J. Mater. Chem. 2005, 15, 1217–1231.

Yarchoan, R., Mitsuya, H., Myers, C.E. and Broder, S. (1989) Clinical Pharmacology of Y-azido-2',Y-dideoxythymidine (zidovudine) and related dideoxynucleosides. New Engl. J. Med. 321,726-738.

Zarzycki J, Naudin F. J Chim Phys Phys Chim Biol 1961;58:830.

Zhao X. S., Lu G. Q., Whittaker A. K., Millar G. J., Zhu, H. Y. *J. Phys. Chem. B* **1997,** *101*, 6525-6531.

Zhdano V.S.P, Kosheleva L.S, Titova T.I. Langmuir 1987;3:960.

Zhu Kake, Bin Yue, Wuzong Zhou and Heyong He. Preparation of three-dimensional chromium oxide porous single crystals templated by SBA-15. Chemical Communications, 2002.

Zhu-Zhu Li, Li-Xiong Wen, Lei Shao, Jian-Feng Chen. Fabrication of porous hollow silica nanoparticles and their applications in drug release control. Journal of Controlled Release 98 (2004) 245– 254.

APÊNDICE

APÊNDICE

1 . Método de Recuperação da SBA-15

A sílica SBA-15, utilizada nos experimentos de complexação com os fármacos naproxeno e estavudina, foi recuperada para futuros testes de complexação com novos fármacos modelo. O processo de recuperação se deu pela mesma metodologia utilizada na complexação dos fármacos, ou seja, foi submetida a uma agitação com o solvente utlizado (metanol) por 2 dias. Posteriormente este material foi sonicado por cerca de três horas com aquecimento (65 ^{o}C) e filtrado em membrana de poliamida com tamanho de poro de 0,45 micra. A seguir o filtro foi submetido a uma secagem a 100 ^{o}C por cerca de 30 minutos e a sílica foi retirada do filtro. A etapa seguinte consistiu em submeter o material à temperaturas elevadas (450 ^{o}C) em mufla. Como provado por resultados de análise térmica (Figura 18 e 19) a sílica SBA-15 possui boa estabilidade térmica, não ocorrendo desestruturação à altas temperaturas. A seguir, o material foi submetido a analises de Termogravimetria (TGA), Calorimetria exploratória diferencial (DSC), Infravermelho por Transformada de Fourier (FTIR) e difração de raios-x (DRX), a fim de comprovar a completa retirada dos fármacos dos poros e da superfície da SBA-15.

2. Resultados e Discussões

As Figuras abaixo mostram resultados da recuperação do material por DCS. Conforme apresentado na figura a sílica não apresenta evento endotérmico característico de fusão tanto do naproxeno quanto da

estavudina, como apresentado nos resultados de complexação do capítulo 5 (Complexos SBA-15).

Percebe-se, pela figura 1, que o perfil da curva DSC da sílica recuperada é semelhante ao perfil da SBA-15 utilizada como padrão.

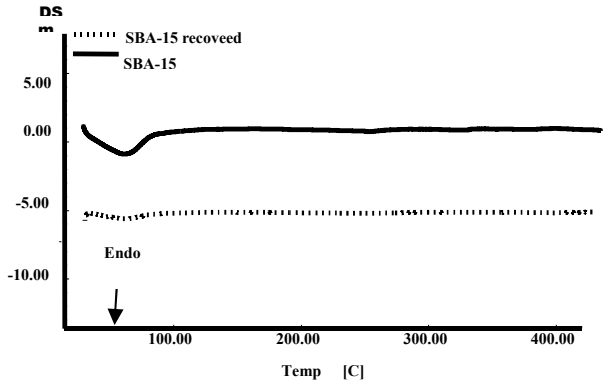

Figura 1 – DSC curve of SBA-15 and AS-15 recovered.

O resultado obtido por DSC é confirmado pela curva TGA (Figura 2) na qual apenas um evento de perda de massa ocorre a temperaturas abaixo de 100 ^{o}C referente à provável perda de água adsorvida na superfície da sílica. Se observarmos a curva da SBA-15 utilizada como referência pode-se também perceber o mesmo perfil quando a SBA-15 foi submetida a analise por TGA.

Estes resultados sugerem uma completa recuperação do material.

As análises por FTIR e DRX a seguir também foram realizadas para comprovar esta teoria.

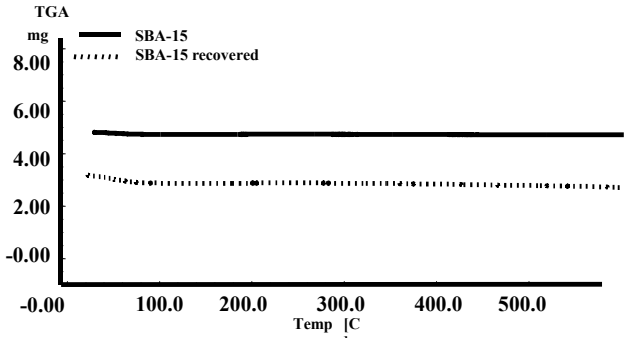

Figura 2 – Curva TGA da sílica SBA-15 e SBA-15 recuperada.

Abaixo é apresentado o resultado das análises por FTIR (Figura 3). Observando os dois espectros de infravermelho (SBA-15 e SBA-15 recuperada), podemos inferir que a recuperação do material foi satisfatória, uma vez que as mesmas bandas de absorção dos principais grupos da SBA-15 utilizada como padrão foram mantidas quando comparadas ao espectro da SBA-15 recuperada.

As principais bandas de absorção da SBA-15 foram já discutidas no capítulo 5 (Complexos SBA-15).

A técnica de FTIR comprova os resultados apresentados anteriormente (Figuras 1 e 2) por TGA e DSC.

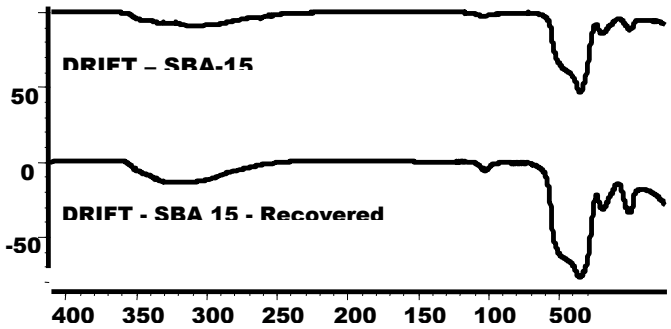

Figura 3 – Espectro FTIR da silica SBA-15 e SBA-15 recuperada.

Abaixo (Figura 4 e 5), temos o resultado das análises por DRX da SBA-15 referência e SBA-15 recuperada. Mais uma vez há a comprovação de que o material foi recuperado com sucesso. Isso pode ser observado comparando-se as analises da SBA-15 referência e SBA-15 recuperada. A SBA-15 apresenta características amorfas (Figura 4), não apresentando região cristalina. Quando observamos a SBA-15 recuperadas (Figura 5) isso poder ser comprovado, pois apresenta as mesmas características da SBA-15 referencia e nenhuma região cristalina referente aos fármacos (naproxeno e estavudina) pode ser observado.

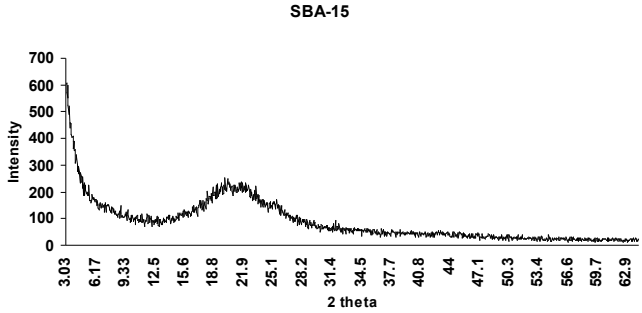

Figura 4 – Difração de raios-X (DRX) da sílica SBA-15.

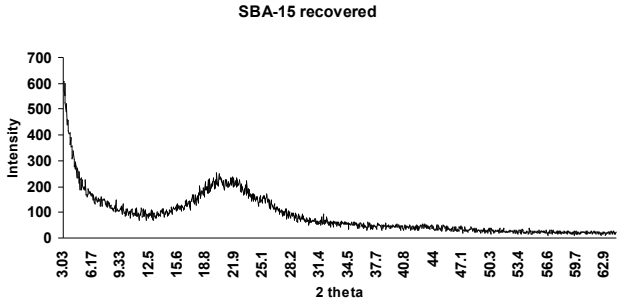

Figura 5 - Difração de raios-X (DRX) da sílica SBA-15 recuperada.

3. Conclusões

Percebe-se pelas técnicas de TGA, DSC, FTIR e DRX que a SBA-15 recuperada apresenta os mesmos perfis apresentados para a SBA-15 utlizada como referência. As análises em questão serviram de suporte para concluir que o material foi recuperado com sucesso.

Análises por HPLC ainda podem ser realizadas para comprovar a inexistência de fármacos na superfície e no interior da SBA-15.

Ainda deveriam ser realizadas novas complexações com o material recuperado para que se possa inferir a manutenção de sua estrutura mesoporosa e seu poder de complexação.